Infectious Bronchitis Virus-Host Interaction: Viral Spike Protein Cell/Tissue Binding Specificity and Immune Responses

by

Saiada Farjana

A dissertation submitted to the Graduate Faculty of
Auburn University
in partial fulfillment of the
requirements for the Degree of
Doctor of Philosophy

Auburn, Alabama
December 14, 2019

Key words: Infectious bronchitis, coronavirus, recombinant spike protein, chicken embryonic kidney cells, spike histochemistry, immune response

Approved by

Vicky L. van Santen, Chair, Professor of Pathobiology
Haroldo Toro, Professor of Pathobiology
Kellye Joiner, Associate Professor of Pathobiology
Ruediger Hauck, Assistant Professor of Pathobiology and Poultry Science

ABSTRACT

The coronavirus avian infectious bronchitis virus (IBV) causes a highly contagious disease in chickens affecting the respiratory tract and, depending on virus strains, reproductive and urogenital tracts. Strains are distinguished and classified based on the amino acid (aa) variation in the S1 domain of spike (S) protein, the major viral attachment protein. The S1 subunit of the IBV spike protein mediates viral attachment and the S2 subunit is involved in fusion to host cells. Although S2 does not have any receptor binding domain, interplay between S1 and S2 synergistically improves host cell attachment. S is the major protein in inducing neutralizing antibodies and in determining host tropism.

Adaptation of an ArkDPI IBV vaccine strain to chicken embryonic kidney (CEK) cells eliminates subpopulations that are selected in and cause problems in vaccinated chickens. The CEK-adapted virus induces protective immune responses in chicken, as demonstrated by reducing viral loads and clinical signs after virulent Ark serotype IBV challenge. Three aa changes in the S protein of CEK-adapted virus, two in S1 and one in the S2, were observed. These aa changes in the S protein of CEK-adapted vaccine virus might allow it to attach more efficiently to CEK cells compared to the ArkDPI vaccine strain, thus contributing to adaptation. Contrary to this expectation, we did not observe detectable binding of CEK-adapted S protein to CEK cells at standard protein concentration. Our results suggested that, in this case, factors other than improved attachment to CEK cells were involved in adaptation to CEK cells.

We also observed severely reduced or abolished detectable binding of recombinant S protein of CEK-adapted ArkDPI IBV vaccine virus to most relevant chicken tissues in vitro, suggesting lower levels of replication in chickens for CEK-adapted ArkDPI vaccine strain than its parental strain. We compared replication in chickens of the CEK-adapted virus to a commercial ArkDPI-derived IBV vaccine, with only two aa differences in S, after ocular inoculation of 1-day-old SPF leghorn chickens with 10^4 or 10^5 EID_{50} CEK-adapted ArkDPI, or 10^4 EID_{50} commercial vaccine virus. Replication of the vaccine viruses in individual chickens was monitored by determining the relative levels of viral RNA in tears 3, 5 and 8-days post-vaccination (DPV) and in choanal and tracheal swabs 5 and 8 DPV. As expected, vaccine viral RNA was consistently statistically significantly lower in all three sample types in chickens inoculated with CEK-adapted vaccine virus compared to the commercial vaccine when the same dose (10^4 EID_{50}) was used and in tracheal swabs even when ten times the dose was used. However, in spite of substantially lower replication of the CEK-adapted vaccine virus in some tissues in chickens, reflected in lower vaccine viral loads in tears, trachea and choana, it provided effective protection against challenge.

IBV variant CalEnt with unusual enteric tropism was believed to have acquired extended tropism due to changes in its S protein. To determine whether this tropism of CalEnt was due to an increased ability of its S protein to bind to the intestinal epithelium, we compared the binding of recombinant S1 proteins derived from CalEnt and Cal99, a typical respiratory IBV variant with an S1 most closely related to CalEnt, to relevant chicken tissues. Contrary to expectations, neither the CalEnt S1 protein, S1-N-terminal domain, nor entire S-ectodomain, showed any binding at the standard protein concentration to respiratory or intestinal tissues. Thus, our results do not support better attachment to intestinal epithelia as a reason for CalEnt's extended tropism. Bioinformatic analyses of CalEnt S protein sequences suggest that CalEnt's S2-coding region was acquired

through a recombination event and encodes a unique aa sequence at the putative recognition site for the protease that activates the S protein for fusion of host membrane and viral envelope during viral entry. Thus, S2 activation by tissue-specific proteases might facilitate CalEnt entry into intestinal epithelial cells and compensate for poor binding by its S1 protein.

Increasing evidence suggested that the practice common in the poultry industry of IBV vaccination early after hatching may not elicit optimal specific immunity and effectively protect chickens. We further investigated the effects of early vaccination on immune responses in chickens primed with ArkDPI-type IBV vaccine at increasing ages followed by booster vaccination. Our results confirmed that IBV vaccination on the day of hatch induces suboptimal IBV immune responses both in the systemic and mucosal compartments. However, booster vaccination seems to overcome poor initial responses.

In spite of extensive vaccination against Ark-type IBV, Ark-type IBV continues to cause problems in the poultry industry. To understand how IBV field strains are able to escape IBV vaccine-induced immune responses, we compared reactivity of antibodies in IBV ArkDPI-vaccinated chickens with the vaccine strain virus and an Ark-type IBV isolated from a vaccinated flock. IBV-specific IgA antibody levels in tears and IgA and IgG antibody levels in plasma measured against the field isolate were lower compared to those against the vaccine strain, suggesting immune escape of the field strain from vaccine-induced immune responses. In order to observe whether differences in antibody levels against the vaccine strain and field isolate in vaccinated chickens included different levels of antibodies recognizing the IBV S proteins, ELISA using trimeric recombinant S-ectodomain proteins with S1 domains representing the vaccine strain and field isolate was conducted. Antibodies in both tears and plasma of vaccinated chickens both post-primary vaccination and post-boost recognized the S-ectodomain containing the field strain

S1 significantly less ($P<0.05$) than they recognized the vaccine strain S-ectodomain. Our results were consistent with the prediction that IBV field strains escape the host humoral immune responses through aa changes within the S1 protein.

AKNOWLEDGEMENTS

I would like to express my sincere gratitude to my advisor Dr. Vicky van Santen for her guidance, encouragement and continuous support during my graduate studies. I am indeed thankful to Dr. Haroldo Toro for his support, valuable contributions and insightful comments provided during my research projects. I would like to gratefully acknowledge Dr. Kellye Joiner and Dr. Ruediger Hauck for their valuable contributions to my research. I would also like to thank Dr. Rodrigo Gallardo for being willing to read the draft of my dissertation and giving valuable feedback.

I am indebted to Fatma Eldemery, Natalia Petrenko, Stephen Gulley, Ramon Zegpi, Cassandra Kitchens, and Cynthia Hutchinson for their support and excellent technical assistance during my research work. I wish to express my appreciation to all people of the Department of Pathobiology for their support throughout my studies.

I would like to express my deepest gratitude to my friends and family, especially my mother-in-law, husband Mohammad Rezaul Huq, sweet daughter Rameesa, and lovely son Radman. This work would not have been possible without their love and incessant support.

Finally, I wish to express my appreciation and sincere thanks for the financial support received from Auburn University.

TABLE OF CONTENTS

Abstract ii

Acknowledgments vi

List of Tables x

List of Figures xi

List of Abbreviations xiii

CHAPTER 1: Literature Review 1

1. Avian Infectious Bronchitis 1

1.1. Economic Losses Associated with IB 1

1.2. Transmission 2

1.3. Pathogenesis, Clinical Signs, and Symptoms 2

1.4. Morbidity and Mortality 3

1.5. Control Measures for IBV 4

2. Infectious Bronchitis Virus (IBV) 5

2.1. IBV Genome 5

2.2. The Spike (S) Protein 6

2.2.1. Genetic Diversity Based on S Protein Variability 7

2.2.2. S Protein in Viral Attachment and Cellular Entry 8

2.2.2.1. IBV Receptor 9

2.2.2.2. Receptor Binding Domain (s) (RBD) of IBV S Protein 10

2.2.3 Role of S Protein in Host Tropism and Pathogenesis 11

2.2.3.1. Role of S Protein in Host Tropism 11

2.2.3.2. Role of Other Viral Protein in Pathogenesis and Tropism 13

2.2.3.3. Role of S Protein in Unusual/Enteric Tropism 14

3. ArkDPI IBV Vaccines 16

3.1. Problems Associated with ArkDPI IBV Vaccines 16

3.2. Effects of Adaptation of ArkDPI IBV Vaccine to Embryonic Kidney Cells 17

4. Immune Responses 18

4.1. Nature of Immune Responses against IBV 18

4.2. Effects of Vaccination Age in Inducing Immune Responses in Chickens against IBV 19

4.3. Role of S Protein Differences in Escaping Vaccine Induced Immune Responses 21

Research Objectives 23

CHAPTER 2: Changes in Avian Infectious Bronchitis Virus Spike Protein Associated with Adaptation to Chicken Embryonic Kidney Cells do not Improve Binding 24

Summary 24

Introduction 25

Materials and Methods 27

Results 30

Discussion 33

CHAPTER 3: Replication Dynamics of CEK Cell-Adapted ArkDPI-Derived Infectious Bronchitis Vaccine in Chickens 38

Summary 38

Introduction 39

Materials and Methods 41

Results 45

Discussion 48

CHAPTER 4: Intestinal Tropism of an IBV Isolate is not Explained by Spike Protein Binding Specificity *Avian Diseases (Submitted 2019)* 56
Summary 57

Introduction 58

Materials and Methods 62

Results 65

Discussion 72

CHAPTER 5: Early Vaccination of Chicken Induces Suboptimal Immunity against Infectious Bronchitis Virus *Avian Diseases (63:38-47, 2019)* 89
Summary 90

Introduction 91

Materials and Methods 92

Results 96

Discussion 102

CHAPTER 6: Role of Changes in S Protein of IBV Field Isolate in Escaping Vaccine-Induced Immune Responses 120
Summary 120

Introduction 121

Materials and Methods 123

Results 125

Discussion 127

CHAPTER 7: Conclusions 130

References 133

LIST OF TABLES

Table 3.1. Selection of vaccine subpopulations in chickens.....55

Table S5.1. Correlations between antibodies against IBV and S1 and between IgA in tears and antibodies in sera.....119

LIST OF FIGURES

Figure 2.1. Binding of IBV Ark-type recombinant spike proteins to CEK cells 35

Figure 2.2. Effects of each of the three amino acid changes in S protein associated with adaption determined by spike histochemistry.....37

Figure 3.1. Protein histochemistry demonstrating recombinant S1 proteins representing vaccine strain and CEK-adapted strain binding to chicken tissues.....51

Figure 3.2. Protein histochemistry comparing binding of recombinant trimeric S-ectodomain protein representing the major population of a commercial ArkDPI vaccine strain and CEK-adapted ArkDPI vaccine strain to relevant chicken tissues 53

Figure 3.3. Relative vaccine virus RNA levels in (A) tears, (B) choanal swabs, and (C) tracheal swabs at different days post vaccination with CEK-adapted or commercial ArkDPI vaccine 54

Figure 4.1. Comparison of amino acid sequences and predicted structures of IBV CalEnt and Cal99 S1 proteins.....78

Figure 4.2. Protein histochemistry demonstrating recombinant S1 proteins of IBV Cal99 and CalEnt variants binding to chicken tissues. 81

Figure 4.3. Protein histochemistry demonstrating recombinant S1-NTD of IBV Cal99 and CalEnt variants binding to chicken tissues. 83

Figure 4.4. Protein histochemistry demonstrating recombinant S-ectodomain protein of IBV CalEnt variant binding to cloaca.....84

Figure 4.5. RDP analysis showing recombination between Malaysian IBV isolate IBS180/2015 (Genbank accession #KU949747; major parent) and Cal99 (minor parent) producing the CalEnt S gene.....85

Figure 4.6. Comparison of amino acid sequences of IBV CalEnt and Malaysian isolate IBS180/2015 S2 (GenBank accession number KU949747) proteins. 86

Figure 4.7. Unique aa sequence present in CalEnt S2 near putative S2' cleavage site.....87

Figure 5.1. IBV antibodies after vaccination (n=15/group) determined by a commercial ELISA (individual values, mean, and SEM).....107

Figure 5.2. IBV antibody levels (n=15/group) after vaccination determined by ELISA using Ark-serotype S1 recombinant protein bound to the wells. 109

Figure 5.3. IBV IgA levels (n=15/group) after vaccination determined by ELISA using plates of commercial origin (individual values, mean, and SEM).....110

Figure 5.4. IBV IgA levels (n=15/group) after vaccination determined by ELISA using recombinant Ark-serotype S1 protein bound to wells (individual values, mean, and SEM).....112

Figure 5.5. Correlations of IBV-specific and S1-specific antibody levels in sera and tears of individual chickens (n=15) vaccinated at 28 days of age. 114

Figure 5.6. $CD4^+$ lymphocytes in HG of chickens 3 weeks after boosting of chickens primed at different ages. 115

Figure 5.7. Linear regression analysis of $CD8^+$ and $CD4^+CD8^+$ cells in CT and spleen of chickens at different ages.....117

Figure 5.8. $CD4^+$ lymphocytes in peripheral blood (n=6 chickens/group) determined by flow cytometry 18 days after prime IBV vaccination (A) and 12 days after booster IBV vaccination (B), and B lymphocytes in CT determined by flow cytometry 18 days after booster IBV vaccination (C) in chickens primed on days 1, 7, 14, or 21 days of age.....118

Figure 6.1. ELISA demonstrating S1- and S-ectodomain-specific IgA antibodies in tears and antibodies in plasma of ArkDPI-vaccinated chickens. 128

LIST OF ABBREVIATIONS

aa	Amino acid
AEC	3-amino-9-ethyl-carbazole
ANOVA	Analysis of variance
Ark	Arkansas
ArkDPI	Arkansas Delmarva Poultry Industry
BLAST	Basic local alignment search tool
Cal 99	California variant 1999
CalEnt	California enteric variant
CAM	Chorioallantoic membrane
CT	Cecal tonsils
CD	Cluster of differentiation
CALT	Conjunctiva associated lymphoid tissue
CTD	C-terminal domain
DOA	Day of age
DPI	Days post inoculation
DPC	Days post-challenge
EID_{50}	50% embryo infectious doses
EM	Electron microscopy
ELISA	Enzyme-linked immunosorbent assay

FITC	Fluorescein isothiocyanate
HEK293T	Human embryonic kidney 293T cells
HRP	Horseradish peroxidase
HG	Harderian gland
IB	Infectious bronchitis
IBV	Infectious bronchitis virus
IgA	Class A immunoglobulin
IgG	Class G immunoglobulin
M41	Massachusetts IBV strain 41
NCBI	National Center for Biotechnology Information
NTD	N-terminal domain
PBMC	Peripheral blood mononuclear cells
qRT-PCR	Quantitative reverse transcriptase polymerase chain reaction
RDP4	Recombination detection program 4
S/P	Sample/positive ratio
S	Spike protein
S1	Spike S1 subunit
S2	Spike S2 subunit
SD	Sub-domain
SPF	Specific-pathogen-free
V	Vaccine major population

CHAPTER 1

Literature Review

1. Avian Infectious Bronchitis

Avian infectious bronchitis (IB) is a viral disease endemic in poultry caused by infectious bronchitis virus (IBV), a *Gammacoronavirus*. The virus is a highly contagious/infectious pathogen that is transmitted by aerosol and replicates mostly in the respiratory tract. IBV can also replicate in the reproductive and enteric tracts, and in the kidneys, depending on the pathogenesis/virulence of the virus strains. It causes reduced and delayed weight gain in broilers and decreased egg production and eggshell malformation in layers and breeders. In addition, the virus may lead to condemnations at processing plants from air-sacculitis due to secondary bacterial infections (1).

1.1. Economic Losses Associated with IB

The World Organization for Animal Health considers IBV an economically important pathogen, affecting performance in all branches of the poultry industry including both meat-type and egg-laying birds in commercial production as well as back yard chickens (1, 2). IBV in the United Kingdom alone has cost over £23 million per year (3). However, the actual costs are difficult to estimate since the losses are not limited to the costs from impaired growth, reduced egg production, and quality due to IBV infection, but are also from the cost of vaccines and vaccination, mortality, and several other additional factors including diagnosis, implementation of specific bio-security conditions, and treatment of secondary bacterial infection. Besides these,

losses due to condemnation of birds in processing plants are also included in the economic burden on the poultry industry (4).

1.2. Transmission

IBV is highly contagious and spreads in all birds in an infected flock within a short period of time. One mode of transmission of the virus is by air-borne route via aerosol or by direct contact from the respiratory contents of infected birds. Mechanical transmission from fomites such as contaminated feed and drinking water, equipment, eggs, working personnel and trucks is also frequent. In addition, the virus can spread via the feces of infected birds, as virus is shed in the feces for several weeks or months (2, 4, 5), and can persist in the litter containing feces for longer periods as well.

1.3. Pathogenesis, Clinical Signs, and Symptoms

Chickens of all ages and breeds are susceptible to IBV, while young chicks are the most severely affected (6). The virus primarily infects and replicates in the epithelium of the upper and lower respiratory tract, usually restricted to the ciliated and mucus-secreting cells including those in the conjunctiva, Harderian gland (7, 8) nasal turbinates, trachea, lungs, and air sacs. Clinical signs vary with age and immune status of the chickens, virulence of IBV strains, and concurrent secondary bacterial infection. Typical clinical signs include common cold-like symptoms with nasal discharge, watery eyes, snicking (like sneezing), coughing, tracheal rales, gasping and lethargy (9, 10). These symptoms usually start 18-24 hours after infection and may last up to 2-3 weeks. Severity and disease outcome vary, ranging from mild respiratory symptoms to severe kidney and oviduct disease (11) depending on the virus strain and the system involved in the

infection, as well, since the virus can also replicate in the urogenital tract (11, 12, 13). Nephropathogenic IBV spreads to the epithelium of renal tubules and produces severe nephritis with tubular necrosis and kidney damage that can lead to death of the chicken (4, 14, 15, 16).

In addition, IBV can infect the ciliated epithelium of the oviduct and cause necrosis and malformation resulting in severe damage in laying hens with decreased or/and permanent loss of production and poor egg quality (9, 11, 12). Moreover, IBV has been also shown to replicate in many parts of the digestive system including esophagus, proventriculus, duodenum, jejunum, bursa of Fabricius, cecal tonsils, rectum, and cloaca, without resulting in significant clinical gastrointestinal disease (9, 13, 17, 18). However, the outcomes of infection depend on several other factors such as age, breed and immune status of chickens, co-infection with immunosuppressive viruses such as Marek's disease virus, infectious bursal disease virus (IBDV), and other environmental conditions, including overcrowding, dust, inadequate ventilation, and presence of ammonia (4, 19, 20, 21, 22).

1.4. Morbidity and Mortality

In broiler flocks, the morbidity rate can reach 100%, whereas mortality is usually low. Mortality may range from 25 to 30% in young chicks but may increase up to 80%, mostly due to mixed infections with other bacterial agents such as *Mycoplasma sp*. or *Escherichia coli* or co-infection with immunosuppressive viruses such as Marek's disease virus and infectious bursal disease virus (23). In younger chicks, nephropathogenic IB strains usually cause high mortality reaching up to 25% (24, 25). However, in experimental conditions, up to 96% mortality was observed following nephropathogenic IBV inoculation in two week-old chicks (26).

1.5 Control Measures for IBV

It is very difficult to control IBV, as several factors are involved. Strict biosecurity with "All-in/All-out" flock management under strict sanitation protocols is essential for the prevention of IBV (23). Since the virus is highly contagious and transmitted by the air-borne route, it is very critical to maintain strict biosecurity.

Besides biosecurity, vaccination is the only measure currently used to control IBV infection. There are numerous serotypes of IBV circulating worldwide, which do not cross protect, and multiple serotypes may be present simultaneously in the same region (11). Moreover, high mutation rate, and genome recombination of IBV results in extensive genetic diversity with frequent emergence of new strains (27). Both live attenuated and inactivated vaccines containing single or multiple serotype(s) are currently used for immunization of chickens against IBV. For attenuation, field strains are serially passaged (generally 75 passages or more) in embryonated eggs (28, 29). Other vaccines such as subunit vaccines using recombinant S protein (30) or vector vaccines expressing S protein of IBV [e.g. fowl adenovirus or Newcastle disease virus vectors (31, 32, 33)] that might have potential success in producing effective immune responses in chickens are under investigation.

Live attenuated vaccines with mild virulence are usually applied via drinking water or by coarse spray to meat-type chickens at one-day of age in the hatchery for managerial convenience and cost reduction. For booster vaccination, more virulent vaccines are given at approximately seven to ten days of age, usually via drinking water or spray. Booster vaccination is particularly practiced in broilers in areas with a high density of farms. In commercial egg layers and breeders, pullets are usually vaccinated with killed inactivated vaccine by subcutaneous injection at thirteen to eighteen weeks of age, after priming with live attenuated vaccines (25). Live attenuated vaccines

induce greater immune responses, especially cell-mediated immune responses, over killed vaccines. However, the greatest drawback for using live vaccines is that there is always the possibility of reversion to virulence (34, 35) and/or persistence in chickens, which increases the chances of emergence of new strains via immune selection and/or recombination between vaccine strains and virulent field strains (36, 37, 38, 39, 40, 41).

2. Infectious Bronchitis Virus

IBV was first reported as a respiratory pathogen infecting chickens in North Dakota, USA in the late 1930s by Schalk and Hawn (42). The virus is the prototype species of the Coronavirus family. Coronaviruses (CoVs) (order *Nidovirales*, family *Coronaviridae*, and subfamily Orthocoronavirinae) are a group of enveloped viruses that primarily infect the respiratory and gastrointestinal tract of a wide range of birds and animal species including humans. They possess four antigenically and phylogenetically related groups which belong to four genera *Alpha-, Beta-, Gamma-,* and *Delta coronavirus (α-, β-, γ- and δ-CoV)* (43); International Committee on the Taxonomy of Viruses, 2011). *Alpha-* and *Beta-coronavirus* genera comprise mostly mammalian coronaviruses while avian coronaviruses are included in *Gamma* and *Delta*-coronavirus genera. IBV belongs to the *Gamma-coronavirus* genus and mostly infects chickens (*Gallus Gallus*).

2.1. IBV Genome

IBV has a non-segmented, single-stranded, positive-sense RNA genome of ~27-kb, which is 5′-capped and 3′-polyadenylated. It encodes four structural proteins in the 3′ one-third of the viral genome, including the phosphorylated nucleocapsid protein (N), which surrounds the viral genome, and three envelope glycoproteins: spike glycoprotein (S); membrane glycoprotein (M)

and small envelope protein (E) (43, 44, 45). The viral genome also encodes fifteen non-structural proteins (NSP2-NSP16) within open reading frame (ORF) 1ab (in the 5` two-thirds of the viral genome), which function in RNA replication and transcription. There are four accessory genes: 3a, 3b, 5a, and 5b that are interspersed among the structural genes (46). The functions of these accessory genes have not been defined, although they were shown to be unessential for IBV replication in vitro (47, 48).

2.2. The Spike (S) Protein

The coronavirus spike (S) protein assembles into trimers on the envelope surrounding the virus particle to form club-shaped 16-21 nm protrusions that make the crown-like appearance when visualized by electron microscopy (46). The protein is a highly-glycosylated class I viral fusion protein (49). S is the largest structural protein encoded by the coronavirus genome. The IBV S protein is post-translationally cleaved into two subunits: the amino (N)-terminal S1 of approximately 520 amino acids and the carboxy (C)-terminal S2 subunit of about 620 amino acids, while the S proteins of some other coronaviruses are not cleaved into subunits although they contain S1 and S2 domains. (43, 50, 51). The S1 subunit or domain possesses two sub-domains, the N-terminal domain (S1-NTD) and C-terminal domain (S1-CTD). The S2 subunits or domains of coronavirus S proteins include an ectodomain, transmembrane domain, and C-terminal cytoplasmic tail domain, and anchor the S protein to the viral envelope. The S2 ectodomain has an internal fusion peptide-like region (FP) associated with two hydrophobic heptad repeat (HR) regions: the N-terminal longer HR1 and the C-terminal shorter HR2 region that is adjacent to the transmembrane region (52).

2.2.1. Genetic Diversity Based on S Protein Variability

The S protein is the most divergent among all proteins encoded by IBV, particularly the S1 subunit, where as little as 45% amino acids identity is observed between different IBV S1 amino acid sequences in GenBank. Most variations are located within the beginning of S1 amino acid sequence, particularly in the approximately 300 residues of its NTD. Although the S2 subunit is more conserved, it is also quite variable, with some IBV S2 aa sequences in GenBank having as little as 64% amino acid identity with each other. High sequence diversity of the S1 accounts for serotypic and genotypic variations of IBV and immunologic escape from vaccine-induced immune responses (53).

A wide range of antigenically and genetically distinct IBV types are distributed worldwide. Serotypes of IBV are determined based on the antigenic variability of the S protein, particularly in the serotype-specific sequences/variation of the S1 subunit (54). Using monoclonal antibody virus neutralization assays five neutralizing antigenic sites/epitopes were detected on S1 that are located within three different hypervariable regions (HVRs) (aa 38–67, 91–141 and 274–387), particularly in the first and third quarters of the S1 subunit (54, 55, 56, 57, 58), indicating that HVRs are associated with the antigenicity and hence, serotype variations. The most common serotype of IBV reported in the poultry industry worldwide is Massachusetts (Mass), while Arkansas (Ark) is the most frequently isolated IBV in the southeastern United States (1). Following Ark-type, Connecticut, Massachusetts, Georgia variants, and California variants are the most prevalent in United States (1, 59).

Differences in partial or complete S1 gene nucleotide sequences have traditionally been used for genotyping of IBV (OIE, 2013). Genotypic variation is thought to be the result of the accumulated mutations in S gene caused by error-prone, viral RNA-dependent-RNA polymerase and by

recombination events between two different strains of IBV during virus replication in the same host cell (36, 60, 61). Mutations caused by nucleotide substitutions, insertions and deletions as well as recombination events along with selection pressure and high viral subpopulation diversity (1) may result in emergence of new IBV serotypes and genotypes. It is likely that only a few amino acid changes in the S1 protein could result in emerging strains, while the other major portion of the virus genome remained unaltered (37, 54). In fact, the presence of mixtures of subpopulations (possessing amino acid differences in S1 protein) within an isolate or a vaccine strain that can be acted by selection pressure upon vaccination/infection of chickens is frequent in IBV (38, 57, 62, 63, 64, 65, 66). Indeed, selection of subpopulations and persistence of viruses similar to virulent parental strains (based on the identity of S1 gene sequences) were observed in chickens vaccinated with commercial ArkDPI-derived vaccines (36, 38, 64).

2.2.2. S Protein in Viral Attachment and Cellular Entry

Coronavirus S proteins are responsible for both virus attachment (binding to target cell receptors) and subsequent entry into host cells. The S1 subunit or domain mediates viral attachment to host receptors. The membrane-anchoring S2 subunit or domain mediates the fusion of the virion with the host membranes for subsequent release of virus RNA into the cytoplasm [reviewed in (67)]. The IBV S protein undergoes proteolytic cleavage at a site within S2 known as S2’ by an unidentified host serine protease (68). Following cleavage at the S2’ site, exposure of the FP and major conformational changes of S2 lead to insertion of the S2 FP into the host membrane, fusion of the viral envelope with host membranes, and viral entry (68, 69). Although the S2 domain is not principally involved in binding to a host cell receptor, the interaction between

S1 and S2 might be involved in conformational changes of the S protein that synergistically affect the avidity and specificity of virus attachment (30, 70).

2.2.2.1. IBV Receptor

Functional receptors, which mediate both attachment and entry, for some human and animal coronavirus that have been identified, and most of them are membrane proteins or glycoproteins that interact with the S protein (71). Relatively little information about IBV attachment and entry has been obtained. Several studies on IBV attachment and entry utilized the highly attenuated, embryo-adapted IBV Beaudette laboratory strain and mammalian cell lines, as the attenuated lab strain was adapted to replicate in established cell lines (68, 72, 73, 74). Several other studies (73, 75) have shown that α2,3-linked sialic acid present on cell membrane proteins plays a crucial role in IBV infection. Removal of α2,3-linked sialic acid or genetic blockage of its cell-surface expression prevented infection by all IBV isolates examined. Wickramasinghe *et al.*, have demonstrated sialic acid-dependent binding of recombinant S1 protein to respiratory epithelial cells in fixed chicken tissues (76).

Sialic acid has been designated a "receptor determinant" for IBV, as binding of IBV S1 to sialic acid is weak compared to other solely sialic-acid-carbohydrate-receptor-utilizing viruses such as influenza viruses (76). Furthermore, IBV differs from other viruses that solely use a carbohydrate receptor in that it does not possess a receptor destroying enzyme like influenza viruses and bovine coronavirus. By using a glycan array, it was demonstrated that IBV S1 binds to only a specific type of α-2, 3-linked sialic acid, whereas, influenza virus uses any α-2, 3-linked sialic acid on the host cell (76). Thus, additional host receptors, either protein or carbohydrate, might be involved in binding with the IBV S1 protein.

The possibility of utilizing a protein co-receptor was hypothesized by Li, based on the available crystal structures of S proteins of coronaviruses (71, 77). He noted that the N-terminal domain (NTD) or C-terminal domain (CTD) of S1, either alone or together, can function as the receptor binding domain(s) [RBD(s)] for different coronaviruses, interacting with sugar and/or protein receptors. Li proposed that all coronaviruses have two potential RBDs through which the S protein interacts with host receptors. The N-terminal carbohydrate-binding domain of S1, structurally conserved among coronaviruses, is observed to be present by default. Usually the C-terminal domain of S1, of variable structure among coronaviruses, interacts with protein receptors on host cells. Thus, Li suggested that the IBV S1-CTD interacts with a host protein co-receptor that remains to be elucidated.

2.2.2.2. Receptor Binding Domain (s) (RBD) of IBV S Protein

Coronavirus S1 subunits or domains include the receptor binding domain(s) (RBDs). For IBV, both the S1-NTD and S1-CTD have been implicated in receptor binding. Promkuntod *et al.* (78) demonstrated that the N-terminal domain with 253 amino acid residues of IBV Massachusetts strain (M41) S1 is necessary and sufficient for binding to α-2,3 linked sialic acids located on the epithelium of formalin-fixed chicken respiratory tract. Shang *et al.* (52) have provided evidence that the IBV S1-CTD also possesses receptor-binding activity for an unknown protein co-receptor. They determined the structure of spike ectodomain of IBV M41, where the core structure of the S1-CTD contains two extended loops that might serve as receptor binding motifs (RBMs). Using two different approaches: flow cytometry live cell binding assay with recombinant IBV S1-CTD and IBV-spike-mediated pseudovirus entry assay in the presence of competing recombinant IBV

S1-CTD, they demonstrated that the IBV S1-CTD has an RBD that interacts with yet to be identified receptor.

2.2.3. Role of S Protein in Host Tropism and Pathogenesis

The S protein is the major determinant of the species, tissue and cell tropism of coronaviruses, including IBV, and thus has a great influence on viral pathogenesis. By using targeted RNA recombination to introduce the S gene from a highly pathogenic strain into the genome of a less neuro-pathogenic murine coronavirus strain, Phillips *et al.*, demonstrated that switching the S protein altered the pathogenicity of the mutant strain similar to the virulent strain in the murine nervous system, indicating that S is the major determinant of coronavirus pathogenesis (79). For IBV, it has been reported that recombination resulting in the replacement of the entire S gene of IBV may have been responsible for the emergence of a new coronavirus, completely changing the host pathogenicity (respiratory to enteric) and host specificity (chicken to turkey) as well (80). In addition, increased virulence of IBV vaccine strains in Ark-type vaccinated chickens associated with differences in the S gene of IBV also reinforces the role of the S protein in pathogenesis (38, 81).

2.2.3.1 Role of S Protein in Host Tropism

Alterations of the S gene sequences of IBV have been shown to be associated with tissue/cell tropism. As for example, Beaudette is the extensively passaged embryo-attenuated Massachusetts-derived strain that has acquired an extended host tropism with the ability to replicate in non-chicken cell lines, including the mammalian cell lines Vero cells and baby hamster kidney cells (BHK-21) (82, 83). However, exchange of the spike gene of a closely related

Massachusetts strain, M41 [3.7% amino acids difference (84)] in the recombinant Beaudette viral genome altered the tropism of the recombinant virus and abolished the broader tropism of the strain, indicating the involvement of differences in the S protein in cell tropism (85).

The role of differences in both the S1 and S2 portions of the S protein in determining tissue and/or species specificity for various coronaviruses, including IBV, has been reported extensively (86). The S1 portion of S affects tropism at the level of virus attachment. Work with the porcine coronavirus transmissible gastroenteritis virus (TGEV) provided an early example that a very few changes in the S1 portion of a coronavirus S protein can alter tropism. This coronavirus lost its enteric tropism and shifted to respiratory tropism after two amino acid changes in the S1 portion of the spike protein (87). Another example is the S1 protein of severe acute respiratory syndromes (SARS) virus, where only two amino acids changes altered the host tropism from palm civet cat to human as well as pathogenicity from asymptomatic to highly severe respiratory syndromes (88). In IBV, two amino acid changes in the S1 protein might be involved in the adaptation of ArkDPI derived attenuated vaccines to chicken embryonic kidney (CEK) cells, i.e. a new host (89).

Recombinant S1 protein of the Beaudette strain IBV is not sufficient for binding to cells in which the virus can replicate, i.e. chicken CAM or mammalian cultured cells, but addition of the Beaudette S2 ectodomain, to generate Beaudette S-ectodomain, enables binding to both types of cells (70). Furthermore, extension of an ArkDPI-type S1 to generate ArkDPI S-ectodomain greatly improves binding to epithelium of relevant chicken tissues (nasal mucosa, trachea, choana, cecal tonsil, cloaca) and allows binding to epithelial cells in additional tissues (lung and kidney) (30). These observations suggest that the interplay between S1 and S2 might synergistically determine the avidity of virus attachment and functions in its tropism, although S2 does not have any receptor binding domain.

S2 can affect tropism at the level of viral entry by its ability to be cleaved by host cell proteases at a site known as S2' to expose its FP (90). The extended host tropism of the IBV Beaudette strain, which has acquired the ability to replicate in mammalian cell lines, has recently been mapped to the S2' recognition site of S2 (85, 91).

2.2.3.2. Role of Other Viral Proteins in Pathogenesis and Tropism

Although the roles of S protein in cell tropism as well as in pathogenesis are well established, accumulating evidence suggests that the genes outside the S gene, particularly in NSP-coding regions might also contribute to pathogenicity of various coronaviruses including IBV (92, 93). Replacement of the spike protein gene in the genome of the apathogenic Beaudette strain by those of virulent M41 or 4/91 IBV resulted in still apathogenic recombinant viruses, indicating that genes in addition to S contribute to pathogenicity (94, 95). Further work with a recombinant virus containing only the NSP-coding genes of the apathogenic strain and rest of the genome from a virulent strain indicated that virulence was affected by the NSP genes (96). Complete genome sequencing of virulent (passage 11) and embryo-attenuated (passage 101) ArkDPI viruses (99.92% similar in their nucleotide sequences) showed three nonsynonymous substitutions, one in NSP 2- and two in the NSP 3-coding regions, besides the changes in S gene of the attenuated strain. This finding indicated that the changes in NSP2 and NSP 3 gene might be involved in attenuation, hence, in altered pathogenicity (97). Furthermore, next generation sequencing of the whole genome showed that an Ark vaccine variant adapted to chicken embryo kidney (CEK) cell culture accumulated changes in the NSP2- and NSP3-coding regions along with the S gene (see below), supporting a possible role for these genes in tropism (89). Although the function of IBV NSP2a is

not known yet, its lack of sequence and structural similarity with other proteins suggested its involvement in host specificity (98, 99).

2.2.3.3. Role of S Protein in Unusual Enteric Tropism

Runting-stunting syndrome (RSS)/malabsorption syndrome is a transmissible enteric disease characterized by diarrhea, impaired growth and poor feed conversion in growing chickens, most commonly in broiler breeds. The etiology of RSS is apparently multifactorial since the identical disease syndrome could not be reproduced under experimental condition using a single agent isolated from the infected chickens (100). Several different viral agents, for example parvoviruses (101, 102), calicivirus (103), rotavirus (104), astrovirus (105, 106), reovirus (107), and birnavirus (108), along with bacterial pathogens, have been reported to be associated with RSS. RSS linked to avian infectious bronchitis virus (IBV) was also documented in a flock of 60,000 14-day-old brown broiler chicks in California during 2012, in which the infected chickens exhibited lethargy, poor growth, and pale and distended small intestines with watery contents, as well as cystic enteritis (13). Due to its association with enteric symptoms, the IBV isolate obtained from this California flock was given the name "CalEnt."

As mentioned earlier, IBV can replicate in many parts of the alimentary tract, including proventriculus, duodenum, jejunum, cecal tonsils, and cloaca, although the infection of enteric tissues very rarely causes any pathology or clinical symptoms (reviewed by (9)). IBV has been isolated from small and large intestines of both naturally-infected and experimentally-inoculated chickens having typical respiratory symptoms but no enteritis (109, 110, 111). Occasionally lesions were observed in the rectum of experimentally infected chickens, but not in other parts of the intestines (24). However, observations in chickens of the flock affected by the California

enteric variant ("CalEnt") revealed an unusual enteric tropism of the virus with gross lesions in the intestines along with other clinical signs as seen in the reported cases of RSS (13). In addition, immunohistochemistry (IHC) of tissues of affected birds showed the presence of IBV antigen throughout the intestine located in the cytoplasm of enterocytes. However, no IBV antigen was detected in respiratory tissues tested (trachea, lung), indicating altered tropism for this enteric variant. Furthermore, during virus isolation from intestinal samples in embryos, IBV could not be detected in chorioallantoic membrane or allantoic fluid using fluorescently labeled antibody, electron microscopy (EM), or RT-PCR. In contrast, IBV was detected by EM and RT-PCR in the embryo's intestine and was recovered from this tissue (13). Following oculonasal inoculation of CalEnt into SPF chickens, IBV antigen and RNA was detected in the intestine and histopathologic lesions of the intestine were reproduced. Consistent with observations of others regarding experimental infection with enteric-origin IBVs, mild respiratory signs and lesions were also observed. IBV antigen was detected in conjunctiva, sinus/turbinate, and trachea, and IBV RNA was present in tears and trachea. According to these observations, it was suggested that the CalEnt variant had acquired extended tropism to enteric tissue while also retaining its original respiratory tropism.

Sequence analysis of the S1 gene of the CalEnt variant isolate along with other available S1 gene sequences in GenBank revealed that the virus was distantly related to most of the IBV genotypes. Although no insertions or deletions in the S1 gene of this CalEnt variant were found in comparison to closely related IBV types, the closest relative, IBV respiratory variant California 99 (Cal 99) showed only 94% S1 nucleotide sequence identity (13). Whether the differences in the S protein of the enteric IBV variant associated with RSS are responsible for its broadened tropism, due to an increased ability of its S1 protein to bind to intestinal epithelial cells, should be addressed.

3. ArkDPI IBV Vaccines

Arkansas (Ark)-type IBV is the most common serotype circulating in the intensive broiler-producing areas of the United States (27), and commercial ArkDPI-derived vaccines are extensively used. The ArkDPI strain of IBV was originally isolated from broiler chickens in the Delmarva Peninsula and partially attenuated at the University of Delaware by 50 passages in embryonated chicken eggs (28). It was then distributed to different vaccine companies and further attenuated by each company, resulting in four similar, but not identical, ArkDPI vaccines.

3.1. Problems Associated with ArkDPI IBV Vaccines

Despite the use of these ArkDPI-derived vaccines, increasing frequencies of Ark-type IBV isolations were reported (59, 62), and experimental and field trials have shown that ArkDPI vaccination does not provide adequate protection (112, 113). In addition, persistence of vaccine virus in vaccinated chickens was reported (112), and ArkDPI vaccine or vaccine-like virus recovered from vaccinated chickens shows certain sequence changes particularly in the S1-coding portion of the S gene (36, 37, 38, 64, 81, 114). The consistent demonstration of these nucleotide changes as early as three days after vaccination supports the concept that ArkDPI vaccines contain viral subpopulations that are selected during a single passage in chickens (36, 38, 64, 81, 114). Different patterns of genetic heterogeneity of S1-coding sequences were observed among the four commercial Ark-serotype vaccines derived from the same un-cloned attenuated ArkDPI field isolate (38). The heterogeneity of the S gene might serve as a source of vaccine-like Ark-virulent field strains or result in emergence of new variants following further replication and selection in chickens and/or recombination between other field strains and positively selected populations of vaccine strains.

ArkDPI-derived vaccines were shown to cause respiratory signs and tracheal damage in experimentally inoculated chicks (81). Vaccine viral loads, incidence of respiratory signs early after vaccination, and severity of tracheal lesions was higher in chickens vaccinated with ArkDPI vaccines containing higher proportions of vaccine subpopulations selected in chickens, suggesting that these vaccine subpopulations are responsible for the tracheal damage and respiratory signs observed.

3.2. Effects of Adaptation of IBV Arkansas Attenuated Vaccine to Embryonic Kidney Cells

Ghetas, *et al.* (89) adapted a commercial ArkDPI vaccine strain to primary CEK cells by serial passage. After seven passages, S gene sequencing revealed two amino acid changes (amino acid positions 163 and 323) in the encoded S1 protein and one amino acid change (amino acid position 889) in the S2 protein encoded. These three changes might affect S protein binding to CEK cells and contribute to adaptation. One difference in S1 (amino acid 163) was in the N-terminal domain, which is sufficient for sialic-acid-dependent binding to tracheal epithelium in protein histochemistry assays (78). The other difference in S1, amino acid 323, in the C-terminal domain, is at a position that differs in the predominant amino acid among the four commercial ArkDPI-derived vaccines (38). Deep sequencing confirmed these changes and provided information on changes in relative proportions of codons encoding different amino acids. In the commercial vaccine prior to passage in CEK cells, S1 amino acid 323 was 73% threonine and 26% arginine, whereas after adaptation it was 99.9% arginine. Deep sequencing also showed that vaccine subpopulations selected in chickens (sharing an alanine codon at S1 codon 213), comprising a total of up to 7% of the vaccine prior to adaptation, had been eliminated during adaptation to CEK culture. Absence of selection of these vaccine populations in chickens after

inoculation of the CEK-adapted vaccine confirmed their elimination. The changes in the S gene do not revert after five back-passages in embryonated eggs or after one passage in chickens (66, 89). The role of amino acid changes in the S protein in CEK-adaptation needs to be addressed.

Vaccination with the CEK-adapted ArkDPI vaccine virus protected chickens against Ark-type IBV virulent challenge, as indicated by reduced challenge viral loads and respiratory signs (66, 89). This indicated that the CEK-adapted virus is able to replicate well enough in chickens to induce protective immunity. Thus, CEK adaptation provides an opportunity to improve commercial ArkDPI-derived vaccines by eliminating vaccine subpopulations that are selected in and persist in chickens. However, the interaction of the CEK-cell-adapted Ark DPI-IBV vaccine strain and its spike proteins with chicken tissues and replication dynamics in different tissues have not been characterized yet.

4. Immune Responses

4. 1. Nature of Immune Responses against IBV

The immune response against IBV is very complex and is influenced by several factors including vaccine strains used, age and breed of the birds, and genetics of the infected chickens, including major histocompatibility complex (MHC) types. The MHC of chickens is the B complex, which includes three antigenic gene classes: MHC class I genes, (homologous to mammals' class I B-F), MHC class II genes, (homologous to mammals' class II B-L) and B-G genes, unique to birds (115). Along with other genes related to immunity, the chicken MHC consists of at least 46 genes, and plays important roles in the regulation of innate and adaptive immune responses and disease resistance (116, 117). MHC B haplotypes are implicated in effective immune responses and differential resistance to IBV infection (118, 119, 120, 121).

During the early stage of life chicks get protection by the passive transfer of maternal antibodies. In addition, in the early stages of the chicken life cycle, innate immunity is crucial for the control of IBV field infections. Receptors such as TLR3, TLR7, or MDA5 recognize IBV and initiate local immune responses in the trachea. The activated pattern recognition receptors then stimulate production of type I IFN and IL-1beta, pro-inflammatory cytokines. Increased production of cytokines may help to prevent viral replication and also aid induction of adaptive humoral immune responses (122, 123, 124).

IBV-induced humoral as well as cell-mediated responses are important in viral clearance and protection against challenge infection (10, 11, 125, 126, 127). A high level of systemic antibodies is correlated with virus clearance in the kidneys and genital tract, as well as with improved egg production and quality (128). IgA antibodies in tears are important in protecting mucosal surfaces from pathogens and IBV-specific lacrimal IgA has been reported to be associated with resistance to IBV inoculated ocularly (129). In addition, cytotoxic T lymphocytes (CTL) are important in controlling IBV infection. An increase in cytotoxic activity in splenocytes was observed to correlate with the reduction of viral loads in lungs and kidneys of IBV-infected chickens (125).

4.2. Effects of Vaccination Age in Inducing Effective Immune Responses in Chickens against IBV

Commercial chickens are routinely vaccinated at 1-day of age against IBV or even prior to hatch against other pathogens by in *ovo* vaccination. As mentioned earlier, despite extensive vaccination, IB outbreaks continue to occur mainly because of the changing nature of these viruses due to mutation and recombination, followed by selection (61). However, increasing evidence

suggests that the practice of IBV vaccination early after hatching in the poultry industry may not elicit optimal specific immunity and effectively protect the birds (22, 128). Innate immunity has also been found to be less developed in young chicks. Indeed, significantly lower levels of TLR7 expression in spleen and small intestine cells were observed in 1-day-old chicks compared to 4- to 5-week-old chickens. TLR21 and TLR15 also displayed reduced expression in the spleen, skin, lung and small intestine in 1-day-old birds (130). Thus, deficient TLR expression in young chicks might affect induction of IBV-specific immunity.

Both structural and functional maturation of mucosal associated lymphoid tissues are important for effectiveness of vaccines against respiratory viruses administered mucosally. For example, although random lymphocyte clusters in CALT have been noted at one week of age, germinal centers and plasma cells appear around 4 weeks after hatching. Increasing numbers of $CD4^+$ and $CD8^+$ T lymphocytes and B lymphocytes have been shown in the CALT by in situ immunohistochemistry as chicks developed from 1 to 4 weeks of age. In addition, the concentration of T-cells, particularly $CD4^+$ cells, in the Harderian gland (HG) is also increased in 4-week-old compared to 1-week-old chickens (131). IgA was undetectable and low levels of IgM were found during the first week after hatch indicating limited immune responses, in particular in the mucosal immune compartment (132). In addition, Lowenthal *et al*. showed that splenic T cells from 1-day old chicks produce some inhibitory factors that affect the proliferation of mature T cells and lead to transient T cell unresponsiveness to immune stimulation *in vitro* and at least a week was required to become fully responsive to that stimulation (133). The study also reported a 70-fold increase in T cell numbers in spleen, the major site of lymphopoiesis, in 1-week old birds compared to day 1 old birds.

Previous work also suggested that early vaccination might limit the immune repertoire and result in reduced mucosal and systemic immune responses. Indeed, chickens primed at day 1 of age showed lower IBV-specific IgA and IgG levels in both tear fluid and sera than birds vaccinated at days 7, 14, 21 or 28 of age (22). In addition, upon challenge with an IBV field strain, birds vaccinated later showed better protection against clinical signs and lesions compared to birds vaccinated immediately after hatch, indicating better protection as a result of vaccination at later ages (22). Thus, to get better insight into the importance of maturation of the chicken immune system for the optimum induction of IBV-specific immune responses, further studies should be done.

4.3. Role of S Protein Differences in Escaping Vaccine Induced Immune Responses

Because the S protein interacts with host receptors, it is the primary target for neutralizing antibodies (57). In addition, it also induces cell mediated immune responses (125). It was observed that immunization with recombinant S1 subunit of S protein protected chickens against challenge with the N1/62 nephropathic IBV strain (126). However, no protection was observed when recombinant nucleocapsid or matrix protein were used for immunization, indicating that S1 is important in inducing protective immune responses.

As stated earlier, S protein heterogeneity originates from nucleotide insertions, deletions, or point mutations and/or from genetic recombination events occurring during viral replication (134, 135, 136). Amino acid changes of as few as 2-3% in S1 (10-15 residues) can alter serotype, which suggests that a small number of immune-dominant epitopes on S1 are recognized by neutralizing antibodies (137)). Amino acids involved in virus neutralization are located within the first and third quarters of the S1 polypeptide, based on observations with the use of neutralizing

monoclonal antibodies and escape mutants (54, 56, 57, 138). When the amino acid sequences of the S1 proteins of seven Massachusetts serotype IBV strains were analyzed, two hyper-variable regions were identified in the region including amino acids 19-122, between residues 38-51 and 99-115 (138). The IBV host RBD of the M41 strain has been mapped to S1 amino acids 19-272 (the S1-NTD) (78). It is interesting that important hyper-variable regions are located in the RBD domain in the M41 S1 protein that mediates host attachment. Emerging strains that accumulate changes in the S1 protein could escape immunity induced by common vaccine types. As for example, an IBV isolated from a Mass serotype H120-vaccinated flock had 5 amino acid substitutions in its S1 aa sequence compared to H120, 4 in the S1-NTD. These changes presumably enabled the virus to successfully evade the Mass vaccine-induced immune response, indicating the important role of a small number of changes in the S protein in host immune escape (139). Interestingly, one of the aa changes was adjacent to an aa position shown to be part of a neutralizing epitope in another Mass-serotype IBV, M41 (138). The continued generation of new IBV variants in the field raises the important question of how mutations in S genes observed in IBV field isolates contribute to immune evasion by those field strains in vaccinated birds. How the IBV-ArkDPI vaccine-induced humoral immune response cross-reacts with Ark-serotype field isolates obtained from IBV-vaccinated broilers and how small amino acid differences in the S1 protein of field isolates might contribute to immune evasion are not understood. Much less information regarding neutralizing epitopes in Ark-serotype S1 proteins in available compared to neutralizing epitopes in Mass-serotype S1 proteins (55).

Research Objectives

1. Identify the basis of adaptation of Ark DPI-IBV vaccine virus to chicken embryonic kidney (CEK) cells, focusing on effects of the amino acid changes in S protein associated with CEK-adaptation on binding efficiency to CEK cells.
2. Characterize the interaction of the spike protein of a CEK-cell-adapted Ark DPI-IBV vaccine strain with chicken tissues *in vitro* and replication of the virus in chicken tissues *in vivo*.
3. Compare the binding to chicken respiratory and intestinal tissues of S1 spike protein of enteric-tropic IBV to that of respiratory-tropic IBV to observe whether the broadened tropism of the enteric IBV variant is due to an increased ability of its S1 protein to bind to intestinal epithelial cells.
4. Determine age-dependence of development of IBV-specific humoral and cell-mediated responses following IBV vaccination of chickens at different ages.
5. Explore the ability of a field isolate to escape IBV vaccine-induced immune protection.

CHAPTER 2

Changes in Avian Infectious Bronchitis Virus Spike Protein Associated with Adaptation to Chicken Embryonic Kidney Cells do not Improve Binding

SUMMARY. Avian coronavirus infectious bronchitis virus (IBV) is one of the most economically important pathogens of chickens. ArkDPI-derived IBV vaccines contain minor subpopulations that are rapidly selected in chickens, resulting in tracheal damage and persistence in chickens. These subpopulations, distinguished by their S1 gene sequences, were eliminated from a commercial ArkDPI-derived vaccine strain during serial passage in chicken embryonic kidney (CEK) cells. In addition, two amino acid changes in the S1 subunit and one in the S2 subunit were observed in the CEK-adapted vaccine strain. Because the S1 subunit of the IBV spike protein mediates viral attachment, we hypothesized that these alterations in the S protein of the CEK-adapted IBV allow the virus to attach more efficiently to CEK cells, thus contributing to adaptation. Trimeric, soluble, *Strep*-tagged recombinant proteins representing S1 and S-ectodomain (S1 plus the portion of the S2 subunit outside the viral envelope) proteins of the commercial ArkDPI vaccine strain and the CEK-adapted ArkDPI vaccine strain were produced in HEK293T cells and their binding to acetone-fixed CEK cells compared in protein histochemistry assays. We observed very little binding to CEK cells by the S1 protein representing the commercial vaccine and no binding by the S1 protein representing the CEK-adapted vaccine virus. The S-ectodomain protein of the commercial vaccine strain showed clear binding to CEK cells. However, contrary to the expected

improved binding to CEK cells, no binding of CEK-adapted S-ectodomain protein was observed. Notably, neither of the two mutations in CEK-adapted S1 alone or combined completely disrupted the binding of S-ectodomain protein to CEK cells, suggesting that the all changes in the S protein in combination affected the binding to CEK cells. Because changes in S protein associated with adaption to CEK cells abolished rather than improved binding to CEK cells, our results suggest that factors other than improved attachment to CEK cells were involved in adaptation of this strain to CEK cells.

1. INTRODUCTION

Avian coronavirus infectious bronchitis virus (IBV) is one of the most economically important respiratory pathogens in the poultry industry. The viral envelope is covered with the clove-shaped trimeric spike (S) protein, a highly-glycosylated class I viral fusion protein (49). The IBV S glycoprotein is cleaved into an amino (N)-terminal S1 subunit of approximately 520 amino acids and carboxy (C)-terminal S2 subunit of about 620 amino acids, which remain non-covalently associated (43, 50, 51). Coronavirus S proteins mediate viral attachment and entry into host cells. S1 subunits include the receptor binding domain(s) and the membrane-anchoring S2 subunits are involved in the fusion of the virion with host membranes [reviewed in (67)]. The role of S proteins in determining the tissue and species specificity and pathogenicity of several coronaviruses, including IBV, is well-documented (76, 85, 86, 90, 91, 140).

Live attenuated ArkDPI IBV vaccines are used extensively in United States. Changes in the ArkDPI genome were documented after 101 serial passages in embryonated eggs of the virulent ArkDPI strain to generate an attenuated vaccine strain. Differences were observed in only 21 nucleotides in the whole genome, resulting in 17 amino acid changes. Differences were

concentrated in the S gene (encoding 8 of 17 aa differences), mostly in the S1 part (97) indicating that changes in the S gene are associated with attenuation. However, commercial ArkDPI-derived vaccines contain minor subpopulations that are rapidly selected in vaccinated chickens, with S gene sequences similar to that of the original virulent ArkDPI strain (38, 64). These minor vaccine subpopulations are likely the cause of tracheal damage and vaccine virus persistence observed in ArkDPI-vaccinated chickens (81, 114). Vaccine subpopulations selected in chickens were eliminated from a commercial IBV-ArkDPI vaccine strain by 7 serial passages in chicken embryonic kidney (CEK) cells (89). During adaptation to CEK cells, two amino acid changes (amino acid positions 163 and 323) in the S1 protein and one amino acid change (amino acid position 889) in the S2 protein also occurred. Importantly, these three changes were all non-conservative changes and thus might affect S protein binding to CEK cells and contribute to adaptation. One difference in S1 was in the N-terminal domain (amino acid 163), which is sufficient for sialic-acid-dependent binding to tracheal epithelium in protein histochemistry assays (78). The other difference in S1, amino acid 323, in the C-terminal domain, is at a position that differs in the predominant amino acid among the four commercial ArkDPI-derived vaccines (38). We hypothesized that these alterations in the S gene of CEK-adapted ArkDPI vaccine strain contributed to adaptation by allowing the virus to attach more efficiently to CEK cells compared to the ArkDPI vaccine strain.

Wickramsinghe *et al*. developed and used an *in vitro* S1 protein histochemistry assay to show that recombinant S1 proteins representing the attenuated Mass serotype H120 vaccine strain bind to tracheal epithelium with lower affinity than recombinant S1 protein representing the virulent M41 strain (76). Thus, binding of recombinant S1 proteins *in vitro* can reflect effects of differences in S1 proteins on viral tropism and pathogenicity. In the case of ArkDPI-type IBV,

recombinant S1 protein representing an ArkDPI-derived IBV vaccine subpopulation that is selected in chickens binds to tracheal epithelium and other chicken tissues with greater affinity than S1 protein representing the negatively selected major vaccine population, consistent with an important role for differences in the S1 protein in selection of that vaccine subpopulation in chickens (141). Interestingly, the S1 protein of this selected vaccine subpopulation differs from that of the negatively-selected major vaccine population in only four amino acid positions (38). Thus the assay is able to detect binding differences resulting from only a few amino acid differences in S1. In addition, the S2 portion of the IBV S protein increases binding affinity in this assay (30, 70), suggesting that effects of differences in S2 that potentially affect virus attachment can be detected by the assay. We used spike protein histochemistry assays to address our hypothesis that the three changes in the S gene of CEK-adapted ArkDPI vaccine strain contributed to adaptation by allowing the virus to attach more efficiently to CEK cells compared to the ArkDPI vaccine strain.

2. MATERIALS AND METHODS

2.1. Spike protein expression plasmids

Expression constructs contained S1- or S-ectodomain-coding sequences flanked by sequences encoding an N-terminal CD5 signal sequence and sequences encoding a C-terminal artificial GCN4 trimerization motif and *Strep*-tag II for affinity purification and detection of recombinant proteins, as described (76). Codon-optimized sequences encoding IBV ArkDPI vaccine S1 (GenBank accession no. ABY66327) [amino acids (aa) 19-539], containing an upstream *Kpn*I and a downstream *Nhe*I restriction site, were obtained from GeneArt (Regensburg, Germany) and cloned into the pCD5 expression vector as previously described (76). To introduce

changes in S1 codon 163 (mutation no. 1) and codon 323 (mutation no. 2) of the codon-optimized vaccine S1 gene corresponding to the changes in CEK adapted S1 gene (89), site directed mutagenesis was performed by overlap extension polymerase chain reaction (PCR) (142) using the Phusion High-Fidelity PCR kit (Thermo Scientific, Waltham, MA, USA). Codon optimized CEK-adapted S1-coding sequences (aa 19-539), were then cloned into *Nhe*I and *Kpn*I-cleaved pCD5 vector.

Codon optimized sequences encoding the S2-ectodomain (aa 545-1098) of ArkDPI vaccine was also synthesized by GeneArt (Regensburg, Germany). *Kpn*I and *Nhe*I sites were added for cloning the S2-ectodomain-encoding sequences into the pCD5 vector already containing sequences encoding the S1 domain to produce constructs encoding S-ectodomain proteins as described (70). To avoid cleavage of the S-ectodomain at the S1/S2 border, sequences encoding the furin cleavage site RRSRR in S were replaced by sequences encoding a GGGVP linker (70). Codon 889 (encoding serine) of codon-optimized ArkDPI vaccine S2-coding sequences was changed to a phenylalanine codon (mutation no. 3), corresponding to the change in S2-coding sequences of the CEK-adapted vaccine virus (89) by site directed mutagenesis by overlap extension PCR. The resulting codon-optimized sequences encoding the CEK adapted vaccine S2-ectodomain were then cloned into the pCD5 vector already containing the coding sequences of the CEK-adapted vaccine S1 using *Kpn*I and *Nhe*I restriction cleavage sites. Expression plasmid constructs containing encoding S-ectodomain containing only one or two of the three amino acid changes found in CEK-adapted vaccine spike protein were also generated as described above. All expression constructs were sequenced to verify correct recombinant protein-coding sequences. The equivalent expression construct encoding the S-ectodomain of the ArkDPI vaccine subpopulation

previously designated C2, eliminated in the CEK-adapted vaccine strain (89), was previously described (30).

2.2. Recombinant S protein expression and purification

Soluble, trimeric *Strep*-tagged recombinant S1 and S-ectodomain proteins of parental ArkDPI vaccine and CEK-adapted vaccine strain were produced in human embryonic kidney (HEK) 293T cells as described (76, 140). In brief, 293T cells were transfected with one of the expression plasmids and cell culture supernatants were harvested at 6 days post transfection. The proteins were then purified using *Strep*-Tactin® Sepharose columns according to the manufacturer's protocols (IBA GmbH). The concentrations of purified proteins were determined by Qubit® 2.0 fluorometer (Invitrogen, Carlsbad, CA). The purified recombinant proteins were visualized by electrophoresis in Mini-PROTEAN®TGX Stain-FreeTM Precast Gels (Bio-Rad, Hercules, CA) and relative concentrations of purified proteins were determined.

2.3. CEK-cell culture and acetone fixation

Monolayers of primary CEK cells were prepared from 19-day-old specific pathogen free (SPF) chicken embryos as described (89). Cells were seeded in 8-chamber slides (Lab-Tek®II Chamber SlideTM, NuncTM, Rochester, NY), in minimal essential medium with 10% fetal bovine serum and 1% antibiotics and incubated at 37 C and 5% CO_2. Cells were fixed in cold acetone when they were ~80% confluent. The acetone-fixed slides were stored at -80 C until used for protein histochemistry.

2.4. Spike protein histochemistry

Acetone-fixed CEK cells on chamber slides were used for spike histochemistry as described (30), omitting the rehydration and antigen retrieval steps at the beginning of the procedure. Briefly, *Strep*-tagged recombinant S1 (100 μg/ml) or S-ectodomain (50 μg/ml, except as otherwise indicated) proteins pre-complexed with *Strep*-Tactin-HRP (IBA GmbH, Göttingen, Germany) were incubated with acetone-fixed CEK cells overnight at 4 C. Bound protein was visualized with chromogenic substrate 3-amino-9-ethyl-carbazole (AEC^+; Dako, Carpinteria, CA) and cells were counterstained with hematoxylin. Images were captured by an Aperio ScanScope CS slide scanner (Leica Biosystems, Buffalo Grove, IL) and visualized using Aperio ImageScope software v12 (Leica Biosystems, Buffalo Grove, IL).

2.5. Protein structure prediction and display

A three-dimensional structure homology model of the S protein of CEK-adapted vaccine strain based on the cryo-electron microscopy structure of trimeric IBV M41-S protein (52) was generated using the I-TASSER server (https://zhanglab.ccmb.med.umich.edu/I-TASSER/) (143, 144, 145). Visualization of the resulting model was performed with CueMol (Version 2.2.3.443, obtained at http://www.cuemol.org/en/).

3. RESULTS

3.1. Binding of S1 proteins to CEK cells

To compare the binding affinity of S1 proteins representing ArkDPI vaccine and CEK-adapted vaccine virus to CEK cells, protein histochemistry was performed. Recombinant S1

protein of the vaccine strain bound detectably to only a few CEK cells as shown in Fig. 1A. However, contrary to the expected improved binding, S1 protein of CEK-adapted vaccine strain exhibited no detectable binding to CEK cells (Fig. 1B), even with 4 times the standard protein concentration (not shown).

3.2. Improved binding after inclusion of S2-ectodomain

Based on the observation that the extension of S1 with the S2-ectodomain improved binding to chicken tissues in protein histochemistry assays (30), we determined whether using the S-ectodomain (containing both S1 and S2 domains, excluding the transmembrane domain and cytoplasmic tail) could improve the binding to CEK cells compared to S1 protein alone. Although S-ectodomain protein of the parental vaccine exhibited improved binding to CEK cells compared to S1 protein (Fig. 1C), binding of the S-ectodomain protein of the CEK-adapted vaccine strain was still undetectable (Fig. 1D). S-ectodomain representing the CEK-adapted vaccine virus showed binding only at higher concentrations (e.g. 3.5-times the concentration used in Fig.1C & Fig.1D) (Fig. 1E), indicating that the S protein of the CEK-adapted virus possesses very low binding affinity for CEK cells compared to the S protein of its parental vaccine strain.

3.3. Binding to CEK cells of S2-ectodomain of vaccine subpopulation eliminated by CEK-adaptation

CEK-adaptation resulted in elimination from the vaccine population of subpopulations selected in chickens (89). If this were due to negative selection in CEK cells, it would be expected that S proteins of these vaccine subpopulations would show less binding to CEK cells compared to vaccine S protein. Therefore the binding of S-ectodomain protein representing the C2 vaccine

subpopulation, one of the subpopulations eliminated in CEK cells, was also compared with the vaccine S-ectodomain protein. Rather than less or poor binding, similar binding to CEK cells of S protein representing the C2 subpopulation was observed (Fig. 1 F).

3.4. Effects of each of the three amino acid changes in S protein associated with adaptation to CEK cells

Effects on binding to CEK cells of each of the three amino acid changes in S protein associated with adaptation to CEK cells were tested individually (Fig. 2). Each of the two amino acid changes in S1 reduced, but did not abolish, binding of spike ectodomain to CEK cells (Figs. 2A and 2B). However, the combination of the two amino acid changes in S1 or the one amino acid change in S2 alone reduced binding of the S-ectodomain to below detectable levels (not shown). Similar to the S-ectodomain protein representing the CEK-adapted virus, containing all three aa changes, the S-ectodomain proteins with both changes in S1 or the single change in S2 were able to bind CEK cells when used at a higher concentration (Figs. 2C and 2D). Taken together, our results suggest that all three changes in the S protein of the CEK-adapted virus more or less contribute to the lack of binding.

3.5. Location in S protein secondary structure of aa changes in CEK-adapted virus

The predicted structure of CEK-adapted S protein, based on the known structure of trimeric IBV M41 S protein demonstrated the location of the three amino acids with changes in the S protein of CEK-adapted Ark vaccine strain associated with CEK-adaptation (not shown). The aa change in the S1-NTD is located at the base of the NTD core and is thus unlikely to directly affect receptor binding, but could affect secondary or tertiary structure of the S protein, thus affecting the

conformation of the receptor-binding site. The aa change in the S1-CTD is located in a loop near the loops identified by Shang *et al*. (52) as putative receptor-binding motifs and thus has more potential to affect receptor binding.

4. DISCUSSION

Contrary to expectation, we found that changes in the S protein associated with adaptation of an ArkDPI vaccine strain to CEK cells greatly decreased, rather than increased, the binding of S1 or S-ectodomain protein to CEK cells. This is in contrast to our findings regarding vaccine subpopulations selected in chickens, where S1 binding assays showed increased binding to relevant chicken tissues of S1 protein representing a vaccine subpopulation selected in chickens, suggesting a role for improved attachment in selection of those subpopulations (141). Also contrary to expectation, the S-ectodomain of a vaccine subpopulation selected in chickens, but eliminated during adaptation to CEK cells, did not bind more poorly to CEK cells than the vaccine S-ectodomain. Taken together, these results suggest that initially the very minor vaccine subpopulation selected in chickens was eliminated in CEK cells by limiting dilution, followed by selection of a subpopulation replicating better in CEK cells during subsequent passages, as evidenced by increasing virus levels (89).

Reduced, rather than improved, binding of S protein due to changes in S protein associated with adaption of the vaccine strain to CEK cells suggests that factors other than improved attachment, associated with other changes in the genome of CEK-adapted vaccine (89), are involved in adaptation to CEK cells and compensate for poor attachment. Whole genome sequencing of the CEK-adapted ArkDPI vaccine strain showed nucleotide changes resulting in three amino acid changes (two in NSP2 and one in NSP3) had occurred in the CEK-adapted virus

genome outside the S gene. One of the changes in NSP2 and the change in NSP3 correspond to positions of 2 of only 9 aa changes outside the S gene of the ArkDPI strain during attenuation by adaptation to embryos (97). In each case, the change noted in the CEK-adapted ArkDPI vaccine represents a reversion to the amino acid found in the virulent ArkDPI strain. Of particular interest is the change in NSP3, because the NSP3 of other coronaviruses has been shown function as a type 1 interferon antagonist (146, 147, 148). While 9-11-day-old embryos, in which embryo-adapted IBV is propagated, do not express type 1 interferons, 20-day-old-embryos, the source of the CEK cells used for adaptation to CEK cells, do (149). Thus, a functional interferon antagonist would present a selective advantage to IBV replicating in CEK cells.

The S protein histochemistry assay we used did not provide evidence for a role of changes in the S protein in adaptation of the ArkDPI vaccine strain to CEK cells. However, it should be noted that the protein histochemistry assay only detects binding of the S1 N-terminal domain to sialic acid receptors and is unable to detect the binding of the S1-CTD to putative protein co-receptors demonstrated by assays using live cells (52, 78). Indeed, the presence of the S1-CTD interferes with binding of the S1-NTD to epithelial cells in the kidney (150). Thus if the aa change in the S1-CTD in CEK-adapted virus did improve binding to the putative protein co-receptor, our assay would not have been able to demonstrate that. Thus a potential contribution of better attachment due to the change in the S1-CTD to adaptation to CEK cells has not been ruled out.

ACKNOWLEDGEMENTS

This work was funded by Alabama Animal Health and Disease Research and an Auburn University Cell and Molecular Biosciences graduate stipend. We are grateful to Dr. Aly Ghetas, Ms. Krystyna Minc, and Ms. Cynthia Hutchinson for assistance with CEK culture, acetone fixation, and

histochemistry assays, respectively. We are grateful to Dr. M. Hélène Verheije (Utrecht University) and members of her lab for constructing the ArkDPI vaccine and C2 subpopulation S1 expression vectors.

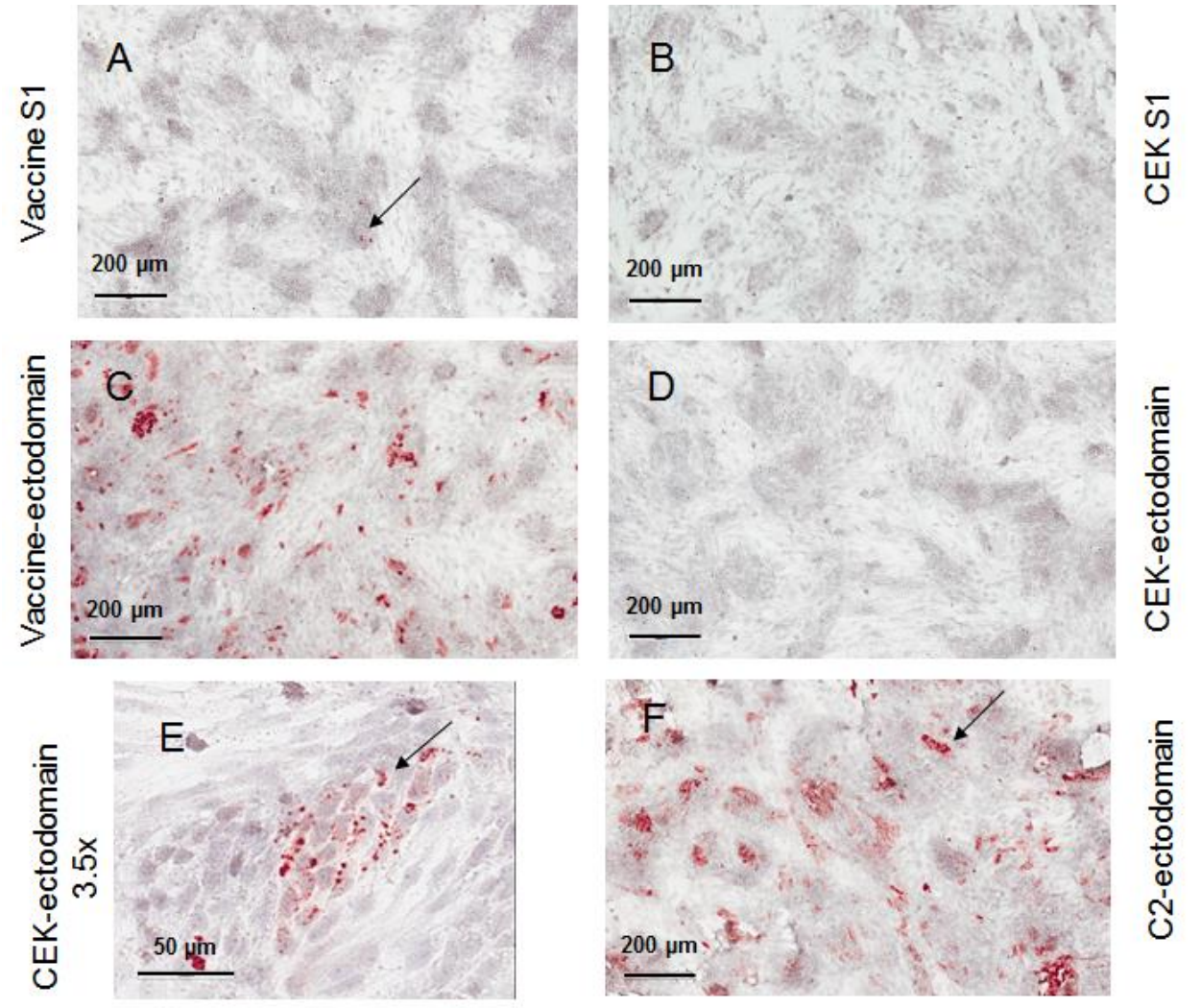

Fig. 2.1. Binding of IBV Ark-type recombinant spike proteins to CEK cells. Purified *Strep*-tag II-tagged trimeric recombinant S proteins were bound to acetone-fixed CEK cells and AEC^{+} chromogenic substrate was used to identify bound spike protein as indicated by red staining (arrows). Spike histochemistry of recombinant S1 protein representing parent (A) or CEK-adapted (B) vaccine strain on acetone-fixed CEK cells. Proteins in A & B were used at 100 µg/ml. Spike

histochemistry of recombinant S-ectodomain representing parent (C) or CEK-adapted (D) vaccine strain on acetone-fixed CEK cells. Recombinant ectodomain protein concentration in C,D, and F was 50 μg/ml, thus, ectodomain proteins were used at approximately one fourth the molar concentration as S1 proteins. (E) S-ectodomain of CEK-adapted vaccine stain binding to CEK cells was detectable at higher concentrations (3.5x). (F) Spike histochemistry of recombinant S-ectodomain protein representing minor subpopulation of the Ark vaccine strain that differs from major vaccine population in four amino acids in the S1 protein to CEK cells (F).

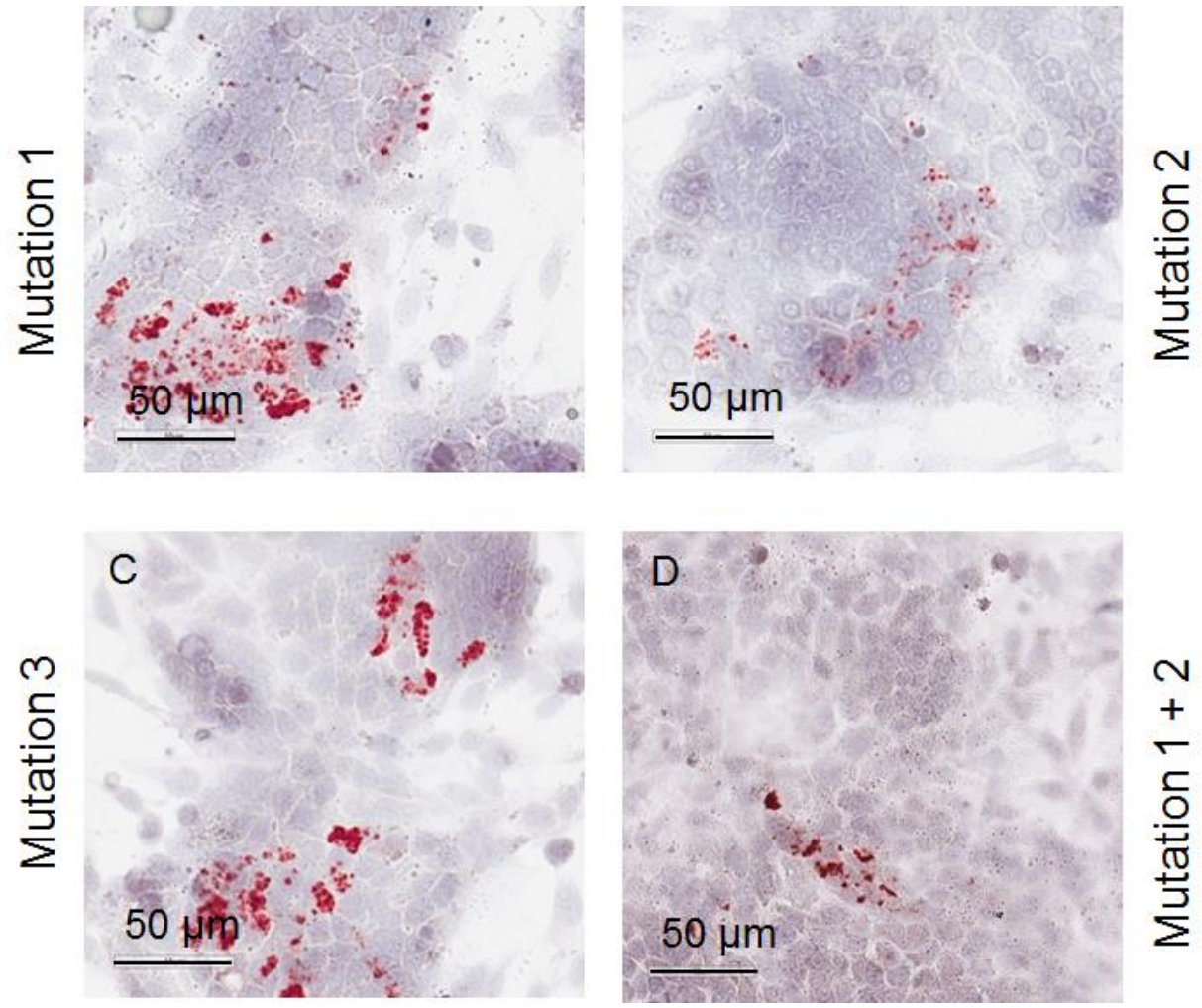

Fig. 2.2. Effects of each of the three amino acid changes in S protein associated with adaption determined by spike histochemistry. Purified *Strep*-tag II-tagged trimeric recombinant S proteins were bound to CEK cells and AEC^{+} chromogenic substrate was used to identify bound spike protein as indicated by red staining (arrows). (A) Vaccine strain S-ectodomain with single aa change in S1-NTD (mutation 1) binding to CEK cells. (B) Vaccine strain S-ectodomain with single aa change in S1-CTD (mutation 2) binding to CEK cells. S-ectodomain proteins in A & B were used at 50 µg/ml. Vaccine strain S-ectodomain with single change in S2 (C) or S-ectodomain with two changes in S1 (D) binding was detectable at higher concentrations (3.5x).

CHAPTER 3

Replication dynamics of CEK cell-adapted ArkDPI-derived infectious bronchitis vaccine in chickens

SUMMARY. We previously eliminated ArkDPI infectious bronchitis virus (IBV) vaccine subpopulations that are selected in chickens and persist in chickens by seven serial passages of a commercial ArkDPI-derived IBV vaccine in chicken embryonic kidney (CEK) cells. The CEK-adapted vaccine strain maintained the ability to protect against homologous IBV challenge. The CEK-adapted ArkDPI vaccine spike (S) protein has three amino acid differences from the original major vaccine population. We observed that recombinant S protein with these changes showed severely reduced or no detectable binding to most relevant chicken tissues *in vitro*, suggesting a reduced replication ability of the CEK-adapted vaccine strain in chickens. We compared replication in chickens of our CEK-adapted ArkDPI vaccine strain to a commercial ArkDPI-derived vaccine, with only two amino acid differences in S, after ocular inoculation of 1-day-old SPF leghorn chickens with 10^4 or 10^5 EID_{50} CEK-adapted ArkDPI vaccine, or 10^4 EID_{50} commercial ArkDPI vaccine. Replication of the vaccine viruses in individual chickens was monitored by determining relative levels of viral RNA in tears 3, 5 and 8 days post-vaccination (DPV) and in choanal and tracheal swabs 5 and 8 DPV by qRT-PCR. Differences in viral loads and kinetics among the groups were most pronounced in tears. At 3 DPV, tears of chickens inoculated with 10^5 EID_{50} of CEK-adapted vaccine and 10^4 EID_{50} commercial ArkDPI vaccine

had similar viral loads, while those of chickens given 10^4 EID_{50} CEK-adapted vaccine were approximately 100-fold lower ($P < 0.0001$). Viral loads in tears of both chicken groups given the CEK-adapted vaccine remained at levels similar to 3 DPV through days 5 and 8 DPV, while those in chickens given the commercial vaccine increased approximately 1000-fold during the same time period ($P < 0.0001$). The sharp increase in viral load in tears of chickens given the commercial vaccine was likely due to efficient replication of minor (<5%) vaccine subpopulations selected in chickens, which are lacking in the CEK-adapted vaccine. Selection of vaccine subpopulations in chickens given the commercial vaccine but not in chickens given the CEK-adapted vaccine was verified by S1 gene sequencing of the IBV genomes in samples from each chicken. Although statistically significant differences among groups were also noted in viral loads in choanal and tracheal swabs, they were less pronounced, with viral loads in groups given 10^4 EID_{50} of either the commercial or CEK-adapted vaccine differing by only 10-20-fold at both 5 and 8 DPV. In contrast to the 38-fold increase between 5 and 8 DPV in viral loads in tears of chickens vaccinated with the commercial vaccine, viral loads in choanal and tracheal swabs of these chickens decreased somewhat (3.7- and 2.6-fold respectively; $P < 0.0001$ and $P< 0.05$ respectively). The ability of the CEK-adapted vaccine to provide effective protection against challenge in spite of substantially lower replication of the CEK-adapted vaccine virus in some tissues in chickens, reflected in lower vaccine viral loads in tears, is likely due to only minimally reduced replication in other tissues, as reflected by vaccine viral loads in choanal and tracheal swabs.

1. INTRODUCTION

Commercial ArkDPI-derived vaccines, which are used extensively in the U.S., contain minor subpopulations that are rapidly selected in vaccinated chickens (36, 38, 64). The selected

subpopulations have spike gene sequences (encoding the viral attachment protein) similar to that of the original virulent ArkDPI strain and are likely the cause of tracheal damage and vaccine virus persistence observed in ArkDPI-vaccinated chickens (81, 114). The selection of these viral subpopulations within 3 days post-vaccination suggests they replicate better in chickens than the predominant virus population in the vaccine prior to inoculation (38, 64). Consistent with a role for improved attachment in selection of the vaccine subpopulations in chickens, recombinant S1 protein representing one of the subpopulations selected in chickens binds better to relevant chicken tissues in spike protein histochemistry assays than recombinant S1 protein representing the major vaccine population (141). The vaccine subpopulations selected in chickens were eliminated from a commercial IBV-ArkDPI vaccine strain by 7 serial passages in chicken embryonic kidney (CEK) cells (89). In addition, during adaptation to CEK cells, two amino acid changes in the S1 protein (amino acid positions 163 and 323) and one amino acid change in the S2 protein (S amino acid position 889) also occurred. Contrary to expectation, these changes severely diminished, rather than improved, the binding affinity of recombinant S-ectodomain protein to CEK cells (Chapter 2).

Despite the absence of vaccine subpopulations selected in chickens and the severe reduction of the S protein binding affinity for CEK cells, the CEK-adapted vaccine strain replicates in chickens well enough to induce an immune response protective against virulent Ark IBV challenge (65, 66). We further explored the ability of the CEK-adapted vaccine strain to replicate in chickens by comparing the binding of its spike protein with that of the major commercial ArkDPI vaccine population to relevant chicken tissues *in vitro* using spike protein histochemistry assays. We also compared replication dynamics of the two viruses in different chicken tissues *in vivo*.

2. MATERIALS AND METHODS

2.1. Spike protein expression plasmids

Expression constructs contained S1- or S-ectodomain-coding sequences flanked by sequences encoding an N-terminal CD5 signal sequence and sequences encoding a C-terminal artificial GCN4 trimerization motif and *Strep*-tag II for affinity purification and detection of recombinant proteins, as described (76). Codon-optimized sequences encoding ArkDPI vaccine S1 (GenBank accession no. ABY66327), [amino acids (aa) 19-539] containing an upstream *Kpn*I and a downstream *Nhe*I restriction site, were obtained from GeneArt (Regensburg, Germany) and cloned into the pCD5 expression vector as previously described (76). Codon changes at S1 codons 163 and 323 of the codon-optimized vaccine S1 gene corresponding to the changes in CEK-adapted vaccine S1 gene (89), were introduced by site directed mutagenesis by overlap extension polymerase chain reaction (PCR) (142) using the Phusion High-Fidelity PCR kit (New England Biolabs, Ipswich, MA). Codon optimized CEK-adapted S1 coding sequences (aa 19-539), were then cloned into *Nhe*I and *Kpn*I-cleaved pCD5 vector.

Codon optimized sequences encoding the S2-ectodomain (aa 545-1098) of ArkDPI vaccine was also synthesized by GeneArt (Regensburg, Germany). *Kpn*I and *Nhe*I sites were added for cloning into the pCD5 vector already containing sequences encoding the S1 domain to produce constructs encoding S-ectodomain proteins as described (70). To avoid cleavage of the S-ectodomain at the S1/S2 border, sequences encoding the furin cleavage site RRSRR in S were replaced by sequences encoding a GGGVP linker (70). Codon 889 (encoding serine) of codon-optimized ArkDPI vaccine S2-coding sequences was changed to a phenylalanine codon, corresponding to the S2 of CEK-adapted vaccine virus (89) by site directed mutagenesis and overlap extension PCR. The resulting codon-optimized sequences encoding the CEK adapted

vaccine S2-ectodomain were then cloned into the pCD5 vector already containing the coding sequences of the CEK-adapted S1 protein using *Kpn*I and *Nhe*I restriction cleavage sites. Expression constructs were sequenced to verify correct recombinant protein-coding sequences.

2.2. Recombinant S protein expression and purification

Soluble, trimeric *Strep*-tagged recombinant S1 and S-ectodomain proteins of parental ArkDPI vaccine and CEK-adapted vaccine strain were produced in human embryonic kidney (HEK) 293T cells as described (76, 140). In brief, 293T cells were transfected with one of the constructed plasmids and cell culture supernatants were harvested at 6 days post transfection. The proteins were then purified using *Strep*-Tactin® Sepharose columns according to the manufacturer's protocols (IBA GmbH). The concentrations of purified proteins were determined by Qubit® 2.0 fluorometer (Invitrogen, Carlsbad, CA). The purified recombinant proteins were visualized by electrophoresis in Mini-PROTEAN®TGX Stain-Free™ Precast Gels (Bio-Rad, Hercules, CA) and relative concentrations of purified proteins were determined.

2.3. Spike protein histochemistry

The binding efficiency of S1 and S-ectodomain proteins to formalin-fixed tissue sections prepared from healthy specific pathogen free (SPF) 40-day old white leghorn chickens was assessed by protein histochemistry as described (30). Briefly, *Strep*-tagged S1 (100 μg/ml) or S-ectodomain (50 μg/ml) proteins pre-complexed with *Strep*-Tactin-HRP (IBA GmbH, Göttingen, Germany) were incubated with deparaffinized and rehydrated tissue sections overnight at 4 C. Lower concentrations of S-ectodomain proteins were used to avoid non-specific background. Bound protein was visualized with chromogenic substrate 3-amino-9-ethyl-carbazole (AEC^+;

Dako, Carpinteria, CA) and tissues were counterstained with hematoxylin. Images were captured by an Aperio ScanScope CS slide scanner (Leica Biosystems, Buffalo Grove, IL) and visualized using Aperio ImageScope software v12 (Leica Biosystems, Buffalo Grove, IL).

2.4. Chickens

White leghorn chickens hatched from specific pathogen free (SPF) eggs (Charles River, North Franklin, CT) were maintained in Horsfall-type isolators in biosafety level 2 facilities. Experimental procedures and animal care were performed in compliance with all applicable federal and institutional animal guidelines. Auburn University College of Veterinary Medicine is an Association for Assessment and Accreditation of Laboratory Animal Care-accredited institution.

2.5. Vaccination and sample collection

Chickens were divided into three groups (n=15/group) and vaccinated at 1 day of age. Each chicken in the first group received 10^4 50% embryo infective doses (EID_{50}) of a commercially available live attenuated ArkDPI-type IBV vaccine in a volume of 100 µl via ocular (25 µl each eye) and nasal (25 µl each nostril) routes. Chickens in the second group received the CEK-adapted vaccine at the same dose as the commercial vaccine (10^4 EID_{50}) and the third group was inoculated with the CEK-adapted vaccine at ten times the dose of the commercial vaccine (10^5 EID_{50}/chicken). An additional group served as unvaccinated controls. Lachrymal fluids were collected 3, 5, and 8 days post vaccination (DPV) as described (151). Choanal and tracheal swabs were collected in tryptose broth 5 and 8 DPV.

2.6. RNA extraction

Total RNA was extracted from tracheal and choanal swabs and tears from each chicken using the TriReagent® RNA/DNA/protein isolation reagent (Molecular Research Center, Cincinnati, OH) following the manufacturer's protocols.

2.7. Viral load by qRT-PCR

Relative IBV RNA levels in lachrymal fluids, choanal swabs and tracheal swabs were determined by Taqman® quantitative reverse transcription polymerase chain reaction (qRT-PCR) targeting the 5' UTR as described (152). Data were analyzed by one-way analysis of variance (ANOVA) followed by Tukey's multiple comparisons post-test. Differences were considered significant at $P < 0.05$.

3.2.8. Sequencing of S1 gene

cDNA for sequencing a portion of the IBV S1 gene was prepared from RNA by RT-PCR using the Qiagen one step RT-PCR kit (Qiagen, Valencia, CA) and primers S17F and S18R (64). The products obtained were visualized by SYBR Green staining after agarose gel electrophoresis. Amplified cDNA was purified using the QIAquick PCR Purification kit (Qiagen, Valencia, CA) and submitted to the Massachusetts General Hospital DNA core facility for sequencing using primers S17F and S1R (64), yielding sequences of the first approximately 700 nt of the S1 coding sequences. Sequences were assembled and aligned using MacVector 15.5 software (MacVector Inc., Cary, NC). The presence of a clear G nucleotide (alone or in combination with a T nucleotide) in sequence chromatograms at S1 position 637 indicated the presence of a vaccine subpopulation selected in chickens (38, 64), and Fisher's exact test was used to determine statistical differences

in incidence of presence of selected subpopulations between time points and groups. Differences with *P* values <0.05 were considered significant.

3. RESULTS

3.1. Differences in binding to chicken tissues of recombinant S1 proteins representing the major ArkDPI vaccine population and CEK-adapted ArkDPI vaccine strain

We compared the ability of trimeric recombinant S1 proteins representing the major ArkDPI vaccine population and the CEK-adapted virus to bind to relevant chicken tissues by protein histochemistry. Very low levels of binding were seen to the glands of choana, nasolacrimal gland, and to the epithelium of the conjunctiva and cloaca by vaccine S1 (Figs.1A, 1C, 1E, and not shown). Binding to other relevant chicken tissues, including tracheal, lung, and kidney tubule epithelium, was not detectable (not shown). CEK-adapted virus S1 showed an even lower level of binding to the epithelium of conjunctiva (Fig. 1F) but no detectable binding to the other tissues tested (Figs. 1B, 1D and not shown), even when four times higher concentration of S1 protein was used (not shown).

3.2. Differences in binding to chicken tissues of recombinant S-ectodomain protein representing the major ArkDPI vaccine population and CEK-adapted vaccine

Because use of the S-ectodomain protein (S1 plus S2 lacking transmembrane and cytoplasmic tail domains) in spike protein histochemistry assays improves binding compared to S1 protein (30, 70), we also compared binding of CEK-adapted vaccine virus and parental virus S-ectodomains to trachea, lung, and kidney (tissues relevant to IBV pathogenesis); conjunctiva, choana, and nasolacrimal gland (sites of IBV replication following ocular inoculation); and cloaca

(through which virus is shed to the environment) (Fig. 2). Modestly or markedly increased binding by the S-ectodomain protein representing the vaccine strain, compared to binding by the S1 protein, was observed to epithelial and secretory cells of trachea, epithelial cells of lung and kidney, secretory cells and epithelium of choana, epithelial cells of conjunctiva, secretory cells in the nasolachrymal gland, and epithelium and secretory cells in the cloaca. However, detectable binding of S-ectodomain representing the CEK-adapted vaccine strain was observed only to trachea, choana, conjunctiva, and cloaca. Furthermore, binding of the S-ectodomain protein of the CEK-adapted virus to trachea and cloaca was markedly reduced compared to that of the vaccine strain. However, binding of S-ectodomain representing CEK-adapted virus to epithelial cells in the choana and conjunctiva was nearly equivalent to that of spike ectodomain representing the parental vaccine virus (Figs. 2C-2F).

3.3. Replication dynamics in chickens

The severely reduced or absence of detectable binding by S-ectodomain protein representing the CEK-adapted vaccine virus, except to choanal and conjunctival epithelium, suggested a reduced replication ability and restricted tissue tropism of the virus in chickens. Therefore we compared replication of the CEK-adapted ArkDPI vaccine strain to a commercial ArkDPI-derived vaccine in different tissues of chickens after ocular inoculation of 1-day-old SPF leghorn chickens with 10^4 or 10^5 EID_{50} CEK-adapted ArkDPI vaccine, or 10^4 EID_{50} commercial ArkDPI vaccine.

Relative levels of viral RNA in tears determined by qRT-PCR 3, 5 and 8 days DPV revealed pronounced differences in viral loads and kinetics among the groups (Fig. 3A). At 3 DPV, tears of chickens inoculated with 10^5 EID_{50} of CEK-adapted vaccine and 10^4 EID_{50} commercial

ArkDPI vaccine had similar viral loads, while those of chickens given 10^4 EID_{50} CEK-adapted vaccine were approximately 100-fold lower ($P < 0.0001$). The viral loads in tears of both chicken groups given the CEK-adapted vaccine remained at levels similar to 3 DPV through days 5 and 8 DPV, while those in chickens given the commercial vaccine increased approximately 1000-fold during the same time period ($P < 0.0001$).

Statistically significant differences among groups were also noted in viral loads in choanal (Fig. 3B) and tracheal swabs (Fig. 3C). However, differences were less pronounced compared to differences in viral loads in tears, with viral loads in groups given 10^4 EID_{50} of either the commercial or CEK-adapted vaccine differing by only 10-20-fold at both 5 and 8 DPV. In contrast to the 30-fold increase between 5 and 8 DPV in viral loads in tears of chickens vaccinated with the commercial vaccine, viral loads in choanal and tracheal swabs of these chickens decreased somewhat (3.7- and 2.6-fold respectively; $P < 0.0001$ and $P < 0.05$ respectively).

3.4. Selection of vaccine subpopulations in chickens

The sharp increase between 3 and 8 DPV in viral load in tears of chickens given the commercial vaccine, not observed in chickens administered the CEK-adapted vaccine (Fig. 3A), was likely due to efficient replication of minor vaccine subpopulations selected in chickens, which are lacking in the CEK-adapted vaccine (89). This supposition was verified by S1 gene sequencing of the IBV genomes in samples from all chickens. Vaccine subpopulations selected in chickens were readily apparent by 5 DPV in nearly all samples collected from chickens vaccinated with the commercial vaccine, while vaccine subpopulations selected in chickens were not observed in any of the samples from chickens vaccinated with the CEK-adapted vaccine strain (Table 3.1).

4. DISCUSSION

Chickens vaccinated with CEK-adapted ArkDPI vaccine virus showed effective protective immune responses against virulent IBV challenge, as evidenced by reduction in viral load and clinical signs following challenge (65, 66), indicating that the virus is able to successfully replicate in chickens. Next generation sequencing of the whole genome and conventional sequencing of the S gene showed three nonconservative amino acid changes in S protein, two in the S1 subunit and one in the S2 subunit, had occurred in the ArkDPI vaccine virus during adaptation to primary CEK cells (89). In this study the effect of those changes in the S protein associated with CEK-adaptation on tissue tropism was investigated by spike protein histochemistry using a wide range of chicken tissues that are relevant for viral replication, pathogenesis, and shedding. Results suggested that the tropism of the CEK-adapted vaccine virus might be restricted to epithelial cells in the head, which would be encountered soon after ocular inoculation, and that replication in trachea would be absent or limited. To examine this possibility, viral tropism *in vivo* was addressed by evaluating replication dynamics of CEK-adapted vaccine virus in epithelial tissues in the head (reflected by viral loads in tears and choanal swabs) and trachea. Results showed lower levels of replication of the CEK-adapted vaccine virus than the commercial ArkDPI vaccine virus in all sample types, but did not support the prediction, based on *in vitro* binding assays of recombinant spike proteins to various tissues, that replication in trachea would be more severely reduced than replication in epithelial cells associated with eyes and choana.

Since the S1 subunit is the receptor binding protein, we initially examined the effect of the two amino acid changes in the CEK-adapted virus S1 protein on the ability of recombinant trimeric S1 protein to bind to relevant chicken tissues. Very low levels or absence of detectable binding of both vaccine and CEK-adapted vaccine S1 were observed, with binding to fewer tissues by the S1

protein of the CEK-adapted virus. The full length S-ectodomain proteins of both Mass and Ark serotype IBV show improvement over S1 protein in attachment to chicken tissues in protein binding assays (30, 70). Therefore, we examined the binding efficiency of S-ectodomains to various chicken tissues. As expected, the S-ectodomain of the ArkDPI vaccine strain showed improved binding compared to the S1 protein to most of the tissues tested. Use of the S-ectodomain representing the CEK-adapted vaccine virus also improved binding to some chicken tissues (such as in choanal and conjunctival epithelium). Thus our results are consistent with those of others, showing that S2 improves binding efficiency of S1 protein. However, markedly lower levels of binding to most chicken tissues by the S-ectodomain protein of CEK-adapted vaccine strain, compared to the ArkDPI vaccine S-ectodomain, were observed, with the exception of epithelial cells of the choana and conjunctiva. These observations suggested that replication of the CEK-adapted vaccine strain would be largely restricted to sites first encountered by the virus administered ocularly, leading to stimulation of immunity in head-associated lymphoid tissues such as Harderian gland and conjunctiva-associated lymphoid tissue (CALT). From an applied perspective, such restriction might be beneficial as it would reduce adverse reactions, due to reduced viral load, and stimulate local immunity as well.

Consistent with reduced binding of its S-ectodomain protein to chicken tissues, the CEK-adapted ArkDPI vaccine strain replicated to lower levels in chickens than the commercial vaccine strain, as expected. However, our results did not support the prediction that replication of the CEK-adapted virus was restricted to certain tissues. Viral loads were not more severely reduced in trachea than in choana or tears, in spite of severe reduction of binding of the CEK-adapted S-ectodomain protein to tracheal epithelium in the protein histochemistry assay. The basis of selection of the CEK-adapted virus in CEK cells, in spite of lack of detectable binding of its S-

ectodomain to CEK cells in the protein histochemistry assay was discussed in the previous chapter. That discussion is relevant to modest reduction of viral loads of the CEK-adapted virus in trachea compared to reduction in tears, in spite of severe reduction of binding of its S-ectodomain to trachea, compared to little or no reduction of binding to conjunctiva. Other factors may contribute to success of the CEK-adapted virus in trachea, such as ability to antagonize the type 1 interferon response, or interact with a protein co-receptor.

Results of protection following challenge of the chickens vaccinated in this study have been reported (66). Chickens vaccinated with both the commercial ArkDPI and CEK-adapted vaccines were protected despite substantially lower replication of the CEK-adapted vaccine virus in some tissues in chickens, reflected in lower vaccine viral loads in tears. The effective protection afforded by the CEK-adapted virus was likely due to only minimally reduced replication in other tissues, as reflected by vaccine viral loads in choanal and tracheal swabs. Nevertheless, protection, as measured by reduction in viral load in tears 5 days post-challenge, was marginally, though statistically significantly, greater in the chickens vaccinated with the commercial ArkDPI vaccine {Zegpi, 2017 #180. Thus higher vaccine viral loads were associated with somewhat greater protection in this study.

AKNOWLEDGEMENTS

This work was funded by Alabama Animal Health and Disease Research and an Auburn University Cell and Molecular Biosciences graduate stipend. We are grateful to Cassandra Kitchens, Stephen Gully and Ramon A. Zegpi for assistance with sample collection. We are grateful to Dr. M. Hélène Verheije (Utrecht University) and members of her lab for constructing the ArkDPI vaccine S1 expression vector.

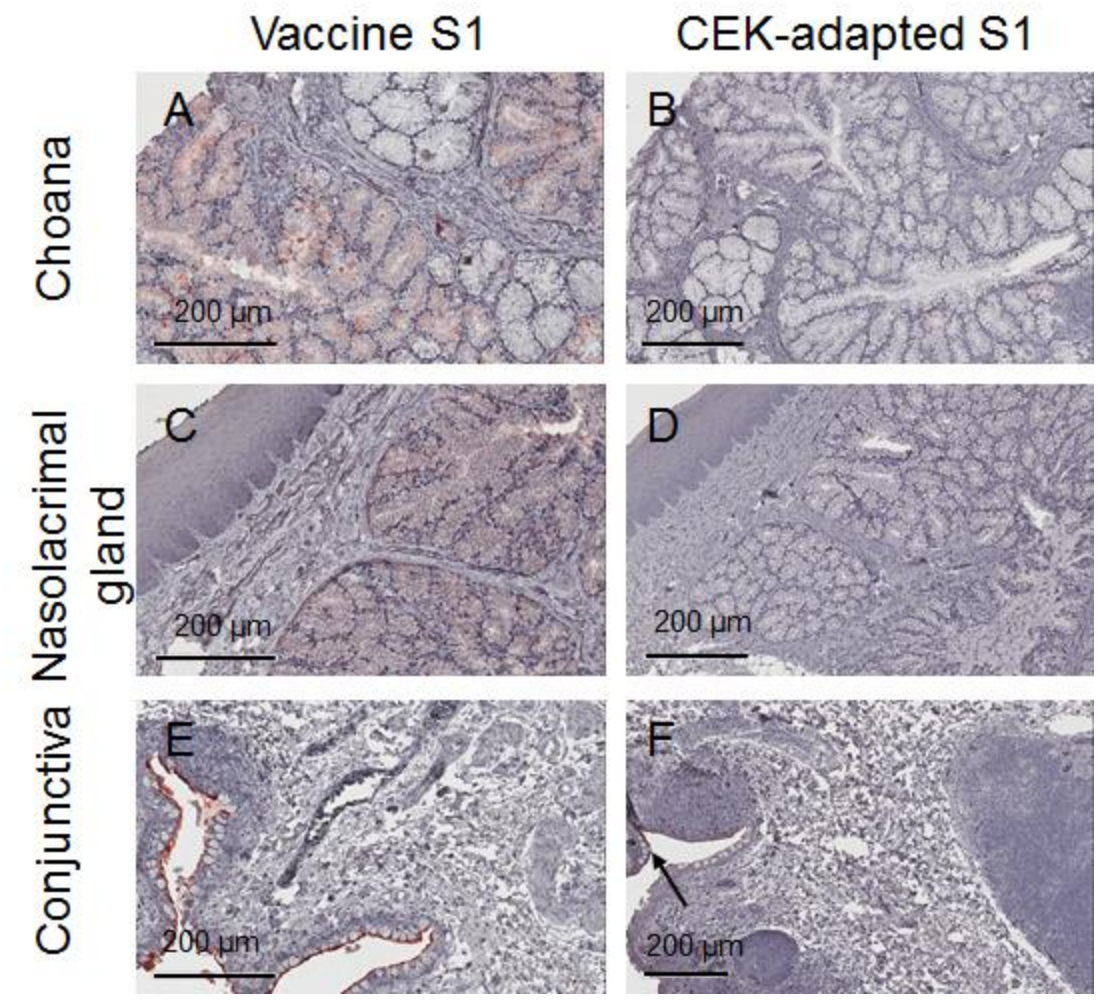

Fig. 3.1. Protein histochemistry demonstrating recombinant S1 proteins representing vaccine strain and CEK-adapted strain binding to chicken tissues. Purified *Strep*-tag II-tagged trimeric recombinant S1 proteins (100 µg/ml) were bound to formalin fixed chicken tissues and AEC^{+} chromogenic substrate was used to identify bound spike protein as indicated by red staining (arrows). In panels A, C, and E, recombinant S1 was from the vaccine strain. In panels B, D, and F, the recombinant S1 was from the CEK-adapted vaccine strain. S1 protein histochemistry is shown for choana (A and B), nasolacrimal glands (C and D), and conjunctiva (E and F).

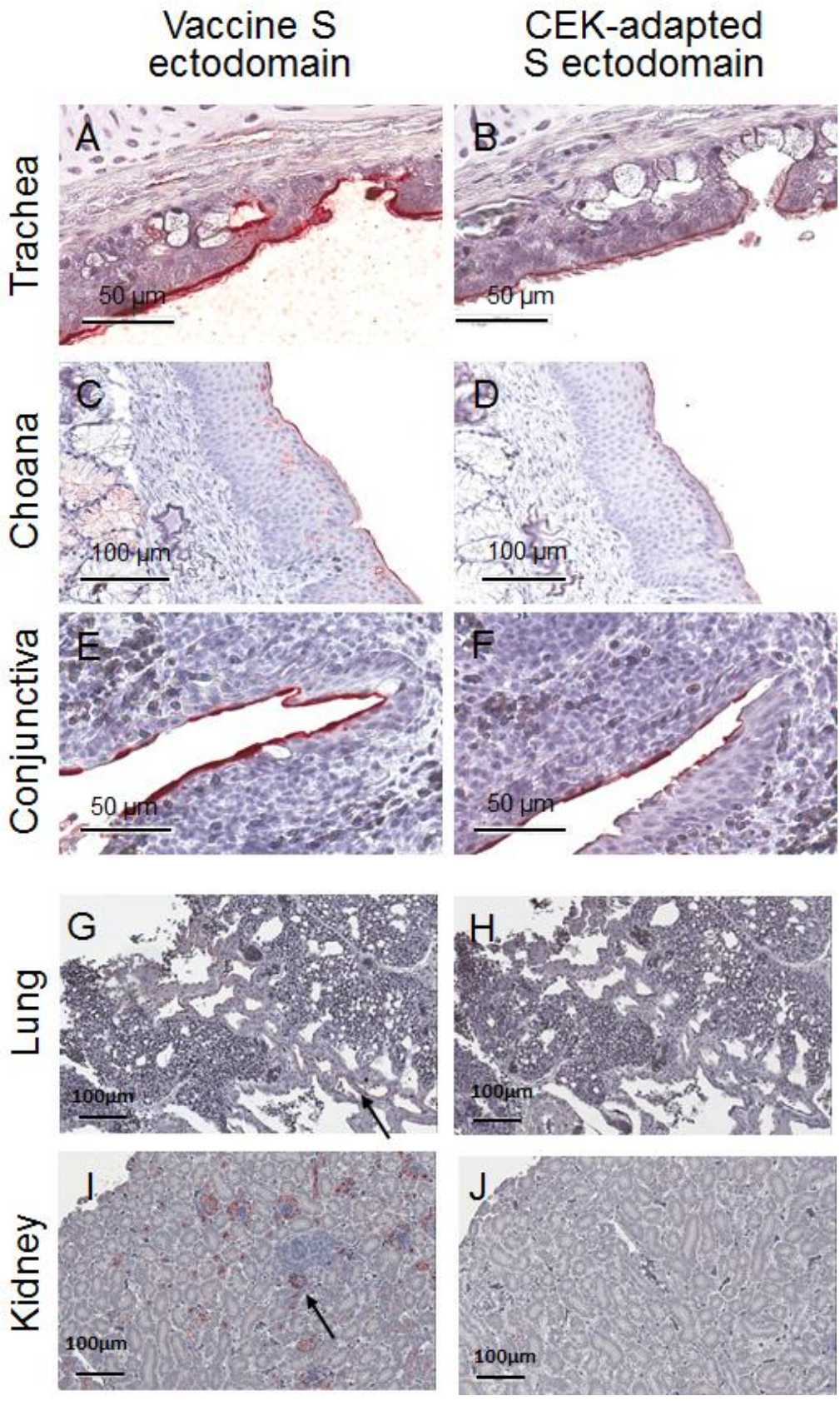
Vaccine S ectodomain
CEK-adapted S ectodomain
Trachea
Choana
Conjunctiva
Lung
Kidney
A
B
C
D
E
F
G
H
I
J
50 µm
100 µm
100µm

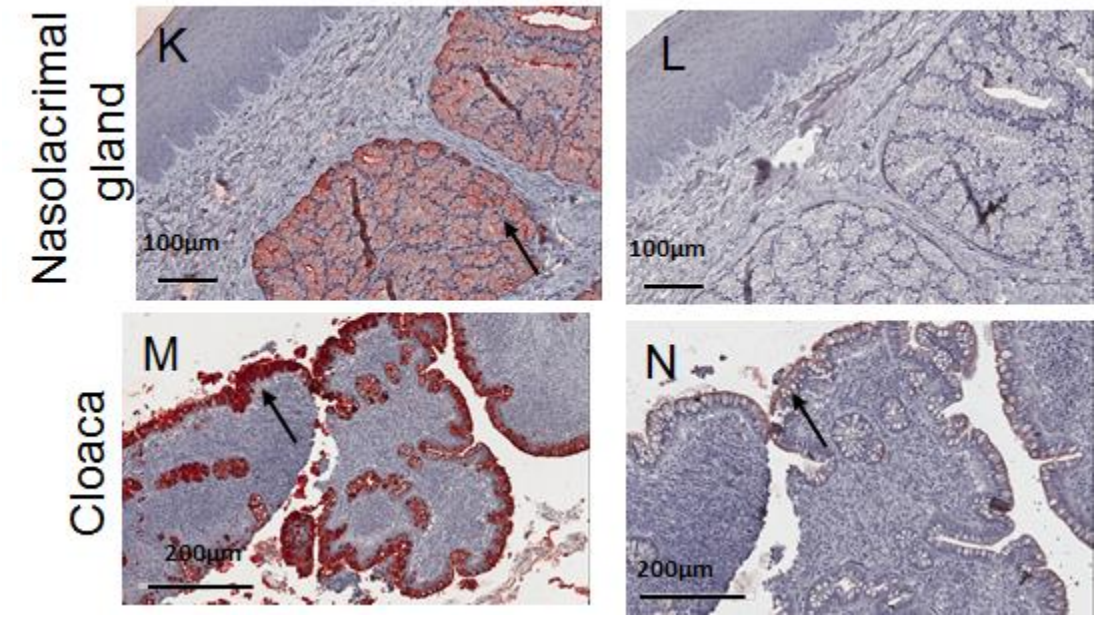

Fig. 3.2. Protein histochemistry comparing binding of recombinant trimeric S-ectodomain protein representing the major population of a commercial ArkDPI vaccine strain and CEK-adapted ArkDPI vaccine strain to relevant chicken tissues. Purified *Strep*-tag II-tagged trimeric recombinant S-ectodomain proteins (50 µg/ml) were bound to formalin fixed chicken tissues and AEC^{+} chromogenic substrate was used to identify bound spike protein as indicated by red staining (arrows). In panels A, C, E, G, I, K, and M, recombinant S-ectodomain protein was from the vaccine major population. In panels B, D, F, H, J, L, and N, the recombinant S-ectodomain protein was from the CEK-adapted vaccine strain. S-ectodomain protein histochemistry is shown for trachea (A and B), choana (C and D), conjunctiva (E and F), lung (G and H), kidney (I and J), nasolacrimal gland (K and L), cloaca (M and N).

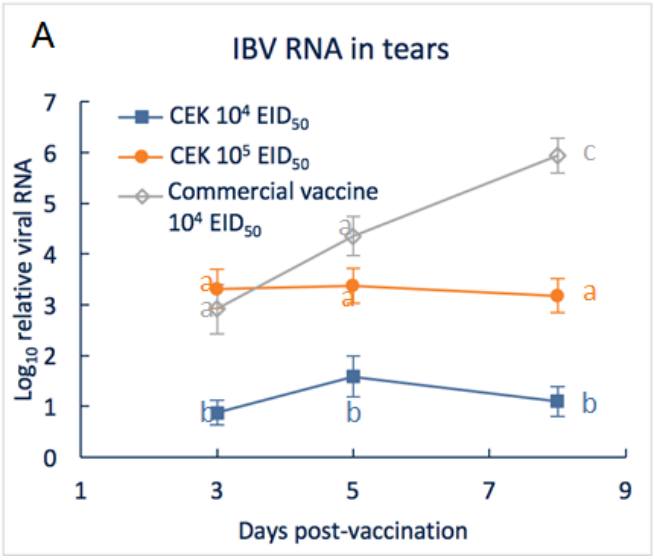

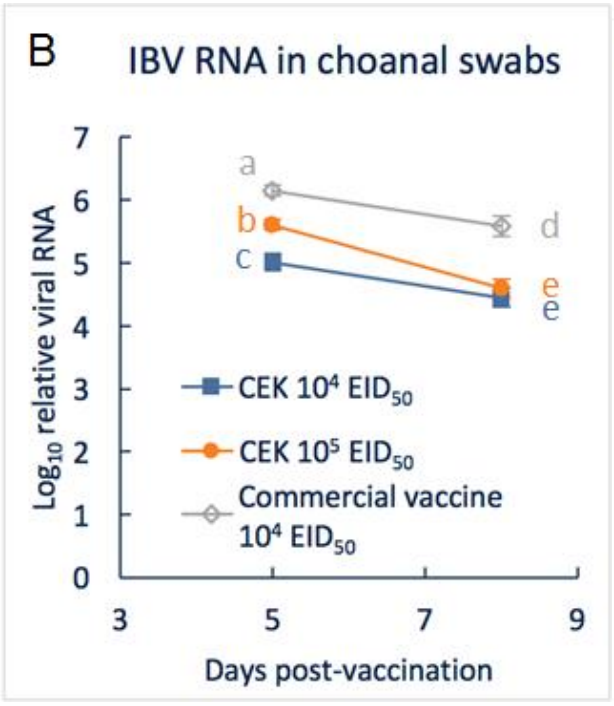

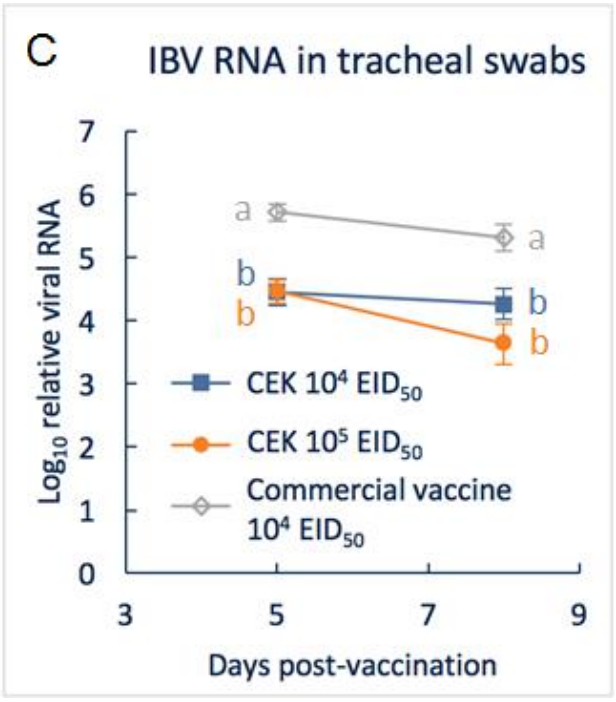

Fig. 3.3. Relative vaccine virus RNA levels in (A) tears, (B) choanal swabs, and (C) tracheal swabs at different days post vaccination with CEK-adapted or commercial ArkDPI vaccine. Mean $\log_{10}$ values ± SEM are shown. Different letters indicate statistically significant differences (One-way ANOVA, Tukey's post-test; $P < 0.05$).

Table 3.1. Selection of vaccine subpopulations in chickens

Chickens vaccinated with:		Number of samples containing selected vaccine populations[A]/number of S1 sequences obtained[B]				
		CEK (10^4 EID_{50})	*P* value[C]	CEK (10^5 EID_{50})	*P* value[C]	Commercial vaccine (10^4 EID_{50})
Sample	DPV					
Tears	3	-[D]		0/2	n.s.	2/6
	5	-		0/2	0.048	5/5
	8	-		0/2	0.046	9/10
Choanal swabs	5	0/15	<0.0001	0/13	<0.0001	13/15
	8	0/13	<0.0001	0/15	<0.0001	15/15
Tracheal swabs	5	0/9	<0.0001	0/4	0.0004	13/13
	8	0/13	<0.0001	0/7	<0.0001	12/12

[A]A hallmark of ArkDPI-derived vaccine subpopulations selected in chickens is a G nucleotide (instead of T) at S1 gene position 637 (64, 38). Therefore the criterion for designation of a sample as containing a selected vaccine subpopulation was that a G nucleotide (alone or as a mixture with T) was clearly discernable at S1 nucleotide 637 in the sequence chromatogram.

[B]Some samples did not contain adequate amounts of IBV RNA for S1 gene sequencing, so for most time points and sample types, 15 sequences/group were not obtained.

[C]*P* values for difference from corresponding samples in commercial vaccine-vaccinated chickens (Fisher's exact test)

[D] - indicates no sequences obtained

CHAPTER 4

Intestinal tropism of an IBV isolate not explained by spike protein binding specificity

Avian Diseases (submitted August 22, 2019)

F. Saiada[a], R. A. Gallardo[b], H.L. Shivaprasad[c], Charles Corsiglia[d], V. L. van Santen[a,e]

[a] Department of Pathobiology, 264 Greene Hall, College of Veterinary Medicine, Auburn University, Auburn, AL 36849-5519.
[b] Population Health and Reproduction, School of Veterinary Medicine, University of California, Davis, CA, 95616.
[c] University of California, California Animal Health and Food Safety Laboratory Tulare Branch, 18830 Rd. 112, Tulare, CA 93274
[d] Foster Farms, 14519 Collier Road, Livingston, California, 95315-9609.

[e] Corresponding author. E-mail: vanvick@auburn.edu

SUMMARY. An infectious bronchitis virus (CalEnt) with unusual enteric tropism was isolated from a California broiler flock exhibiting runting-stunting syndrome. IBV was detected in the small intestine, but not in respiratory tract or kidney. During virus isolation in embryos, it did not replicate in chorioallantoic membrane (CAM), but could be recovered from intestines. Its S1 protein showed 93% amino acid sequence identity to a California variant isolated in 1999 (Cal99). Intestinal lesions were reproduced following ocular/nasal inoculation of specific pathogen free (SPF) chickens, but respiratory signs and lesions were also present. The virus was detected in both respiratory and intestinal tissues. To determine whether the novel tropism of IBV CalEnt was due to an increased ability of its S1 protein to bind to the intestinal epithelium, we compared the binding of soluble trimeric recombinant S1 proteins derived from CalEnt and Cal99 to chicken tissues. Contrary to expectations, CalEnt S1 protein did not bind to small intestine, and, unlike Cal99 S1, did not bind to the respiratory epithelium or CAM. Using only the CalEnt S1-N-terminal domain or including the S2-ectodomain (lacking membrane and cytoplasmic domains), which have been shown to improve ArkDPI S1 binding, did not lead to detectable binding at the standard protein concentration to any tissue tested. Our results indicate no/poor binding of the CalEnt spike protein to both respiratory and intestinal tissues and thus do not support better attachment to intestinal epithelial cells as a reason for CalEnt's extended tropism. These results might reflect shortcomings of the assay, including that it does not detect potential contributions of the S1-C-terminal domain to attachment. We used bioinformatic approaches to explore the possibility that the unique tropism of CalEnt might be a result of functions of the S protein in cell entry steps subsequent to attachment. These analyses suggest that CalEnt's S2-coding region was acquired through a recombination event and encodes a unique amino acid sequence at the putative recognition site for the protease that activates the S protein for fusion. Thus S2 activation by tissue-

specific proteases might facilitate CalEnt entry into intestinal epithelial cells and compensate for poor binding by its S1 protein.

1. INTRODUCTION

The avian infectious bronchitis coronavirus (IBV) is an economically important, highly contagious respiratory pathogen of chickens, which is endemic in the poultry industry worldwide, affecting the performance of both meat-type and egg-laying birds {Jackwood, 2012 #76}. IBV replicates initially in the epithelium of the upper respiratory tract, and, following viremia, also in the epithelium of non-respiratory tissues including those in the urogenital tract. Depending on the IBV strains, disease outcome varies, ranging from mild respiratory symptoms to severe kidney and oviduct disease (11). IBV is frequently isolated from cecal tonsils or cloacal swabs from breeder or layer flocks with or without respiratory disease, but the isolated strains cause respiratory disease during experimental infection (153, 154). Some IBV isolates have been shown to have a wider enteric tissue distribution and longer persistence in enteric tissues compared to other isolates, but all cause respiratory disease and lesions during experimental infection (109, 110, 155, 156). These isolates have been obtained from many parts of the alimentary tract of experimentally infected chickens, including proventriculus, duodenum, jejunum, caecal tonsils, and cloaca (24, 109, 110), although evidence for viral replication in those tissues has been obtained only for enterocytes in the ileum and rectum (24) and glandular epithelium in the proventriculus (157). In partial agreement, ten IBV isolates originating from fecal swabs or gut tissues were all able to replicate in proventriculus organ cultures, half were able to replicate in cecal tonsil or rectum organ cultures, but none replicated in duodenum, jejunum, or ileum organ cultures (9). Presence of IBV in enteric tissues very rarely causes any pathology/clinical symptoms (reviewed by (9)). Occasionally lesions

were observed in the rectum of experimentally infected chickens, but not in other parts of the intestines (24). Chacon, *et al*. recently compared the pathogenicity and tropism of two genetically similar Brazilian IBV isolates, one isolated from enteric content of a broiler flock with diarrhea and poor growth rate and one isolated from respiratory tissues of a broiler flock with respiratory disease(158). They found no important differences in tropism or disease in experimentally-inoculated chickens. Whether inoculated orally or oculonasally, both isolates caused respiratory disease, while the agent could be detected by nested RT-PCR in both respiratory tissues and enteric content. The enteric-origin virus did not reproduce the disease it was associated with in the commercial flock.

An IBV was isolated from intestines of chickens in a broiler flock exhibiting clinical signs of runting-stunting syndrome and designated "California enteric variant" (CalEnt) due to its unusual tropism (13). IBV antigen was detected within the cytoplasm of enterocytes in all segments of the intestine (duodenum, jejunum, rectum/cloaca) of the affected birds as well as in the proventriculus and pancreas, indicating viral replication in these tissues. However, no IBV antigen was detected in respiratory tissues, including trachea, lung, and air sac, or conjunctiva. Most remarkably, during virus isolation from intestinal samples in embryos, IBV could not be detected in chorioallantoic membrane or allantoic fluid using fluorescently labeled antibody, electron microscopy (EM), or RT-PCR. In contrast, IBV was detected by both EM and RT-PCR in the embryo's intestine and was recovered from this tissue (13). Following oculonasal inoculation of CalEnt, IBV antigen and RNA were detected in the intestine and histopathologic lesions of the intestine were reproduced in SPF chickens. Consistent with observations of others regarding experimental infection with enteric-origin IBVs, mild respiratory signs and lesions were also observed. IBV antigen was detected in conjunctiva, sinus/turbinate, and trachea, and IBV

RNA was present in tears and trachea. Thus, CalEnt exhibited a broadened tropism, causing lesions in both intestine and respiratory tract.

Coronavirus spike (S) proteins mediate viral attachment and cell entry and are major determinants of coronavirus species specificity and tissue tropism (77, 86). The IBV S glycoprotein is cleaved into an amino (N)-terminal S1 subunit of approximately 520 amino acids and carboxy (C)-terminal S2 subunit of about 620 amino acids, which remain non-covalently associated (43, 50). Coronavirus S1 subunits or domains include the receptor binding domain(s) and are essential for viral attachment. The membrane-anchoring S2 subunits or domains are involved in the fusion of the viral envelope with host membranes (reviewed in (67)). Coronavirus S1 subunits or domains comprise at least two sub-domains, the N-terminal domain (S1-NTD) and C-terminal domain (S1-CTD), where either or both of the sub-domains can function as the receptor-binding domain for different coronaviruses, interacting with sugar and/or protein receptors (77). For IBV, both the S1-NTD and S1-CTD have been implicated in receptor binding. Promkuntod, *et al*., (78) demonstrated that the S1-NTD of IBV strain M41 is necessary and sufficient for binding to α-2,3 linked sialic acids located on the epithelium of the chicken respiratory tract, which serve as receptor determinants for the virus (73, 75, 76). Shang, *et al*., (52) have provided evidence that the IBV S1-CTD also possesses receptor-binding activity for an unknown protein co-receptor. The IBV S1 subunit contains two additional subdomains, designated subdomain (SD)1 and SD2, which connect the rest of the S1 subunit with the S2 subunit (52). The role of SD1 and SD2 in IBV S protein function is unknown, but may provide structural constraint of the S2 subunit until it is activated for its fusion function.

The S1 portions of coronavirus spike proteins affect tropism at the level of virus attachment. The porcine coronavirus transmissible gastroenteritis virus provided an early example

that a very few changes in the S1 portion of a coronavirus S protein can alter tropism and pathogenicity. This coronavirus lost its enteric tropism and shifted to respiratory tropism after two amino acid changes in the S1 portion of the spike protein (87). Wickramasinghe, *et al*., (159) have demonstrated that S1 proteins of avian enteric coronaviruses turkey coronavirus, guineafowl coronavirus, and quail coronavirus have a glycan binding specificity distinct from that of IBV S1 protein and bind only to intestinal tissues, whereas the IBV S1 protein binds to both enteric and respiratory tissues.

Subsequent to attachment mediated by the S1 portion of the spike protein, coronavirus viral entry is mediated by the S2 portion of the spike protein. Following proteolytic activation by cleavage at a site within S2 known as S2', exposure of the fusion peptide and major conformational changes of S2 lead to insertion of the S2 fusion peptide into the host membrane, fusion of the viral envelope with host membranes, and viral entry (69). Thus tropism can be affected at the level of viral entry by the ability of S2 to be cleaved by host cell proteases at its S2' cleavage site (90). In the case of IBV, with the exception of the Beaudette strain, the host protease responsible for S2' cleavage is an unidentified serine protease (68). The extended host tropism of the IBV Beaudette strain, the extensively passaged embryo-attenuated Massachusetts-derived strain that has acquired the ability to replicate in mammalian cell lines, was shown to be conferred by its S protein (85), and has recently been more precisely mapped to its S2' protease recognition site (87), which can be cleaved by furin (68).

We examined the possibility that the broadened tropism of IBV CalEnt was due to an increased ability of its S1 protein to bind to intestinal tissues. Because IBV Cal99 is the IBV isolate with a known complete S protein amino acid sequence that is most similar to CalEnt S1 (92.6% amino acid identity), we compared binding of recombinant trimeric CalEnt S1, S-ectodomain, and S1-NTD to relevant chicken tissues with that of corresponding Cal99 recombinant proteins. We

used bioinformatic approaches to consider the possibility that differences in CalEnt S2 might contribute to its altered tropism at the stage of cell entry.

2. MATERIALS AND METHODS

2.1. Protein structure prediction and display

Three-dimensional structure homology models of S proteins of Cal99 and CalEnt variants based on the cryo-electron microscopy structure of trimeric IBV M41-S protein (52) were generated using the SWISS-MODEL (https://swissmodel.expasy.org) (160) and I-TASSER servers (https://zhanglab.ccmb.med.umich.edu/I-TASSER/) (143, 144, 145). Visualization and analysis of the resulting models were performed with CueMol (Version 2.2.3.443, obtained at http://www.cuemol.org/en/).

2.2. Construction of expression plasmids

Expression constructs contained S1-, S-ectodomain- or S1-NTD-coding sequences flanked by sequences encoding an N-terminal CD5 signal sequence and sequences encoding a C-terminal artificial GCN4 trimerization motif and *Strep*-tag II for affinity purification and detection of recombinant proteins, as described (76). Codon-optimized sequences encoding Cal99 S1 (IBV variant California 99, GenBank accession no. AAS00080.1) and CalEnt S1 (enteric variant CalEnt, GenBank accession no. ANG58739.1), [amino acids (aa) 19-539] containing an upstream *Nhe*I

and a downstream *Pac*I restriction site, were obtained from GeneArt (Regensburg, Germany) and cloned into the pCD5 expression vector as previously described (76). Codon optimized sequences encoding the S2 ectodomains [aa 545-1098] of Cal99 and CalEnt were also synthesized by GeneArt (Regensburg, Germany). *Kpn*I and *Pac*I sites were added for cloning the S2-ectodomain-encoding sequences into the pCD5 vector already containing sequences encoding the S1 domain to produce constructs encoding S-ectodomain proteins as described (70). To avoid cleavage of the S-ectodomain at the S1/S2 border, sequences encoding the furin cleavage sites RRSRR in Cal99 S and RRFRR in CalEnt S were replaced by sequences encoding a GGGVP linker (70). For the cloning of the S1 N-terminal domain (NTD) [aa 19-279], the appropriate segment of the S1-encoding gene was amplified from each S1 gene construct by polymerase chain reaction (PCR) and cloned into *Nhe*I and *Kpn*I-cleaved pCD5 vector using the In-Fusion® HD PCR cloning kit (Takara Bio USA, Inc., Mountain View, CA). All expression constructs were sequenced to verify correct recombinant protein-coding sequences. These S1-NTD expression constructs, based on that of (70) of the M41 NTD, encoded the S1-NTD, SD2' and SD1' portions of the S1 subdomains, and the first three amino acids of the S1-CTD (see Fig. 4.1).

2.3. Recombinant S protein expression and purification

Soluble, trimeric *Strep*-tagged recombinant S1, S1- NTD, and S-ectodomain proteins of Cal99 and CalEnt variants were produced in human embryonic kidney (HEK) 293T cells as described (76, 140). In brief, 293T cells were transfected with one of the constructed plasmids and cell culture supernatants were harvested at 6 days post transfection. The proteins were then purified using *Strep*-Tactin® Sepharose columns according to the manufacturer's protocols (IBA GmbH). The concentrations of purified proteins were determined by Qubit® 2.0 fluorometer (Invitrogen,

Carlsbad, CA). The purified recombinant proteins were visualized by electrophoresis in Mini-PROTEAN®TGX Stain-Free™ Precast Gels (Bio-Rad, Hercules, CA) and relative concentrations of purified proteins were calculated.

2.4. Spike Protein histochemistry

The binding of trimeric recombinant S1 proteins, S1-NTDs and S-ectodomains to formalin-fixed tissues from healthy SPF white leghorn chickens was assessed by protein histochemistry as described (30). Intestinal tissues were obtained from 4-week old chickens, trachea and kidney were obtained from 8-week old chickens, and chorioallantoic membrane was obtained from 11-day embryos. Briefly, equimolar concentrations of *Strep*-tagged S1 (100 µg/ml) or S1-NTD (54 µg/ml) proteins pre-complexed with *Strep*-Tactin-HRP (IBA GmbH, Göttingen, Germany) were incubated with deparaffinized and rehydrated tissue sections overnight at 4 C. Bound protein was visualized with chromogenic substrate 3-amino-9-ethyl-carbazole (AEC$^+$; Dako, Carpinteria, CA) and tissues were counterstained with hematoxylin. Lower concentrations of S-ectodomain proteins (50 µg/ml) were used to avoid non-specific background. Images were captured by an Aperio ScanScope CS slide scanner (Leica Biosystems, Buffalo Grove, IL) and visualized using Aperio ImageScope software v12 (Leica Biosystems, Buffalo Grove, IL).

2.5. Recombination analysis

To detect evidence of recombination within the S gene of the CalEnt variant, the recombination detection program (RDP4) v.4.16 was used. IBV S gene sequences to be included in the analysis were identified by Basic Local Alignment Search Tool (BLAST) searches at the National Center for Biotechnology Information (NCBI) (https://blast.ncbi.nlm.nih.gov/Blast.cgi)

using S1 and S2 gene sequences of CalEnt separately. Seventeen sequences with >90% nucleotide identity to either CalEnt S1 or S2 gene sequences were identified and retrieved from GenBank. The seventeen nucleotide sequences (seven full-length S gene sequences, nine S1 gene sequences, and one S2 gene sequence) and the CalEnt S gene sequence were aligned by CLUSTALW using MacVector version 17 (MacVector Inc., Cary, NC) and recombination analysis was conducted using RDP, GENECONV, Chimaera, Maximum Chi Square, BootScan, Sister Scan, and 3Seq methods implemented in the RDP4 program with the default settings (161, 162).

2.6. Protein cleavage site prediction. Potential protease recognition sites in S2 amino acid sequences were detected by the PROSPER protease specificity prediction server at https://prosper.erc.monash.edu.au/(163) and the PeptideCutter server at https://web.expasy.org/peptide_cutter/ (164).

3. RESULTS

3.1. Differences between IBV CalEnt and Cal99 S1 proteins

The predicted amino acid sequence of CalEnt variant mature S1 protein has the highest (93-94%) amino acid sequence identities with IBVs of California variant 99 (Cal99) molecular type, typical respiratory field isolates of IBV. Amino acid differences between the CalEnt S1 protein sequence and a representative Cal99 S1 protein sequence are mostly non-conservative differences and are found in all four of the structural domains of S1 (Fig. 4.1A). The highest concentration of aa differences is in the signal peptide, but these differences are not directly relevant to the function of mature S1 protein. The largest number of aa differences (13) is in the S1-NTD. However, when the number of total amino acids in each subdomain is considered, aa

differences are more concentrated in SD1" and SD2", with 11% and 13% aa differences, respectively, compared to only 6% difference within the S1-NTD. The predicted structures of Cal99 and CalEnt S1 proteins, based on the known structure of trimeric IBV M41 S protein, are largely identical (Fig. 4.1B), which is expected since the predictions are based on the same known structure. An exception is one of the loops comprising part of the "partial ceiling" over the putative sugar-binding site on the S1-NTD core identified by Shang, *et al*. (52), where the backbone of the amino acid chain takes divergent paths in Cal99 and CalEnt S1 protein predicted structures (Figs. 4.1B, 4.1C). In Cal99 S1, amino acids 139 (K-lysine) and 141 (E-glutamic acid), near one end of this loop, are oppositely charged and their side chains are in close contact in the model (Fig 4.1E). In CalEnt S1, amino acid 141 (G-glycine) is uncharged, leaving negatively-charged amino acid 139 (E-glutamic acid) to interact with positively charged amino acid 140 (K-lysine) in the model, and changing the orientation of this lysine side chain compared to its orientation in Cal99 S1 (Fig. 4.1D). The remainder of the amino acids in the loop are the same in Cal99 and CalEnt S1s. Oppositely charged amino acids at S1 positions corresponding to CalEnt aa 139 and 140 are rare among IBV S1 aa sequences, present in only 2.9% of IBV S1 aa sequences in GenBank. Most of those have the opposite configuration as CalEnt S1; they have basic amino acid lysine at position 139 and positively charged glutamic acid at position 140. However, structural models of these S1 proteins do not show interaction of aas 139 and 140, and the path of the loop containing them follows a path similar to that of Cal99 S1 (not shown). Only 0.44% of IBV sequences in GenBank have an acidic aa (glutamic acid) at 139, a basic amino acid (lysine of histidine) at 140, and an uncharged aa (glycine) at 141, like CalEnt S1. The pathway of the loop containing these aas in structural models of S1 proteins is similar or identical to that of CalEnt S1. The models shown in Fig. 1B-E were generated by SWISS-MODEL. Models generated by I-TASSER also showed a

different structure of this loop between CalEnt and Cal99, and proximity of charged side chains of amino acids 139 and 140 in CalEnt S1 and those of amino acids 139 and 141 in Cal99 S1 (not shown).

3.2 Differences in binding of CalEnt and Cal99 recombinant S1 proteins to chicken tissues

To determine whether the attachment specificity of the S1 protein of IBV CalEnt reflects the unusual tropism of CalEnt, we used spike histochemistry to compare binding of trimeric CalEnt and Cal99 recombinant S1 proteins to relevant chicken tissues (Fig. 4.2). Consistent with its respiratory tropism, Cal99 S1 protein bound to the apical surface and cilia of the tracheal epithelium Fig. 4.2A. However, binding to tracheal epithelium by CalEnt S1 protein was not detected (Fig. 4.2B) even when a five times higher concentration of CalEnt S1 protein was used (not shown). Cal99 S1 bound to the inner epithelium of duodenum (Fig. 4.2C), but no binding to jejunum or ileum was detected (Fig. 4.2E and 4.2G). A few foci of binding to cecal tonsil epithelium (Fig. 4.2I) and more extensive binding to cloacal epithelium and glands (Fig. 4.2K) by Cal99 S1 were observed. Contrary to expectation, no detectable binding to duodenum (Fig. 4.2D), jejunum (Fig. 4.2F), ileum (Fig. 4.2H), or cecal tonsil (Fig. 4.2J) was seen for the S1 of the CalEnt variant, not even when the concentration of S1 protein was increased five times (not shown). However, binding of CalEnt S1 to epithelium and glands of cloaca was observed (Fig. 4.2L), although less than that by Cal99 S1. Cal99 S1 also bound to the epithelium of renal tubules (Fig. 4.2M), but CalEnt S1 did not (Fig. 4.2N). Consistent with the inability to detect or recover the CalEnt virus from CAM or allantoic fluid during virus isolation in embryos (13), CalEnt S1 protein did not show any binding to CAM from 11 day old embryos (Fig. 4.2P), while Cal 99 S1 did bind to the allantoic epithelium (Fig. 4.2O).

3.3. Differences in binding of CalEnt and Cal99 recombinant S1-NTDs to chicken tissues

Enteric avian coronavirus S1 proteins have a glycan binding specificity distinct from that of IBV S1 protein and bind only to intestinal tissues (159). Promkuntod, *et al*. (78) showed that the S1-NTD (aa 19-272) of IBV M41 was necessary and sufficient for alpha-2,3 sialic acid-dependent binding to chicken respiratory tract, indicating that the protein histochemistry assay depends on the glycan-binding specificity of the S1-NTD. We previously confirmed that the S1-NTD (aa 19-279) of Ark serotype S1 was necessary and sufficient for binding and also found that it showed increased binding to all relevant chicken tissues compared to full length S1 (30). These observations led us to consider the possibility that results of protein histochemistry binding assays using the S1-NTD of CalEnt would better reflect its broadened tropism. Therefore we compared binding of CalEnt and Cal99 S1-NTDs (aa 19-279) to trachea, intestinal tissues, kidney, and CAM (Fig. 4.3). In contrast to results expected, Cal99 S1-NTD bound extremely well to epithelial cells in all intestinal tissues tested (Figs. 4.3C, 4.3E, 4.3G, 4.3I, 4.3K) in addition to trachea (Fig. 4.3A), while CalEnt S1-NTD binding was not detectable to any intestinal tissues tested (Figs. 4.3D, 4.3F, 4.3H, 4.3J) except cloaca (Fig. 4.3L). Binding of CalEnt S1-NTD to cloaca, although clearly detectable, was much less than that of Cal99 S1-NTD. Cal99 S1-NTD binding was reproducibly detected to epithelium of duodenum and ileum collected from some chickens, but not others (not shown). Like binding to trachea and intestinal tissues, Cal99 S1-NTD binding to kidney (Fig. 4.3M) and CAM (Fig. 4.3O) was greater than that of Cal99 S1. Additionally, while Cal99 S1 was observed to bind only to tubular epithelium in kidney tissue (Fig. 4.2M), Cal99 S1-NTD was observed bound to both tubular epithelium and epithelial cells of the parietal and visceral layers of the Bowman's capsules (Fig. 4.3M). In contrast, binding of CalEnt S1-NTD to neither kidney nor CAM was detected (Figs. 4.3N and 4.3P). CalEnt S1-NTD binding to tracheal epithelium was

quite evident when double the concentration of protein was used (Fig. 4.3B'), but at a much lower level than Cal99 S1-NTD binding. However, CalEnt S1-NTD at twice the concentration did not bind detectably to any of the other tissues tested (not shown). CalEnt S1-NTD binding to cloaca at double concentration was not tested, because binding had already been demonstrated at the standard concentration.

3.4. Effect of S2 ectodomain on CalEnt S1 binding to chicken tissues

Addition of the S2 ectodomain to recombinant Beaudette (70) or Ark (30) S1 proteins to generate S-ectodomain enabled or improved binding to relevant tissues. These previous observations suggested that spike histochemistry assays using CalEnt S-ectodomain might better reflect its tropism. However, extension of recombinant CalEnt S1 with CalEnt S2 ectodomain did not enable detectable binding to most tissues tested (not shown). Like CalEnt S1-NTD, binding of CalEnt S-ectodomain was detectable only to cloaca. However, the binding pattern of CalEnt S-ectodomain to cloaca differed somewhat from that of CalEnt S1-NTD. Whereas CalEnt S1-NTD bound to both cloacal secretory cells and apical surface of the epithelium (Fig. 3L), CalEnt S-ectodomain binding was restricted to secretory cells (Fig. 4.4).

3.5. Recombination within CalEnt S gene

After finding that the enteric tropism of CalEnt IBV could not be explained by the tissue binding specificity of its spike protein as demonstrated in protein histochemistry assays, even when the S2 ectodomain was included, we considered the possibility that properties of the S2 subunit of the CalEnt S protein might contribute to the tropism of the CalEnt virus by affecting functions of the S protein subsequent to attachment. While CalEnt and Cal99 mature S1 subunits have 93% aa sequence identity, their S2 subunits have only 85% aa sequence identity, an unexpected

observation because IBV S2 subunits are generally more conserved than S1 subunits (11). This observation led us to suspect recombination between the S1 and S2 coding regions of the CalEnt S gene. To identify potential origins of the CalEnt S2-coding sequence, a BLAST search of GenBank sequences was conducted with the CalEnt S2-coding sequence. Results indicated that the CalEnt S2 coding region nucleotide sequence was most similar (92% nucleotide identity) to S2 nucleotide sequences of four IBV isolates collected in Malaysia during 2014 and 2015 (IBS037A/2014, IBS037B/2014, IBS051/2014, IBS180/2015; GenBank accession numbers KU949737, KU949738, KU949739, KU949747) (165). Consistent with the similarity of S2 nucleotide sequences, phylogenetic analysis of the CalEnt S2 aa sequence and 576 IBV S2 amino acid sequences by neighbor-joining with 1000 bootstrap replicates placed CalEnt S2 in a distinct group along with S2 aa sequences of those four Malaysian IBV isolates, plus one more isolate from Malaysia collected in 2004 (isolate V9/04; Genbank accession # FJ518782), with strong bootstrap support (93%) (not shown). Consistent with the possibility of recombination, phylogenetic analysis of the CalEnt S1 aa sequence and GenBank IBV S1 aa sequences did not group CalEnt with the Malaysian IBV isolates. Recombination analysis identified a putative recombination event between Cal99 and Malaysian IBV isolate IBS180/2015 genomes with the breakpoint at nucleotide position 1375 (99% confidence interval nucleotides 1286-1381), with 96.6% nucleotide identity between Cal99 and CalEnt S gene sequences preceding the breakpoint and 90.6% nucleotide identity between IBS180/2015 and CalEnt S gene sequences following the breakpoint (Fig. 4.5). This putative recombination event was identified by all seven recombination detection programs used, with Bonferroni-corrected *P* values each $<5x10^{-14}$. The breakpoint identified corresponds to codon 459 (99% confidence interval codons 429-461), consistent with

the high density of amino acid differences between CalEnt and Cal99 following aa 459 in SD1" and SD2" portions of S1 (Fig. 4.1).

3.6. Unique sequence of CalEnt putative S2' protease recognition sequence

Alignment of CalEnt and IBS180/2015 S2 aa sequences revealed aa acid differences concentrated near the amino-terminal and carboxyl-terminal regions of the S2 ectodomain (Fig 4.6). Slightly over half (55%) are non-conservative differences. Of particular note is a cluster of four non-conservative aa differences immediately preceding the putative S2' cleavage site and fusion peptide. These four aa substitutions in CalEnt, along with the substitutions found in the two preceding positions in both CalEnt and IBS180/2015 S2, are rare; they are each found at the corresponding positions in ≤ 5% of IBV S2 aa sequences in GenBank (Fig. 4.7B). The last of these aa, glycine at aa position 695, and the exact aa sequence of CalEnt S2 at aa positions 689-694 are found exclusively in CalEnt S2 among IBV S protein sequences in GenBank. In the predicted structure of CalEnt S2, this unique 7 aa sequence (aa 689-695) is found in an exposed loop (Fig. 4.7A). A striking feature of the sequence of this loop in CalEnt S protein compared to other IBVs is the presence only one proline, in the first position. Most other IBV S sequences in GenBank, including IBS180/2015, have two or three prolines in this loop (Figs. 4.7C and 4.7D), usually in positions 2, 3, and 6 (Figs. 4.7C and 4.7D). The reduced number of prolines in CalEnt S2 would be expected to increase the flexibility of this loop (166, 167, 168), with unknown consequences for its function.

Among the few IBV S2 sequences having only one proline in the region corresponding to the unique sequence in CalEnt S2 are those of Beaudette strains, with its single proline at position 3. The basic aa arginine replaces the highly-conserved proline at position 6. Two additional aa

substitutions surrounding the S2' cleavage site allow Beaudette S2 to be cleaved by furin, resulting in Beaudette's broadened tropism to include mammalian cell lines (91). To explore the possibility that the unique sequence in CalEnt S2 might contribute to CalEnt's broadened tropism, we examined CalEnt, Cal99, and IBS180/2015 S2 aa sequences for potential protease cleavage sites. In addition to the conserved putative S2' trypsin or other serine protease cleavage site (90) indicated by thick arrows in Figs. 4.7B, 4.7C, and 4.7D, additional sites predicted to be cleaved by digestive enzymes pepsin and chymotrypsin and by the endosomal protease Cathepsin K were found in this region only in the CalEnt S2 sequence (Fig. 4.7B).

4. DISCUSSION

An unusual enterotropic IBV isolate CalEnt was detected in the intestines of a California broiler flock and recovered from embryonic intestine during virus isolation. However, upon experimental inoculation into SFP chickens the virus also caused mild respiratory symptoms (13). These findings suggested that the virus had gained extended enteric tropism while retaining respiratory tropism to some extent. In this study, we examined the possibility that the extended tropism of IBV CalEnt was due to an increased ability of its S1 protein to bind to intestinal tissues. Since CalEnt S1 showed the highest amino acid identity among IBV S protein sequences in GenBank to the S1 of California variant Cal99, a typical respiratory IBV, we compared binding of CalEnt and Cal99 S1 to relevant chicken tissues.

Previous studies in experimentally infected chickens with different IBV isolates indicated that the viruses could be recovered from many different parts of the alimentary tract (24, 109, 110). Consistent with these studies, our finding of binding of Cal99 S1 to trachea and some enteric tissues (duodenum, cecal tonsils) was expected, even though infection with this virus did not

produce any noticeable enteric symptoms in experimentally inoculated chickens (169). Contrary to expectations, no detectable binding of CalEnt S1 to any enteric tissues was observed. In addition, CalEnt S1 did not bind to trachea. Decreased binding ability of CalEnt S1 to tracheal epithelium compared to Cal99 S1 might have been due to the predicted structural difference near the putative sugar-binding site and/or additional potential structural differences not identified by structural modeling based on the same known IBV S1 structure.

The NTD of S1 or the full length S-ectodomain of other IBV types (Ark, Mass) shows improvement over S1 in the attachment to chicken tissues in protein binding assays (30, 70, 150). Therefore we also tested binding of CalEnt S1-NTD and S1-ectodomain to intestinal tissues. We found that Cal99 S1-NTD also showed improved binding compared to whole S1 to all tissues tested, as expected. However, neither the S1-NTD nor the S-ectodomain of CalEnt altered the scenario of no binding to any intestinal tissues. In contrast, CalEnt S1-NTD did bind to tracheal epithelium, but only when used at twice the standard concentration, indicating that it bound with a lower affinity compared to Cal99 S1-NTD. Poor binding of CalEnt S1-NTD to tracheal epithelium is consistent with the finding that CalEnt infection resulted in mild respiratory symptoms in chickens after experimental inoculation (13), which had suggested that the virus had not lost its respiratory tropism. In addition, lack of binding of CalEnt S-ectodomain and S1-NTD to CAM explained the fact that virus could not be detected in CAM or allantoic fluid during virus isolation attempts (13). Although the virus could replicate in embryo intestine (13), we did not test binding of CalEnt S-NTD to embryonic intestine.

Although the IBV S1-NTD is necessary and sufficient for binding to carbohydrate receptors on respiratory epithelium in the protein histochemistry assay we used (78), Shang, *et al*. (52), demonstrated that the IBV S1-CTD could bind to live cells. The CryoEM structure of trimeric

IBV S protein shows that S1-CTD contains two extended loops on the core structure that were designated as putative receptor-binding motifs, assumed to interact with a yet-to-be-identified protein receptor/co-receptor (52). One of the non-conservative substitutions in the CalEnt S1-CTD compared to Cal99 (glutamic acid to glutamine at aa 284) is within one of those motifs. Glutamine (a polar, uncharged aa) at the corresponding aa position is found in only 4.5% of over 900 IBV S1 aa sequences retrieved from GenBank. Other IBV S1s have either the charged aa glutamic acid (50%) or non-polar aa leucine (45%) at the corresponding position. However, because receptor binding by the S1-CTD is not detected by the assay we used, we could not determine the effect of this aa substitution or any of the other aa substitutions in CalEnt's S1-CTD on binding to intestinal epithelial cells. Thus, our finding that CalEnt S1 protein does not bind to intestinal epithelium might be due to this limitation of the protein histochemistry assay. It remains possible that poor binding of CalEnt S1-NTD to carbohydrate receptors on intestinal epithelium is balanced by improved interaction of CalEnt S1-CTD with other receptors or co-receptors on intestinal epithelial cells.

Binding properties of S1 proteins are not the only determinant of tropism. Mork, *et al*. (170) found that although recombinant S1 protein from the nephropathogenic IBV strain B1648 and an IBV QX strain associated with reproductive disease in addition to kidney disease each bound well to primary oviduct epithelial cells, only the QX strain infected those cells. Apparently infection of oviduct epithelial cells was limited at a step subsequent to the initial attachment detected by their binding assay. This provides an example converse to that of CalEnt, where we found that binding by S1 to intestinal epithelium was not detected, yet infection of epithelial cells resulting in tissue damage occurs *in vivo* (13). In the case of CalEnt, it is possible that poor binding by S1 is compensated in intestinal epithelial cells at a later step in infection. One such potential

step is activation of the S2 protein for membrane fusion required for viral entry by cleavage at a site designated S2' (90). The extended host tropism of the extensively laboratory-passaged IBV Beaudette strain for mammalian cell lines is due to the presence of a furin cleavage site at its S2' site (68, 91). CalEnt S2 has a unique amino acid sequence at its S2' site not found in any other IBV S protein sequence in GenBank. This unique sequence includes predicted recognition sites for digestive enzymes pepsin and chymotrypsin, and an endosomal protease Cathepsin K. The tissue distribution of Cathepsin K in chickens is not known. However, activation of CalEnt S2 protein for viral entry by host enzymes in the digestive tract might facilitate viral entry into intestinal epithelial cells, overcoming poor viral attachment.

We performed recombination analysis of the complete S gene of the CalEnt isolate to elucidate the possible source/origin of the virus. A predicted recombination event was accepted by all seven algorithms tested, where a California strain (Cal99-like) donated most of the sequences encoding S1 and a strain similar to Malaysian isolate IBS180/2015 contributed the rest of the S gene, including its S2-coding portion. The information available about the Malaysian isolates with S2 sequences most similar to CalEnt indicates that one of them was isolated from a layer flock with a clinical history of respiratory disease (171). The GenBank entries of four of them indicate that the isolates are nephropathogenic, but the published paper only indicates swollen kidneys in association with one of the isolates (165). Recombination analysis of the full genome sequence of CalEnt should be done to reveal evidence of other potential recombination events that might have occurred outside of the S gene. Interestingly, the two putative parental strains identified were isolated from two widely separated geographical locations. In addition, the putative recombinant CalEnt was isolated from the region from where one of the putative parental strains was isolated and is still predominant in that region. This might hint that at the time CalEnt was isolated (2012),

the recombination event had happened recently, in California. The unique sequence at the S2' cleavage site apparently evolved after the recombination event and perhaps facilitated the ability of the virus to infect and damage intestinal epithelium. Selective pressure might increase the poor binding affinity of CalEnt S1 for intestinal epithelium as has been observed in the case of the S1 protein of the enterotropic Guinea fowl coronavirus within a three-year period in France (172). Thus enteric IBV strains have the potential to become more prevalent in California if appropriate selective pressure is present.

In this study, we first tried to discover the basis of the unusual enteric tropism of CalEnt IBV at the stage of virus attachment to carbohydrate receptors mediated by the S1 protein. However, the spike protein binding assay did not reflect the tissue tropism. This assay could not rule out a possible role for the S1-CTD in interacting with a yet-to-be-identified receptor or co-receptor, which remained undetected in our protein binding assay. Another possible basis of CalEnt's unique tropism is the presence of a unique sequence within the S2' cleavage site of S2 which has the potential to affect tissue tropism at the stage of viral entry. Further study is needed to uncover the role of this unique sequence in tissue tropism.

ACKNOWLEDGEMENTS

We thank Cynthia Hutchinson and Natalia Petrenko for excellent technical assistance. This work was funded by the State of Alabama Animal Health and Disease Research, Center for Food Animal Health UC Davis, and the Poultry Medicine Programs.

A

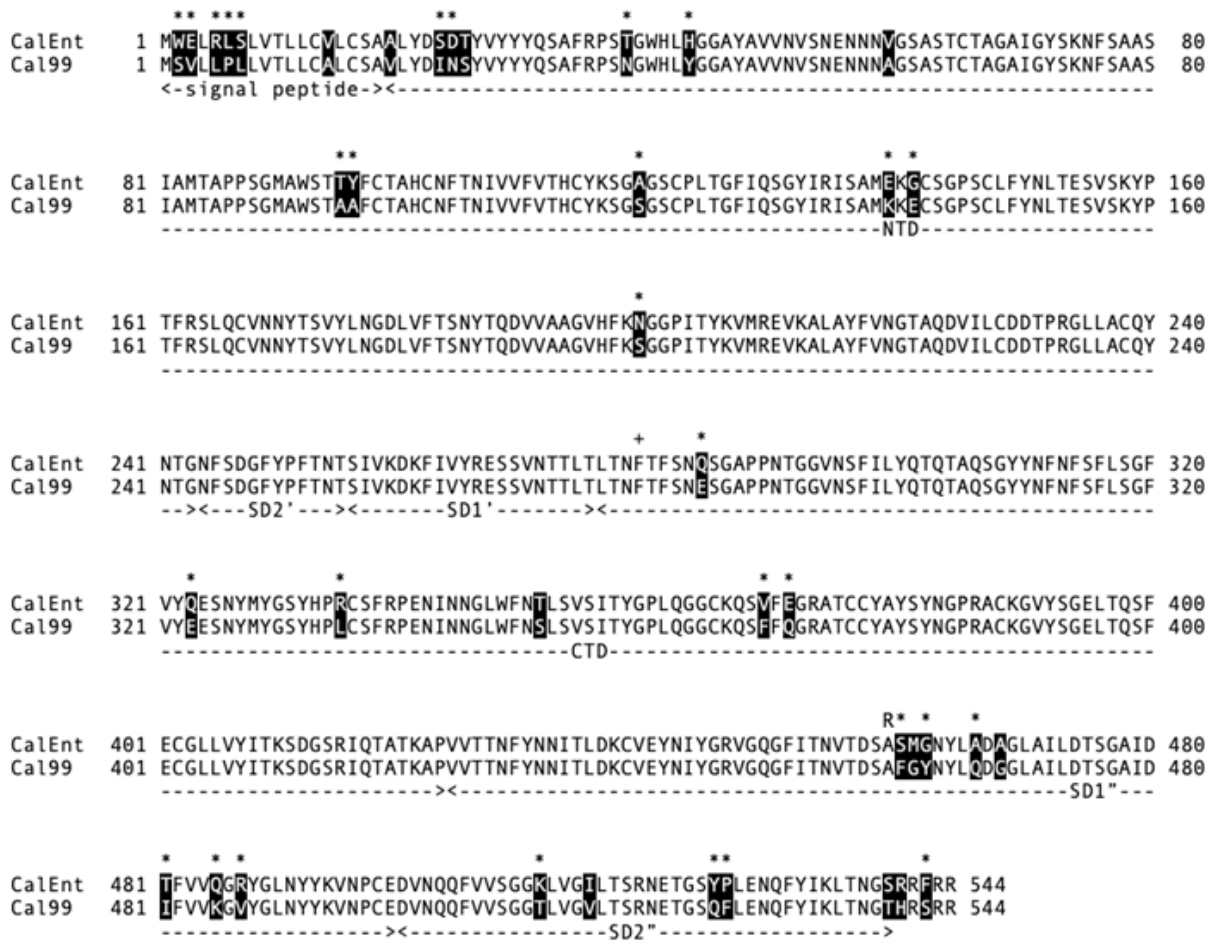
CalEnt 1 MWELRLSLVTLLCVLCSAALYDSDTYVYYYQSAFRPSTGWHLHGGAYAVVNVSNENNNVGSASTCTAGAIGYSKNFSAAS 80
Cal99 1 MSVLLPLLVTLLCALCSAVLYDINSYVYYYQSAFRPSNGWHLYGGAYAVVNVSNENNNAGSASTCTAGAIGYSKNFSAAS 80
<-signal peptide-><
CalEnt 81 IAMTAPPSGMAWSTTYFCTAHCNFTNIVVFVTHCYKSGAGSCPLTGFIQSGYIRISAMEKGCSGPSCLFYNLTESVSKYP 160
Cal99 81 IAMTAPPSGMAWSTAAFCTAHCNFTNIVVFVTHCYKSGSGSCPLTGFIQSGYIRISAMKKECSGPSCLFYNLTESVSKYP 160
NTD
CalEnt 161 TFRSLQCVNNYTSVYLNGDLVFTSNYTQDVVAAGVHFKNGGPITYKVMREVKALAYFVNGTAQDVILCDDTPRGLLACQY 240
Cal99 161 TFRSLQCVNNYTSVYLNGDLVFTSNYTQDVVAAGVHFKSGGPITYKVMREVKALAYFVNGTAQDVILCDDTPRGLLACQY 240
CalEnt 241 NTGNFSDGFYPFTNTSIVKDKFIVYRESSVNTTLTLTNFTFSNQSGAPPNTGGVNSFILYQTQTAQSGYYNFNFSFLSGF 320
Cal99 241 NTGNFSDGFYPFTNTSIVKDKFIVYRESSVNTTLTLTNFTFSNESGAPPNTGGVNSFILYQTQTAQSGYYNFNFSFLSGF 320
--><---SD2'---><-------SD1'-------><
CalEnt 321 VYQESNYMYGSYHPRCSFRPENINNGLWFNTLSVSITYGPLQGGCKQSVFEGRATCCYAYSYNGPRACKGVYSGELTQSF 400
Cal99 321 VYEESNYMYGSYHPLCSFRPENINNGLWFNSLSVSITYGPLQGGCKQSFFQGRATCCYAYSYNGPRACKGVYSGELTQSF 400
CTD
CalEnt 401 ECGLLVYITKSDGSRIQTATKAPVVTTNFYNNITLDKCVEYNIYGRVGQGFITNVTDSASMGNYLADAGLAILDTSGAID 480
Cal99 401 ECGLLVYITKSDGSRIQTATKAPVVTTNFYNNITLDKCVEYNIYGRVGQGFITNVTDSAFGYNYLQDGGLAILDTSGAID 480
><SD1"---
CalEnt 481 TFVVQGRYGLNYYKVNPCEDVNQQFVVSGGKLVGILTSRNETGSYPLENQFYIKLTNGSRRFRR 544
Cal99 481 IFVVKGVYGLNYYKVNPCEDVNQQFVVSGGTLVGVLTSRNETGSQFLENQFYIKLTNGTHRSRR 544
><SD2"-->

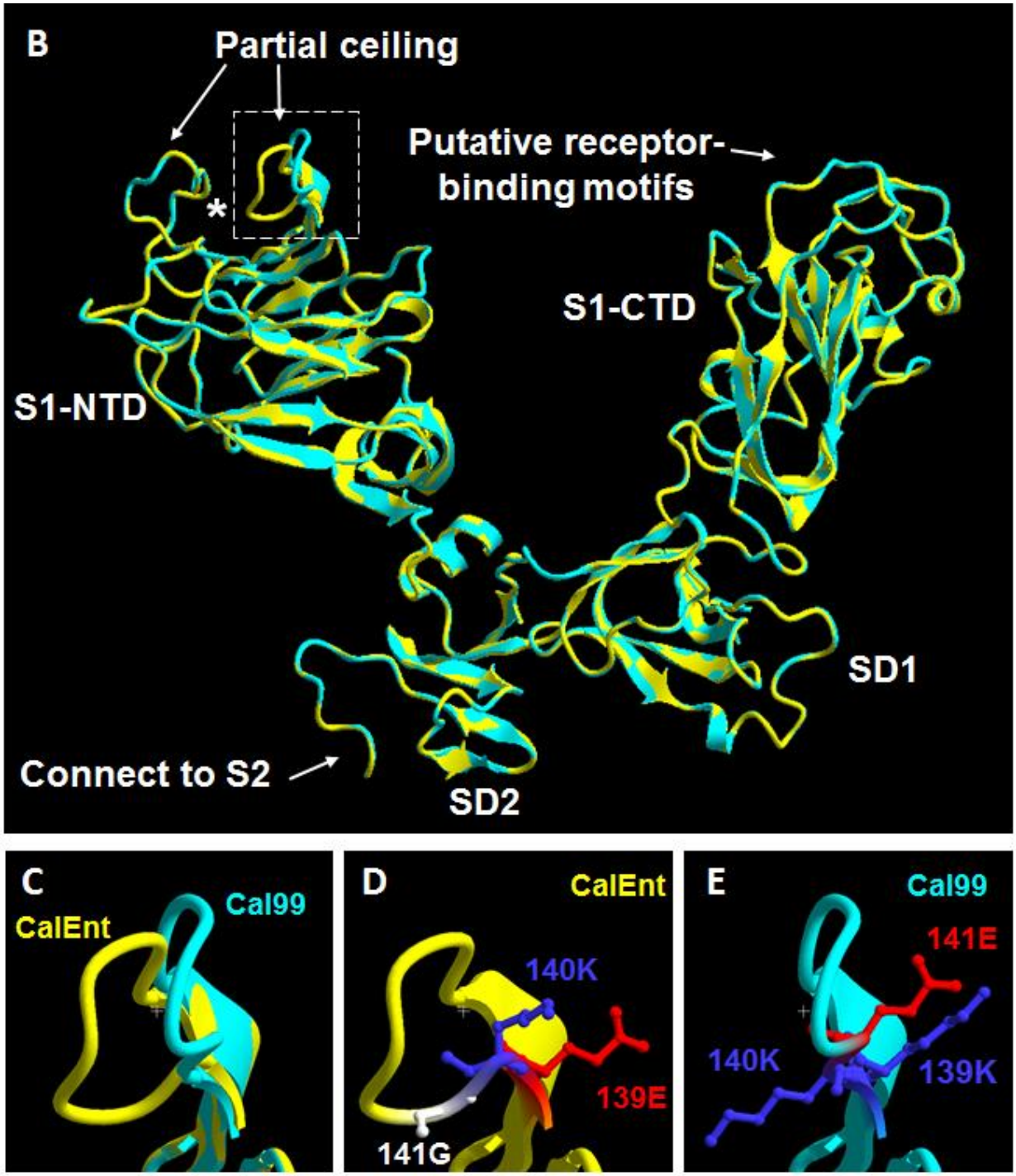

Fig. 4.1. Comparison of aa sequences and predicted structures of IBV CalEnt and Cal99 S1 proteins. (A) CLUSTALW aa sequence alignment of CalEnt and Cal99 (GenBank accession # AAS00080.1) S1 proteins. Aa differences are highlighted in black. Non-conservative aa

differences are indicated by asterisks above each line of the alignment. Most of the differences are non-conservative (29/38 = 76%). The codon within which recombination analyses predicts a recombination event is indicated by an R above the aligned sequences. The extent of each of the S1 subdomains as defined by (52) is indicated below each line of the alignments. SD1' and SD1" together form SD1. Likewise SD2' and SD2" form SD2. The last S1 aa included in recombinant S1-NTD proteins (aa 279) is indicated by a + above the alignment. (B) Alignment of predicted structures of S1 proteins from Cal99 and CalEnt variants. Predicted structures of S1 monomer within the S trimer were generated by SWISS-MODEL based on the known structure of IBV M41 trimeric S. Ribbon models of Cal99 (cyan) and CalEnt (yellow) S1 proteins are overlaid. S1-NTD, S1-CTD, SD1, and SD2 and other structural features identified by (52) are labeled. * indicates putative sugar-binding site, protected by a partial ceiling (52). Putative receptor-binding motifs identified by (52) are based on location of receptor-binding motifs in other coronavirus S1-CTDs. The box around one side of the partial celling indicates the region shown in panels C-E, where the predicted structures of Cal99 and CalEnt proteins differ somewhat. (C) Enlarged view of the boxed region in (B), showing the different predicted pathways of the amino acid backbone in this region of Call99 (cyan) and CalEnt (yellow) S1 proteins. In (D) and (E) ball and stick models of aa side chains at positions 139 -141 have been added. Cal99 and CalEnt S1 differ at aa positions 139 and 141. The side chain of the lysine (K) at aa position 140 is predicted to be oriented differently in Cal99 and CalEnt S1. Ball and stick aa side chain models and the aa labels are colored according to side chain chemical properties: red, acidic; blue, basic; white, non-polar.

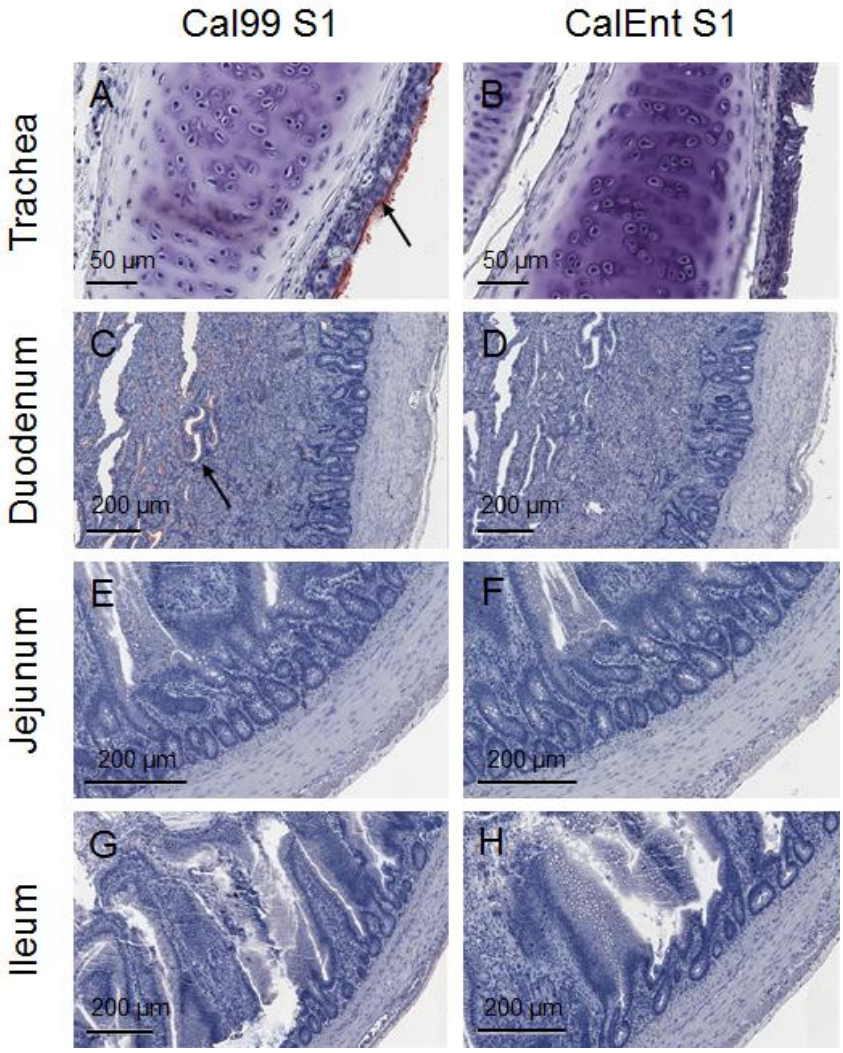
Cal99 S1
CalEnt S1
Trachea
Duodenum
Jejunum
Ileum
A
B
C
D
E
F
G
H
50 µm
200 µm

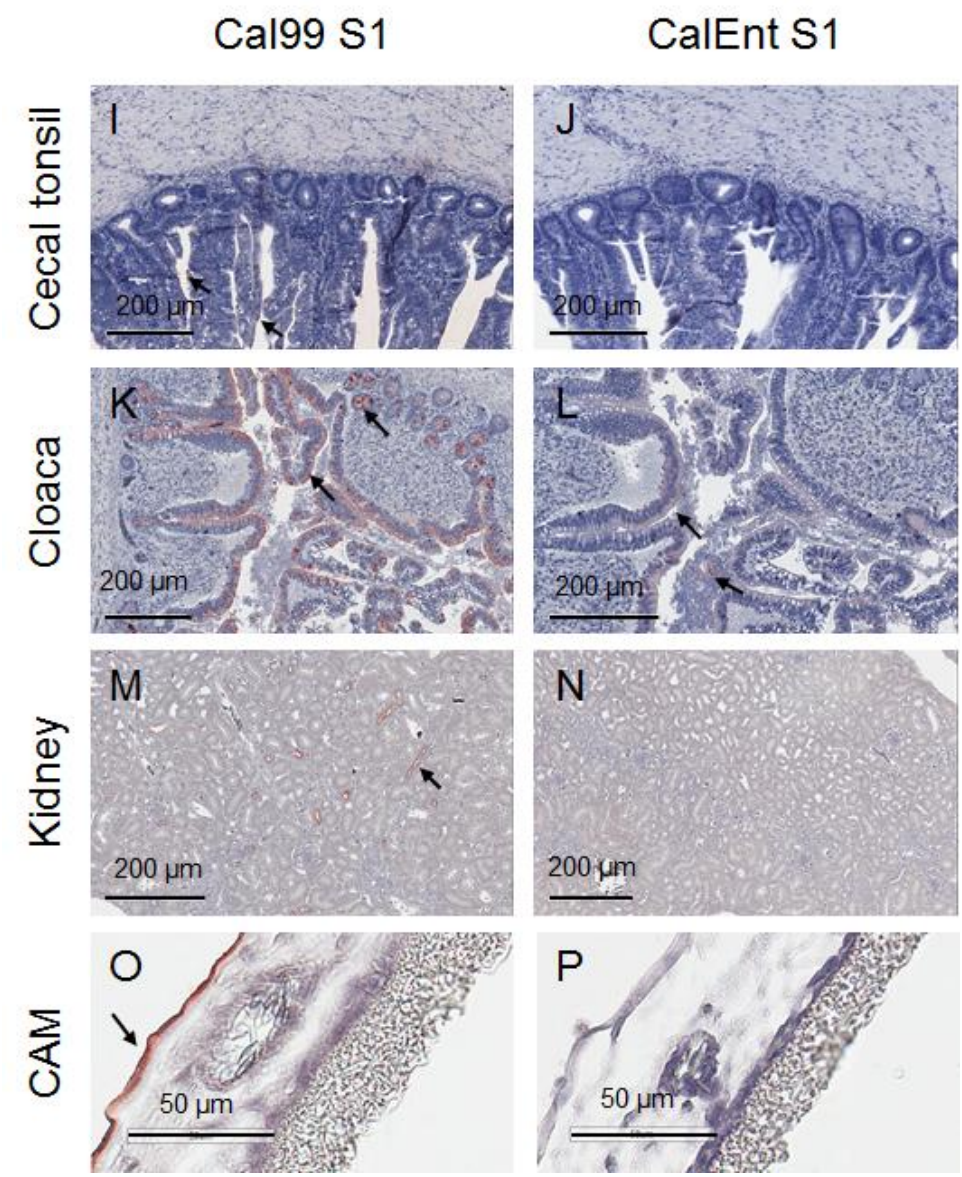

Fig. 4.2. Protein histochemistry demonstrating recombinant S1 proteins of IBV Cal99 and CalEnt variants binding to chicken tissues. Purified *Strep*-tag II-tagged trimeric recombinant S1 proteins (100 µg/ml) were bound to formalin fixed chicken tissues and AEC^{+} chromogenic substrate was used to identify bound spike protein as indicated by red staining (arrows). In the left panels recombinant S1 was from the Cal99 variant. In the right panels, the recombinant S1 was from CalEnt enteric variant. S1 protein histochemistry is shown in trachea (A and B), duodenum (C and

D), jejunum (E and F), ileum (G and H), cecal tonsil (I and J), cloaca (K and L), kidney (M and N), CAM (O and P). CAM=chorioallantoic membrane.

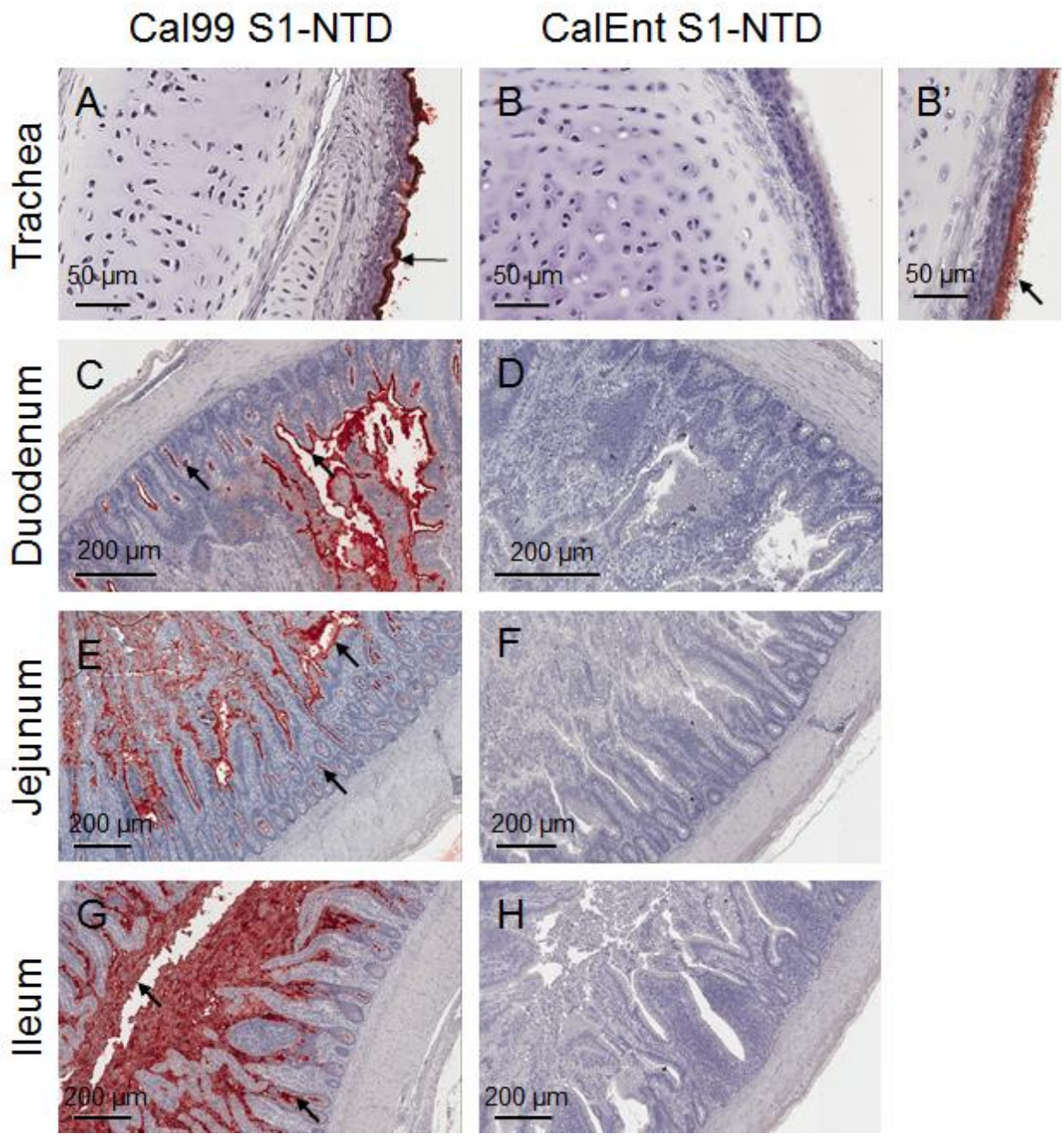

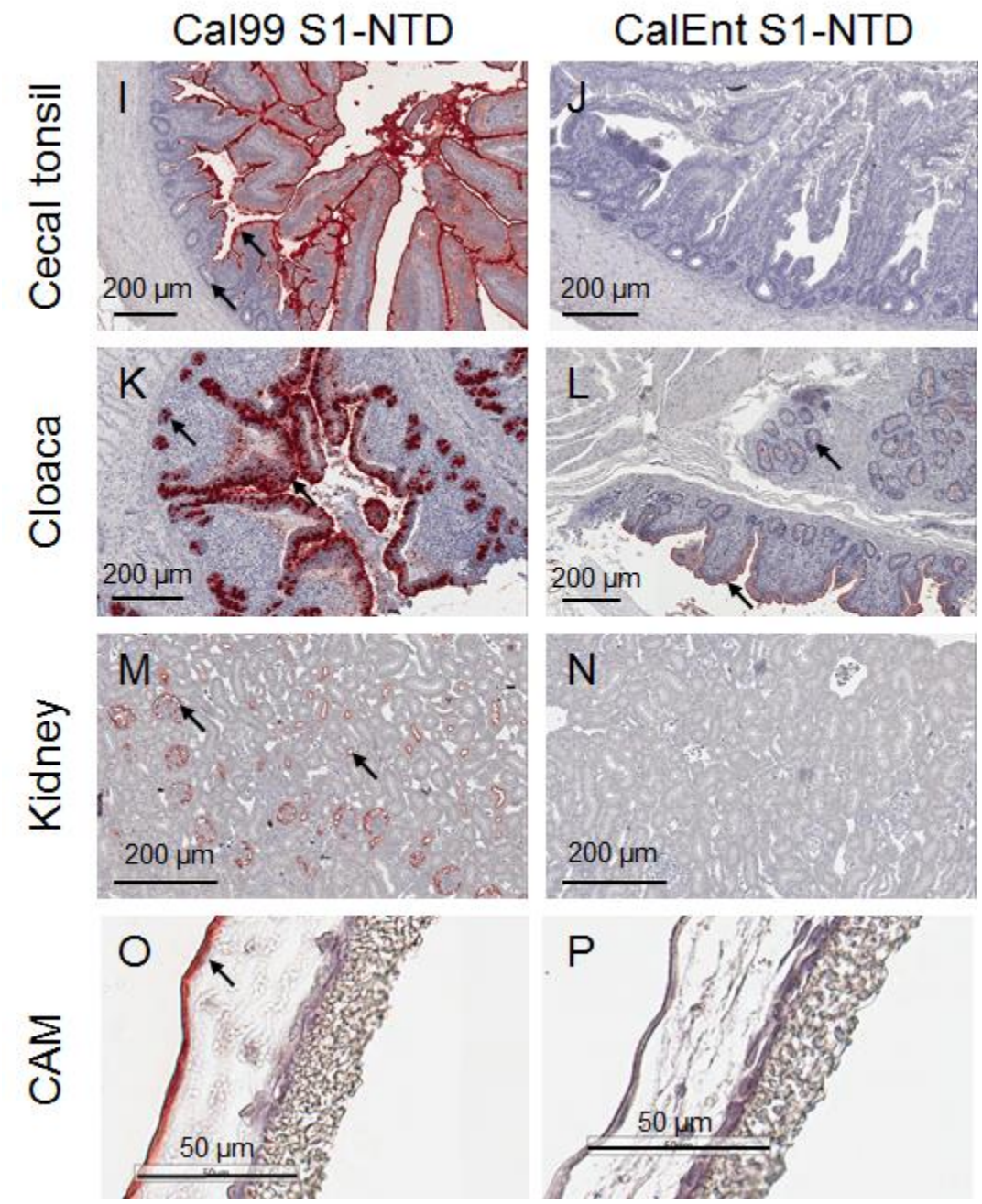

Fig. 4.3. Protein histochemistry demonstrating recombinant S1-NTD of IBV Cal99 and CalEnt variants binding to chicken tissues. Purified trimeric *Strep*-tag II-tagged recombinant S1-NTDs (54 µg/ml) were bound to formalin fixed chicken tissues and AEC^{+} chromogenic substrate was used to identify bound proteins as indicated by red staining (arrows). In the left panels recombinant

S1-NTD was from the Cal99 variant. In the right panels, the recombinant S1 was from CalEnt enteric variant. S1-NTD protein histochemistry is shown in trachea (A and B), duodenum (C and D), jejunum (E and F), ileum (G and H), cecal tonsil (I and J), cloaca (K and L), kidney (M and N), CAM (O and P). CAM=chorioallantoic membrane. (B') Protein histochemistry using 108 µg/ml CalEnt S1-NTD protein and trachea.

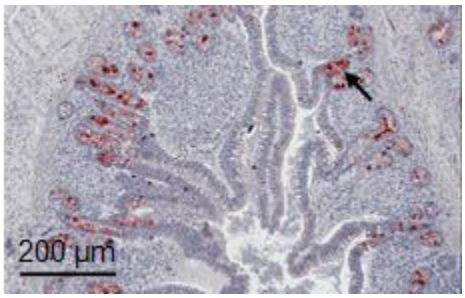

Fig. 4.4. Protein histochemistry demonstrating recombinant S-ectodomain protein of IBV CalEnt variant binding to cloaca. Purified trimeric *Strep*-tag II-tagged recombinant S-ectodomain (50 µg/ml) was bound to formalin fixed chicken choana and AEC^{+} chromogenic substrate was used to identify bound proteins as indicated by red staining (arrows).

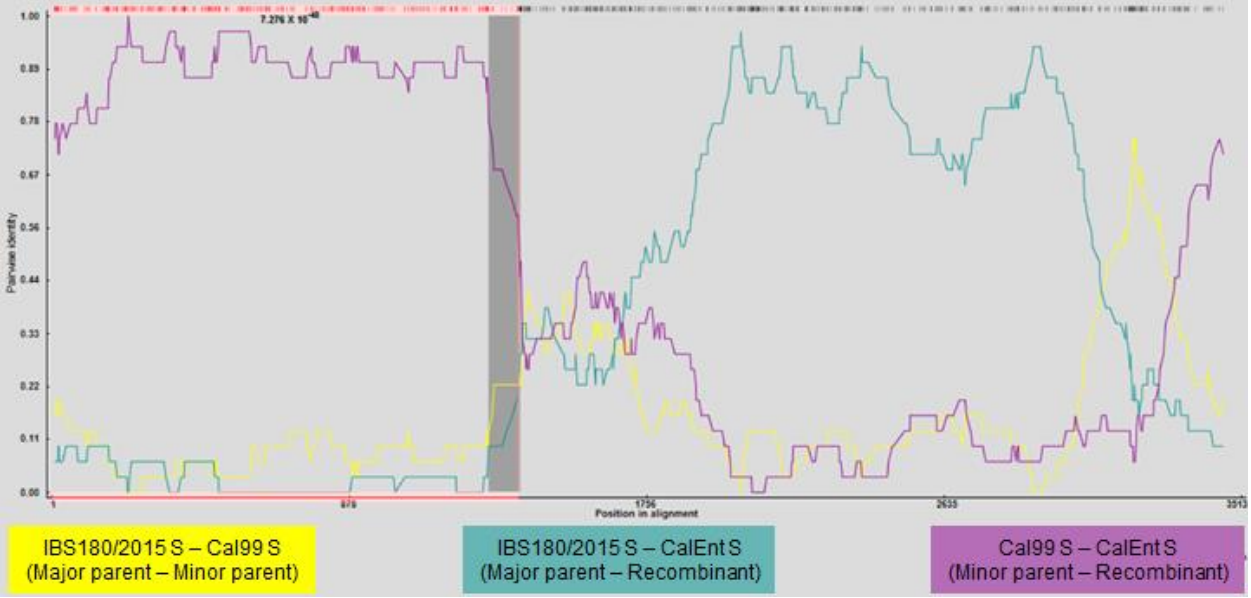

Fig. 4.5. RDP analysis showing recombination between Malaysian IBV isolate IBS180/2015 (Genbank accession #KU949747; major parent) and Cal99 (minor parent) producing the CalEnt S gene. The Y-axis shows percentage nucleotide identity for the indicated sequence pairs against the position in the alignment on the X axis. The short vertical lines at the top indicate positions of variability. Grey shaded area shows the 99% confidence interval for putative recombination break point at nucleotide position 1375 (marked by pink line). Bonferroni-corrected *P* values for each of the seven recombination detection programs for this recombination event were each $<5x10^{-14}$.

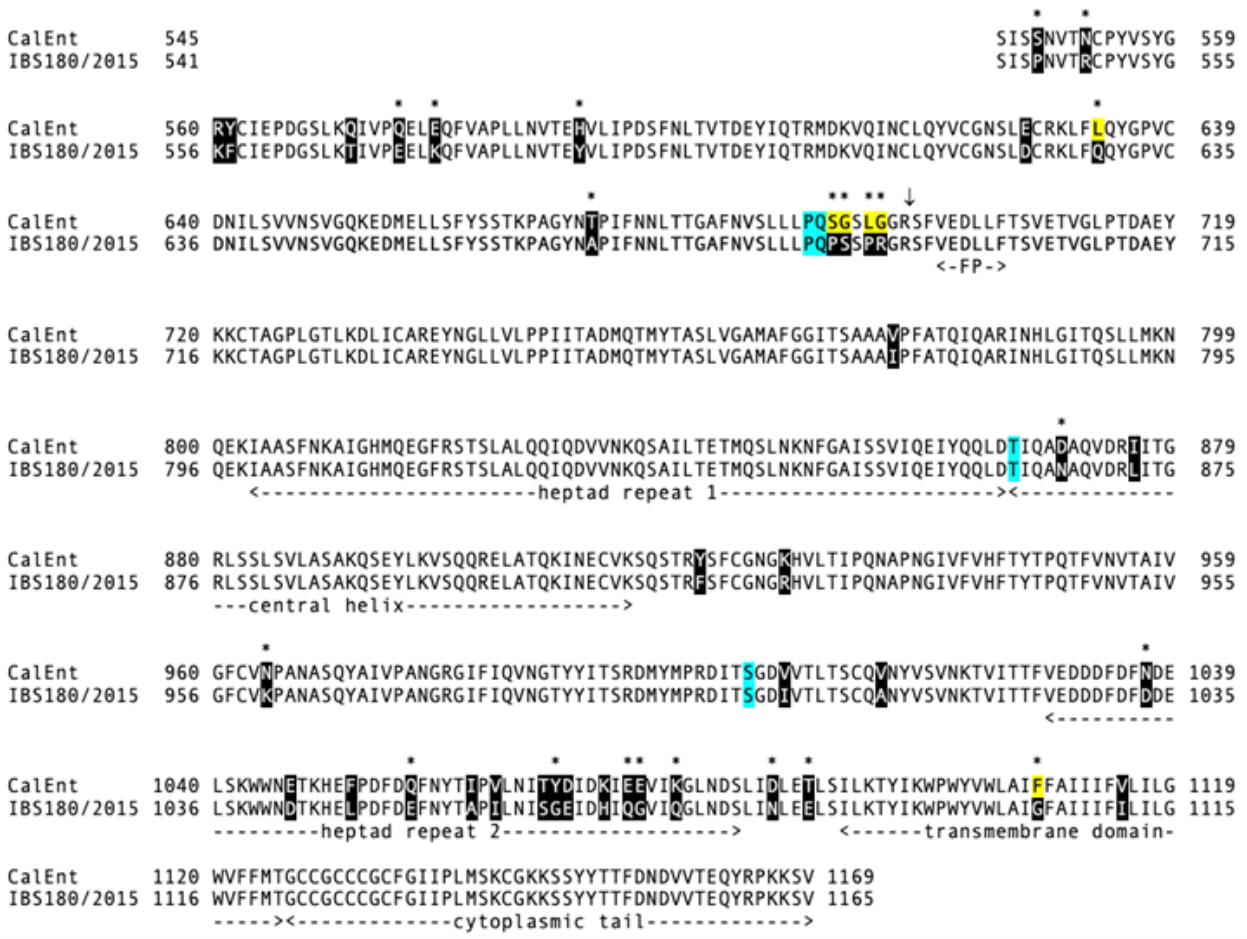

Fig. 4.6. Comparison of amino acid sequences of IBV CalEnt and Malaysian isolate IBS180/2015 S2 (GenBank accession number KU949747) proteins. A CLUSTALW amino acid sequence alignment is shown. Amino acid differences are highlighted in black or yellow. Non-conservative aa differences are indicated by asterisks above each line of the alignment; 55% (22/40) differences are non-conservative. The extent of IBV S2 subdomains as defined by Millet and Whittaker (90) (FP=fusion peptide), Shang, *et al*. (52) (heptad repeats, central helix, and transmembrane domain), and Lontok, *et al*. (173) (cytoplasmic tail) is indicated below each line of the alignments. The vertical arrow above the aligned sequences indicates the putative S2' cleavage site (90). Cyan highlighting indicates rare (≤5% of sequences in GenBank) non-conservative aa substitutions in

both Cal Ent and IBS180/2015. Yellow highlighting indicates rare (≤5% of sequences in GenBank) non-conservative aa substitutions in CalEnt. Conservative rare aa substitutions are not marked.

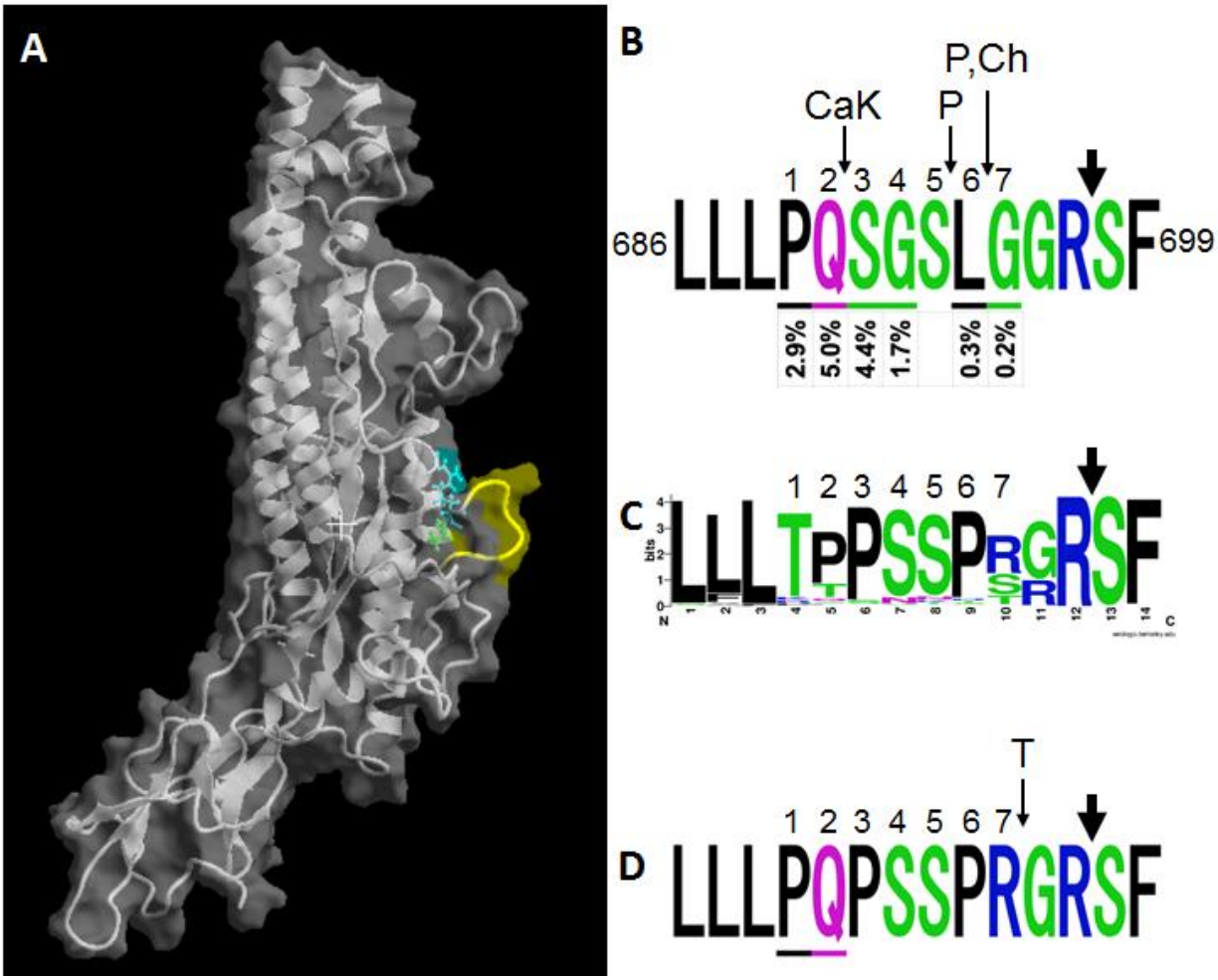

Fig 4.7. Unique amino acid sequence present in CalEnt S2 near putative S2' cleavage site. (A) Predicted structure of CalEnt S2 monomer (based on known structure of M41 S trimer). Ribbon model is overlaid with space-filling model. Portion of CalEntS2 with unique aa sequence is indicated in yellow. Putative S2' cleavage site is between Arg (cyan) and Ser (green), which are indicated by ball and stick models. (B-D) Comparison of putative S2' recognition sequences of CalEnt (B), IBV consensus (C), and Malaysian IBV isolates with S2 sequences most similar to CalEnt. Amino acids numbered 1-7 are those indicated in yellow in panel (A). Flanking sequences of CalEnt S2 matching the consensus are included at each end. Amino acids are colored according

to their chemical properties: polar amino acids (G,S,T,Y,C,) are green, polar amino acids with amido groups (N,Q) magenta, basic (K,R,H) blue, acidic (D,E) red and hydrophobic (A,V,L,I,P,W,F,M) amino acids are black. The thick black arrows above each sequence indicate the putative S2' trypsin or other serine protease cleavage site (90). Thin arrows above the CalEnt aa sequence in B and the Malaysian IBV aa sequence in D indicate predicted endosomal protease cleavage sites and digestive enzyme cleavage sites predicted by PROSPER and PeptideCutter. CaK = Cathepsin K, P = pepsin, Ch = chymotrypsin, T = trypsin. Rare amino acids at each position in the CalEnt and Malaysian IBV sequences are underlined. The frequency among 585 IBV S2 aa sequences in GenBank of the rare amino acids observed in the CalEnt sequence are indicated below the CalEnt sequence. The consensus logo in (C) was generated from 576 S2 sequences from S genes most closely related to CalEnt S using the WebLogo server at https://weblogo.berkeley.edu.

CHAPTER 5

Early Vaccination of Chickens Induces Suboptimal Immunity against Infectious Bronchitis Virus

Avian Diseases 63(1):38-47, 2019

F. Saiada, F. Eldemery, R.A. Zegpi, S.L. Gulley, A. Mishra, V.L. van Santen, H. Toro [a]

Department of Pathobiology, Auburn University, Auburn, AL 36849

[a] Senior and corresponding author. E-mail: torohar@auburn.edu

SUMMARY. Infectious bronchitis virus (IBV) is highly prevalent in broiler chickens despite extensive vaccination commonly conducted early after hatch. The effects of early vaccination on immune responses were further investigated in chickens primed at increasing ages followed by booster vaccination with an attenuated Arkansas-Delmarva Poultry Industry (ArkDPI)-type vaccine. Results show that vaccination on day one of age elicits significantly lower systemic and mucosal antibody responses compared to vaccination at later time points in the life of the chicken. The increase of IBV antibodies in serum from secondary responses after booster vaccination was more dramatic and significantly higher when measured by an Ark-S1 protein enzyme linked immunosorbent assay (ELISA) compared to measuring by non-Ark serotype whole virus ELISA, which underlines the immunogenic importance of the virus' spike at inducing antibodies. However, the levels achieved following boosting did not differ significantly between ages of priming. Thus, it seems that the booster vaccination mitigated the differences detected after prime immunization. In contrast to the continued rising of systemic antibodies after booster vaccination, the levels of mucosal IBV-specific IgA decreased after booster vaccination. The recruitment/expansion of $CD4^+$, $CD8^+$, and $CD4^+/CD8^+$ T cell populations in different immune effector sites was increased with age, however remained unaltered by IBV vaccination. In contrast, peripheral blood $CD4^+$ cells showed a significant increase in IBV-vaccinated chickens compared to non-vaccinated age-matched controls both after primary and booster immunization. The results of the current study confirm that IBV vaccination on the day of hatch induces suboptimal IBV immune responses both in the systemic and mucosal compartments. This routine practice may be contributing to the virus' immunological escape and increased persistence of vaccine virus in vaccinated chickens. However, booster vaccination seems to overcome poor initial responses.

1. INTRODUCTION

Avian infectious bronchitis (IB) virus (IBV), belonging to the genus *Gammacoronavirus*, continues to cause important economic losses worldwide. IB outbreaks occur despite extensive vaccination with attenuated vaccines covering multiple serotypes that do not induce cross-protection (11). In addition to lack of cross-protection among prevalent and emerging serotypes, another reason for suboptimal vaccine protection may be that chickens are routinely vaccinated on day of hatch. Accumulating evidence indicates that newly hatched chickens exhibit immature innate and adaptive immune responses (e.g. (174, 175, 176, 177, 178)). Both structural and functional maturation of the mucosa-associated lymphoid tissues are important for effective administration of respiratory virus vaccines and defense against mucosal respiratory pathogens. Although random lymphocyte clusters in conjunctiva associated lymphoid tissue (CALT) have been detected at one week of age, germinal centers and plasma cells appear around four weeks after hatching. Cluster of differentiation (CD)4^+, $CD8^+$, and B-lymphocytes in the CALT have been shown by *in situ* immunohistochemistry to increase in number as chickens developed from one to four weeks of age. In addition, the numbers of $CD4^+$ T cells in the Harderian gland (HG), are also increased in four-week- compared to one-week-old chickens (131). Previous work also suggests that early vaccination might limit the immune repertoire and induce reduced mucosal and systemic immune responses. Indeed, chickens primed at day one of age showed lower IBV-specific IgA and IgG levels in both tear fluid and sera compared to chickens vaccinated on days 7, 14, 21 or 28 of age (22). In addition, birds vaccinated later showed a lesser extent of clinical signs and lesions upon challenge with an IBV field strain compared to birds vaccinated on day of hatch, indicating better protection as a result of vaccination at later ages (22). The current study was

aimed at further understanding the association between age of IBV vaccination and optimum immune responses. Chickens were vaccinated at increasing ages and IBV-specific mucosal and systemic antibody responses against whole virus or a recombinant S1 protein were determined. Furthermore, relative frequency of T and B cells in different immune effector sites was determined after primary and booster immunization.

2. MATERIALS AND METHODS

2.1. Chickens

White leghorn chickens were hatched from specific-pathogen-free eggs (Charles River, North Franklin, CT) and maintained in Horsfall-type isolators in biosafety level 2 facilities. Experimental procedures and animal care were performed in compliance with all applicable federal and institutional animal use guidelines. Auburn University College of Veterinary Medicine is an Association for Assessment and Accreditation of Laboratory Animal Care-accredited institution.

2.2. Vaccination

Chickens were vaccinated ocularly (priming and boosting) with 3×10^5 50% embryo infectious doses (EID_{50}) of a commercially available live attenuated Ark-DPI-type IBV vaccine in a volume of 100 µl. This dose, approximately 100-fold higher than recommended by the manufacturer, is the same vaccine dose used in earlier work demonstrating increased protection as a result of vaccination at later ages (22).

2.3. Experiment 1

Chickens were divided into five groups (n=15/group) and vaccinated (primed) at 1, 7, 14, 21 or 28 days of age. An additional group served as unvaccinated controls. Two weeks after priming chickens were boosted. Lachrymal fluids(151) and sera were collected two weeks after priming and two weeks after boosting for antibody determination by ELISA (described below). Three weeks after boosting nine chickens of each group were euthanized and HGs, cecal tonsils (CT) and spleens collected and placed in complete RPMI medium. Flow cytometry to evaluate T cell populations was conducted on three pools of cells from each organ from vaccinated chickens and a pool of cells from each organ of three unvaccinated age-matched control chickens.

2.3.1. IBV ELISA

Individual serum and tear samples were tested using a conventional commercially available IBV ELISA kit, which utilizes whole non-Arkansas (Ark) serotype virus as antigen (IDEXX Laboratories, Inc., Westbrook, ME). Sera were diluted 1:500 in accordance with the manufacturer's recommendations while tear samples were diluted 1:100. Serum antibody levels were expressed as sample/positive (S/P) ratios, and ratios above 0.2 were considered positive in accordance with kit instructions. IBV-specific IgA levels in tears were determined using horseradish peroxidase-conjugated polyclonal goat–anti-chicken IgA antibodies (Southern Biotechnology Associates Inc., Birmingham, AL) instead of the secondary antibody in the kit and tetramethylbenzidine substrate (Invitrogen, Frederick, MD). Absorbance was measured at 450 nm. Data were analyzed using GraphPad Prism5 software (GraphPad Software Inc., San Diego, CA) by tests indicated in the figure legends. Antibody levels were considered significantly different among groups at $P \leq 0.05$. To determine if age of priming had an effect on magnitude of increase of antibodies upon boosting,

linear regression analysis of the $\log_{10}$ of the fold difference in S/P ratios and OD after boosting compared to after priming versus age of prime vaccination was conducted.

2.3.2. Recombinant S1 protein ELISA

The S1 subunit of the spike (S) protein is the most variable protein among IBV (54) and responsible for the induction of neutralizing antibodies (179). In order to measure Ark S1-specific antibodies in sera and IgA in tears, an S1-specific ELISA was developed. Soluble trimeric recombinant S1 protein was produced in human embryonic kidney (HEK)-293T cells as described (76, 140). In brief, an expression vector encoding a codon-optimized S1 gene of isolate AL/4614/98 (GenBank accession #DQ458217), an Ark-serotype IBV (59), was transfected into HEK293T cells and recombinant S1 protein purified from tissue culture supernatants six days post-transfection using *Strep*-Tactin® Sepharose columns according to the manufacturer's instructions (IBA GmbH, Göttingen, Germany). The concentration of purified protein was determined by Qubit® 2.0 fluorometer (Invitrogen, Carlsbad, CA). The purified S1 protein was visualized by electrophoresis in Mini-PROTEAN®TGX Stain-Free™ Precast Gels (Bio-Rad, Hercules, CA). ELISA plates (Nunc MaxiSorp™, San Diego, CA) were coated with 100 µl of phosphate buffered saline (PBS) containing 0.25 µg/ml of recombinant S1 protein per well during incubation at 4 C overnight. Wells were blocked for 1 hour at room temperature with 200 µl/well of PBS containing 1% bovine serum albumin and 0.05% Tween 20. Individual chicken sera and tear samples diluted 1:100 in PBS were incubated in the wells for 30 min at room temperature. Relative levels of anti-S1 antibodies in serum were determined using reagents of a commercial ELISA kit (IDEXX Laboratories, Inc., Westbrook, ME) and relative anti-S1 IgA levels in tears determined as described above.

2.3.3. Relative frequency of $CD4^+$ and $CD8^+$ T cells

CT, HG and spleen were minced with scissors and then forced through the stainless steel sieve provided in the Sigma cell dissociation sieve - tissue grinder kit with the glass pestle also provided in the kit. Live mononuclear cells were then isolated by density centrifugation over a Histopaque density gradient (1.077 g/ml) (Sigma). Cells were then collected and live cells counted using trypan blue exclusion on a Bright-Line hemocytometer (Hausser Scientific, Horsham, PA) (8). T cell population relative frequencies were determined by flow cytometry as previously described with changes (8). Briefly, $1x10^6$ cells total cells were stained with fluorescein isothiocyanate (FITC)-conjugated mouse anti-chicken CD8b, or biotin-labeled mouse-anti-chicken CD4 (Southern Biotech) and Alexa 660-conjugated streptavidin (Invitrogen). All washes were performed with PBS containing 1% bovine serum albumin and 0.1% sodium azide at 4 C. Unlabeled cells were used as negative controls. The washed cells were fixed in 1% paraformaldehyde PBS overnight at 4 C. Cells were filtered through a 50-µm nylon mesh (Small Parts Inc., Miami Lakes, FL) before analysis on an Accuri C6 flow cytometer. Live cells were gated for lymphocytes and analyzed using CFlow Plus software. Results were expressed as percent positive-stained lymphocytes. Data were analyzed by Student's *t*-test or one-way analysis of variance (ANOVA) followed by Tukey's post-test. Differences were considered significant at $P \leq 0.05$.

2.4. Experiment 2

Cell responses (frequency of B cells and $CD4^+$, $CD8^+$, and $CD4^+CD8^+$ cells) were determined in peripheral blood and CT. Chickens were separated into four vaccinated groups (n=12/group) and vaccinated on days 1, 7, 14, or 21 of age as described for experiment 1.

Additional aged-matched unvaccinated groups served as controls. Each vaccinated group was further divided into two subgroups; a subgroup primed only (n=6), and a subgroup boosted two weeks after priming (n=6). Blood samples (approximately 1 ml) were collected from the brachial vein into EDTA-treated tubes 12 and 18 days after priming or boosting, and CT following euthanasia 18 days after priming or boosting, for both T and B cell determinations in peripheral blood mononuclear cells (PBMC) and CT.

2.4.1. Relative frequencies of T and B cells in PBMC

PBMC were isolated from blood by density centrifugation over a Histopaque density gradient (1.077 g/ml) (Sigma). CD4+ and CD8+ T cell relative frequency was determined as described above. For B cells, staining was conducted using phycoerythrin-conjugated mouse-anti-chicken Bu-1 antibody (Southern Biotech). Further steps and data analysis were conducted as described above.

3. RESULTS

3.1. Experiment 1

3.1.1. IBV antibody responses measured in serum

IBV antibody levels after prime vaccination measured using a commercial IBV ELISA kit (whole virus non-Ark IBV) are shown in Fig. 5.1A. Antibody levels statistically significantly higher than in unvaccinated control chickens were detected in all vaccinated groups ($P<0.05$). However, lower antibody responses were detected in chickens vaccinated at earlier ages compared to levels in chickens vaccinated later in life. Only one chicken vaccinated at 1 day of age achieved

antibody levels considered "positive," above the S/P ratio of 0.2. Only the chickens vaccinated at 28 days of age exhibited S/P ratios over 0.2 for all chickens in the group. Regression analysis of the data, shown in Fig. 5.1B, demonstrated a highly significant positive correlation between level of primary antibody response and increasing age of the birds at vaccination ($P<0.0001$).

The serum IBV antibody levels two weeks after booster vaccination of birds that were primed on days 1, 7, 14, 21 or 28 are shown in Fig. 5.1C. Surprisingly, antibody levels increased significantly after booster vaccination only in groups primed at 1 and 7 days of age. Interestingly, a highly significant negative correlation was found between the magnitude of increase of serum antibody levels following booster vaccination and increasing age of prime vaccination ($P<0.0001$). Unlike the primary antibody response, antibody levels achieved after booster vaccination did not differ significantly among the groups vaccinated at different ages except that birds that were primed on day 1 of age still exhibited lower levels than those primed at 28 day of age. Consistent with these findings, no correlation was found between antibody level and age of booster in regression analyses (not shown). However, chickens primed at 28 days of age remained the only group with "positive" IBV antibody S/P ratios in all chickens after boosting.

3.1.2. S1 antibody responses in sera

Fig. 5.2 shows specific serum antibody levels detected by the Ark S1 recombinant protein ELISA. As seen in Fig. 5.2A, antibody levels in response to primary vaccination showed a trend similar to antibody responses using the commercial IBV ELISA kit (with whole virus) (see Fig. 5.1A). Earlier vaccination, on days 1 and 7, resulted in significantly lower antibody levels ($P<0.05$) than vaccination on days 14 and 21. A significant increase ($P=0.0007$) in antibody response with increasing age at prime vaccination was demonstrated using linear regression analysis (Fig. 5.2B).

Fig. 5.2C shows ArkS1-specific antibody levels in sera after booster immunization. Unlike results obtained with the commercial (whole virus) ELISA, antibody levels increased in all groups after booster vaccination. However, the magnitude of increase of antibody levels following booster vaccination was less with increasing age of prime vaccination ($P<0.0001$), and no significant differences in ArkS1 antibody levels achieved after boosting were detected among sera of chickens primed at different ages.

3.2.3. IBV IgA levels in lacrimal fluids

IBV IgA levels determined in lacrimal fluids are shown in Fig. 5.3. The same pattern shown by serum antibodies was observed, i.e., lower IBV-specific IgA levels were detected after primary immunization in chickens vaccinated on day 1 compared to responses of chickens vaccinated at later ages (Fig. 5.3A). The regression analysis shown in Fig. 5.3B demonstrates a significant positive correlation of level of IBV-specific IgA antibody response with increasing age of the birds at vaccination ($P=0.0005$).

Fig. 5.3C shows IBV-specific IgA levels detected in tears after booster vaccination of birds that were primed on days 1, 7, 14, 21 or 28 of age. As was found for serum antibodies, boosting eliminated most of the differences in IBV-specific IgA in tears observed after priming at different ages. Following boosting, IBV-specific IgA levels in tears of chickens prime vaccinated at day 1 of age remained statistically significantly lower than those in chickens that were primed on day 14 or 28 of age. Unlike the rising antibody responses observed in sera after boosting, considerably lower IBV-specific IgA levels in tears were detected after booster vaccination. The reduction of the IgA antibodies in tears was significant ($P<0.05$) after booster vaccination of chickens that had been primed on days 7, 21 and 28. Linear regression analysis indicated that the magnitude of

reduction following booster vaccination increased with increasing age of prime vaccination (P=0.0035). Indeed, chickens prime vaccinated one day 1 of age showed no reduction.

3.1.3. S1-specific IgA levels in lacrimal fluids

Fig. 5.4 shows IgA antibody levels in tears detected by ELISA using ArkS1 recombinant protein. Prime vaccination on day 1 of age elicited significantly lower S1-specific IgA levels than chickens vaccinated at later time points (Fig. 5.4A). Although no statistically significant differences in tear ArkS1-specific IgA levels among birds primed at later time points were detected when all data were analyzed together, linear regression analysis of S1-specific IgA levels in chickens vaccinated on days 1, 7, and 14 days of age showed a significant positive correlation of antibody responses with increasing age of vaccination (Fig. 5.4B; P=0.0010). As is clear from Fig. 5.4A, this correlation did not continue beyond 14 days of age. The apparent decline of S1-specific IgA levels in tears with age of vaccination between 14 and 28 days of age was not significant; linear regression analysis did not identify a significant negative correlation.

The S1 specific IgA response to booster vaccination is shown in Fig. 5.4C. No significant differences in tear S1 IgA levels were detected among groups that were primed at different ages. A comparison of IgA antibody level in tears after primary and secondary immune responses shows a significant increase of IgA after booster vaccination only in chickens that were primed on day 1 of age.

3.1.4. Age-of-vaccination-dependent correlations between IBV-specific and S1-specific antibodies

Levels of IBV-specific and S1-specific antibodies in sera were positively correlated both post-prime vaccination and post-booster vaccination (Table 5.1). The degree of correlation of these antibody levels post-prime vaccination increased with age of prime vaccination and was significant only in chickens vaccinated at 14, 21, or 28 days of age. The highest degree of correlation was observed in chickens vaccinated at 28 days of age (Fig. 5.5A). The degrees of correlation post-booster vaccination remained low and not statistically significant regardless of age of vaccination (*e.g*. Fig. 5.5B). Likewise, levels of IBV-specific IgA and S1-specific IgA in tears were positively correlated. The degree of correlation of antibodies in tears increased with age of prime vaccination both after prime vaccination and booster vaccination and was statistically significant following prime vaccination in chickens vaccinated at 14, 21, and 28 days of age and after booster vaccination of chickens first vaccinated at 21 and 28 days of age. The highest degrees of correlation were observed in chickens first vaccinated at 28 days of age (Fig. 5.5 C,D). Although weak positive correlations were observed between IBV antibody levels in sera and IBV-specific IgA tears and between S1 antibody levels in sera and S1-specific IgA in tears, these correlations did not increase with age of vaccination and were below the level of statistical significance with the exceptions of IBV-specific antibodies post-booster vaccination in chickens first vaccinated at 7 days of age and S1-specific antibodies post booster vaccination in chickens first vaccinated at 1 day of age.

3.1.5. T cell responses

Significantly greater proportions of $CD4^+$ cells in HG of chickens prime vaccinated at 1 day of age were detected following boost compared to age-matched control chickens (Fig. 5.6).

No other significant differences were detected in proportions of $CD8^+$, $CD4^+$, or double positive $CD8^+/CD4^+$ cells in the HG, CT or spleen between vaccinated and boosted chickens and aged matched unvaccinated controls (not shown). Regardless of vaccination status, significant positive correlations were found between the proportions of $CD8^+$ and double positive $CD8^+/CD4^+$ T cells in CT and spleen and increasing age (Fig. 5.7A-D). The significant increase in proportion of $CD8^+$ T cells with age without a concomitant increase in the proportion of $CD4^+$ T cells (not shown) led to an age-associated increase in CD8/CD4 ratios in CT and spleen (Fig. 5.7 E,F). CD8/CD4 ratios were significantly higher in CT than in spleen at all ages tested except at 7 weeks, when the difference did not reach statistical significance.

3.2. Experiment 2

3.2.1. T and B cell responses in peripheral blood

Few significant differences between vaccinated chickens and age-matched controls were seen in B and T cell populations in PBMC and CT after prime or boost vaccination. $CD4^+$ cells were significantly higher in PBMC of vaccinated chickens compared to age-matched controls after prime vaccination and after boost vaccination in some of the groups primed at 1, 7, or 14 days of age (Fig. 5.8A, B). Although $CD4^+$ cells in PBMC of chickens prime vaccinated between 1 and 21 days of age exhibited an increase with age of prime vaccination, $CD4^+$ cells also increased with age in the unvaccinated controls. Thus, the magnitude of significant differences in proportion of $CD4^+$ cells between vaccinated and unvaccinated chickens was similar for chickens prime vaccinated at different ages, ranging from 1.2-1.4 fold. In CTs, the proportion of B cells in vaccinated chickens was significantly greater than in unvaccinated controls only after boosting of chickens prime vaccinated at 14 days of age (Fig. 5.8C). The increase in double positive

$CD8^+/CD4^+$ T cells in CT with age observed in experiment 1 was also observed in experiment 2, for both CT and PBMC (not shown).

4. DISCUSSION

Consistent with our findings, a study by Gelb *et al.*, although not directed toward comparing immune responses of chickens vaccinated at different ages, showed lower antibody responses in both sera and tears in chickens vaccinated with IBV on day one of age versus chickens vaccinated on day 14 of age (180). In a more directed study, van Ginkel *et al* showed that the concentration of IBV-specific IgG in plasma and lacrimal fluid increased significantly when IBV vaccination was performed on day 14 instead of day one of age(22). First vaccination on days 21 or 28 did not further improve the antibody responses (22). The current results confirmed that increasing age of IBV vaccination is highly associated ($P<0.0001$) with the magnitude of the systemic specific antibody response (Fig. 5.1B). This observation is also true for IBV mucosal IgA where increasing age of vaccination and level of the mucosal IgA antibody is also highly significant ($P=0.0005$) (Fig. 5.3B). The fact that antibodies determined by a commercial ELISA, which contains whole virus bound to the wells, showed both similar results and trend as when S1 protein was used on the ELISA plates underlines the immunogenic importance of the virus' spike at inducing antibodies. Although there was significant positive correlation between antibodies against whole virus and S1 following prime vaccination at 14 days of age and older, such correlation was lacking in chickens vaccinated at earlier ages. Thus further work is necessary to determine which antibodies best correlate with protection in chickens vaccinated prior to 14 days of age. Because antibodies against S1 include virus-neutralizing antibodies, it is likely that antibodies against S1 will better predict protection. Virus-neutralizing antibodies, both systemic and mucosal, are

important for host protective immune responses (129, 138, 179). IBV challenge in chickens vaccinated at one-day-old resulted in significantly increased tracheal damage compared to chickens vaccinated later in life (22). The results of the commercial ELISA show a slight increase of serum antibody levels after booster vaccination (Figs. 5.1A and 5.1C). The increase of specific IBV antibodies from secondary responses after booster vaccination was more dramatic and significantly higher when measured by the more specific S1 protein ELISA in chickens of all vaccination age groups (Figs. 5.2A and 5.2C). However, even though a trend for higher/stronger secondary responses was apparent (as the average antibody levels continued to increase), the levels achieved did not differ significantly between chicken groups that were primed at different ages. Thus, it seems that the booster vaccination mitigated the differences detected after prime immunization. The weaker antibody response seen when prime vaccination is performed on the day of hatch could be explained by a less than optimal lymphocytic clonal expansion and subsequent memory cell response. However, it seems that a hypothetical difference in memory cell numbers activated during priming is not enough to make differences apparent during the secondary response.

Lacrimal IBV-specific IgA levels have been associated with resistance against IBV ocular challenge (129). However, others have reported that IgA was undetectable and only low levels of IgM were found during the first week after hatch (132). Chickens primed on day one of age with an ArkDPI type vaccine produced weaker IgA responses compared to chickens vaccinated two weeks later (22). Similarly, in the current study mucosal IgA levels in tears (both whole virus and S1-specific) of chickens vaccinated at different ages demonstrated that early prime vaccination results in induction of lower IgA levels compared to chickens primed later. In contrast to the continued rising of systemic antibodies after boost, the current results showed decreased levels of

mucosal IBV-specific IgA after booster vaccination (Figs. 5.3A and 5.3C). Absence of mucosal immune responses in tears and in tracheal lavage fluids of chickens following IBV booster immunization or challenge following primary immunization has also been observed by others, e.g., (180, 181).The decrease in IBV-specific lacrimal IgA after booster vaccination cannot be explained in the current study. One speculative explanation involves a shift of IBV vaccine induced immune responses from mucosal to systemic compartments. Gurjar *et al*. (182) demonstrated increased interferon gamma (IFN-γ) expression in the head associated lymphoid tissues after primary immunization. However, booster vaccination resulted in decreased expression of IFN-γ in mucosal compartments but significantly increased expression in systemic immune compartments. In addition, while IBV-specific IgA predominates in tears following primary vaccination, IgG predominates after booster vaccination (183). It is possible that these IgG antibodies originated systemically; transfer of IgG from serum to tears has been demonstrated (151). Another possible explanation might be that a more mature mucosal immune system responds earlier so that at the time of sampling (day 14 after vaccination in the current study) the levels of IgA were already waning. Regarding the possibility of a primary mucosal immune response and shift of the secondary response to the systemic compartment, it is interesting to note that in our present work $CD4^+$ cells in the HG were significantly increased three weeks post boost compared to control chickens only in chickens first vaccinated at 1 day of age. The level of IBV-specific IgA in tears did not decrease post boost in chickens prime vaccinated at 1 day of age, and the level of S1-specific IgA increased post boost only in chickens prime vaccinated on 1 day of age. These observations are all consistent with a very poor response to primary vaccination at day 1 of age, such that a response characteristic of a primary response occurs following the second vaccination, with $CD4^+$ cells in the HG acting as helper cells to aid the mucosal antibody response.

Cell mediated immune responses have also been demonstrated to be age-dependent. For example, Lowenthal *et al.* (133) showed that splenic T cells from 1-day-old chickens produce inhibitory factors affecting the proliferation of T cells, which leads to transient T cell unresponsiveness to immune stimulation. They also reported a 70-fold increase in T cell numbers in the spleen of one-week-old compared to one-day-old chickens. At the mucosal level, a gradual increase in the concentration of $CD4^+$ and $CD8^+$ lymphocytes was observed in the CALT of chickens aged from one to four weeks (131). The current results are in agreement with those findings as higher concentrations $CD8^+$ and double positive $CD8^+/CD4^+$ T cells were detected in the tissues of both vaccinated and aged-matched controls as age increased. Others have also observed an increase in the proportion of $CD8^+$ cells in spleen with age, reaching approximately 50% by 7 or 8 weeks of age (184, 185). Increases in $CD8^+$ cells in CT with age, likely due to colonization by commensal bacteria (186), have also been observed by others (187). In peripheral blood, $CD4^+$ cells and double positive $CD8^+/CD4^+$ cells significantly increased with age while no significant differences were detected in PBMC $CD8^+$ cells. Cell mediated immunity has been shown to be essential in IBV clearance and protection (125, 127). However, significant differences were not detected in $CD8^+$, $CD4^+$, or double positive $CD8^+/CD4^+$ cells in the HG, CT or the spleen between chickens primed at increasing age and boosted, and aged matched unvaccinated control chickens, with the exception of the increase in $CD4^+$ T cells in the HG of boosted chickens following prime vaccination at 1 day of age already noted. These results do not contradict the results of Collisson *et al* (125) because they found increased $CD8^+$ mediated cytotoxic lymphocyte activity peaking at 10 days post-inoculation. They indicated that this response was 50% greater than the response of lymphocytes collected 7 or 15 days after infection. More interesting was the finding that $CD4^+$ cells in peripheral blood showed a significant increase in IBV vaccinated

chickens versus non-vaccinated age-matched controls both after primary and booster immunization in chickens primed on days 7 or 14. Increased $CD4^+$ cells are associated with a more optimal activation of B cells and is likely associated with the significant increase of antibody responses occurring when vaccination was performed later in the life of the chicken. The increase in $CD4^+$ cells in PBMC following booster vaccination was accompanied by an increase in B cells in CT.

The results of the current study confirm that IBV vaccination on the day of hatch induces suboptimal IBV immune responses both in the systemic and mucosal compartments. Less than optimal specific immunity may be contributing to the virus' immunological escape as well as increased persistence of vaccine virus in vaccinated chickens. It is interesting however, that booster vaccination seems to compensate for poor initial responses. Nevertheless, considering that outbreaks of IBV occur most commonly in broiler flocks after 30 days of age, first vaccination could be delayed in order to optimize the primary antibody response and avoid problems associated with vaccine virus persistence. Our study was conducted in IBV-antibody-free white leghorn chickens, and it is possible that different results would be found in commercial broilers with maternal antibody. Furthermore, the economic and labor saving advantages of vaccinating large broiler populations at day of hatch contrast with its immunological disadvantages. Chicken populations more limited in size, such as layer and breeder hens, might benefit from postponing the first IBV vaccination.

ACKNOWLEDGMENTS

We thank Ms. Allison Bird and Ms. Cassandra Kitchens for their great technical assistance. Funding for this work provided by research grant USDA NIFA #2016-67015-24916.

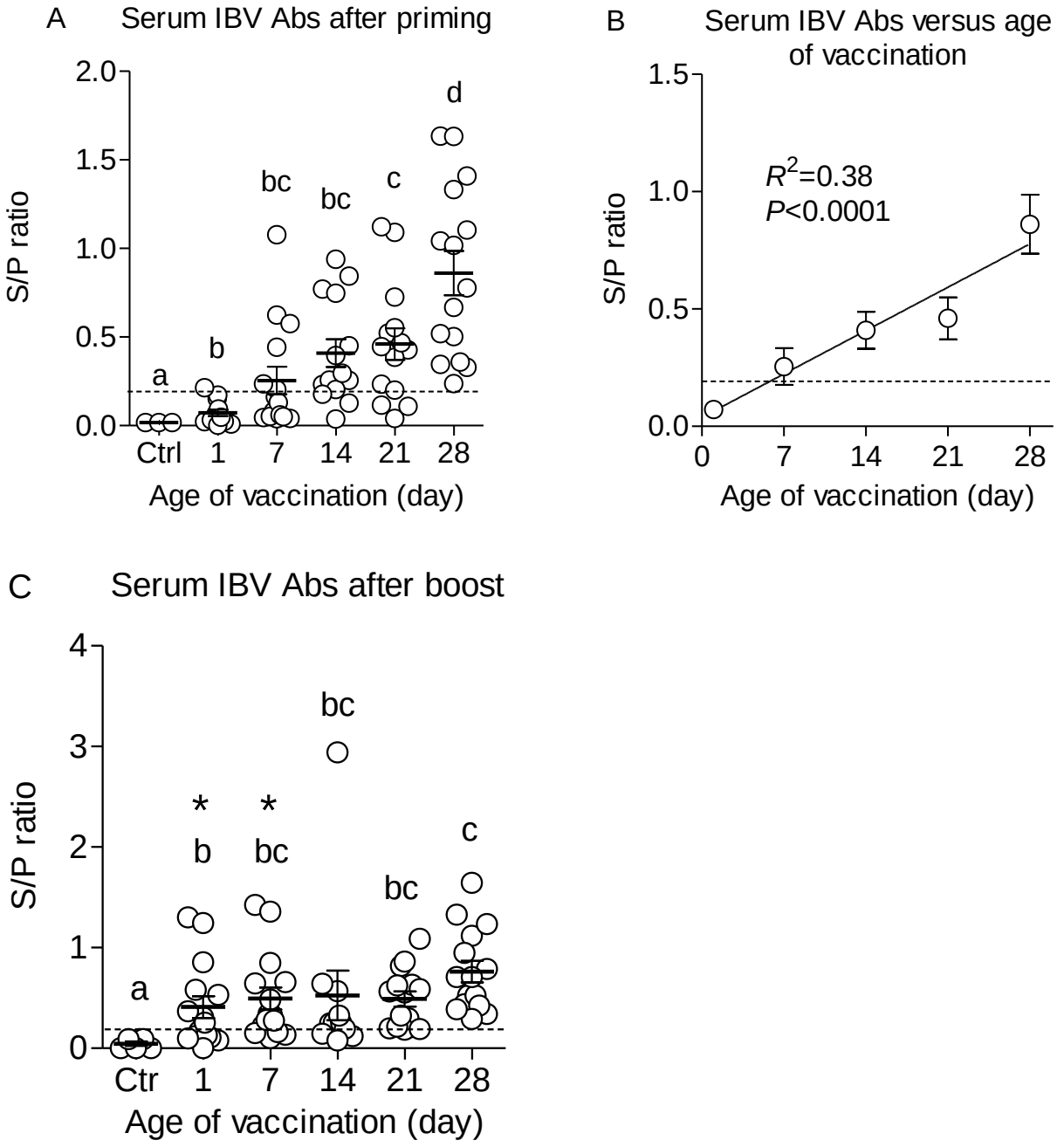

Fig. 5.1. IBV antibodies after vaccination (n=15/group) determined by a commercial ELISA (individual values, mean, and SEM). A) Serum IBV antibody (Abs) two weeks after prime vaccination on days 1, 7, 14, 21, or 28 of age with an attenuated ArkDPI-type vaccine. B) Linear regression analysis of antibody response and increasing age of vaccination. Mean values for each

age are shown, but linear regression analysis was carried out using data from individual chickens. C) Serum IBV antibody two weeks after booster vaccination of chickens primed at increasing ages. In all graphs error bars indicate SEM. Ctr=unvaccinated controls. In A and C different letters indicate significant differences at $P<0.05$. Differences between vaccinated groups and a small number of unvaccinated control samples were determined by one-sample *t*-tests. In A differences among vaccinated groups were analyzed by ANOVA with Tukey's post-test. In C differences among vaccinated groups were evaluated by Kruskal-Wallis test followed by Dunn's post-test. In C asterisks indicate significant increases from antibody levels following prime vaccination ($P<0.05$), determined by two-tailed *t*-tests. Note the difference in Y-axis scales between parts A and C.

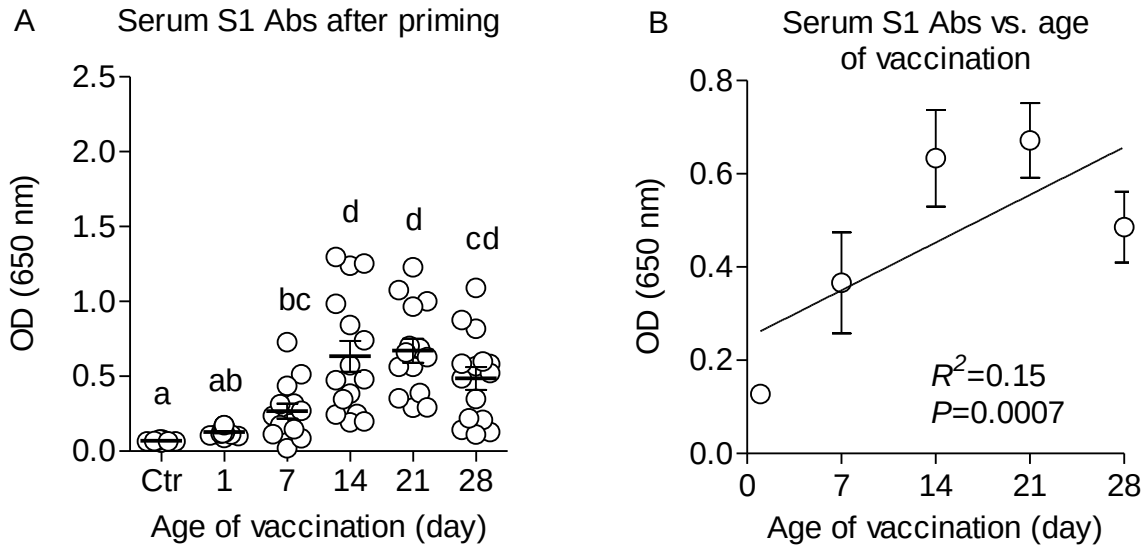

Fig. 5.2. IBV antibody levels (n=15/group) after vaccination determined by ELISA using Ark-serotype S1 recombinant protein bound to the wells (individual values, mean, and SEM). A) Serum S1 antibody two weeks after prime vaccination on days 1, 7, 14, 21, or 28 of age. B) Linear regression analysis of S1 antibody response and increasing age of vaccination. Mean values for each age are shown, but linear regression analysis was carried out using data from individual chickens. C) Serum S1 antibody two weeks after booster vaccination of chickens primed at increasing ages. In all graphs error bars indicate SEM. Ctr=unvaccinated controls. In A and C different letters indicate significant differences at $P<0.05$. Analyses were carried out using $\log_{10}$-transformed data. Differences of each vaccinated group from unvaccinated controls were evaluated by ANOVA with Holm-Sidak's multiple comparisons post-test, and differences among vaccinated groups were evaluated by ANOVA with Tukey's correction for multiple comparisons. In C asterisks indicate significant increases from antibody levels following prime vaccination ($P<0.05$) determined by two-tailed *t*-tests.

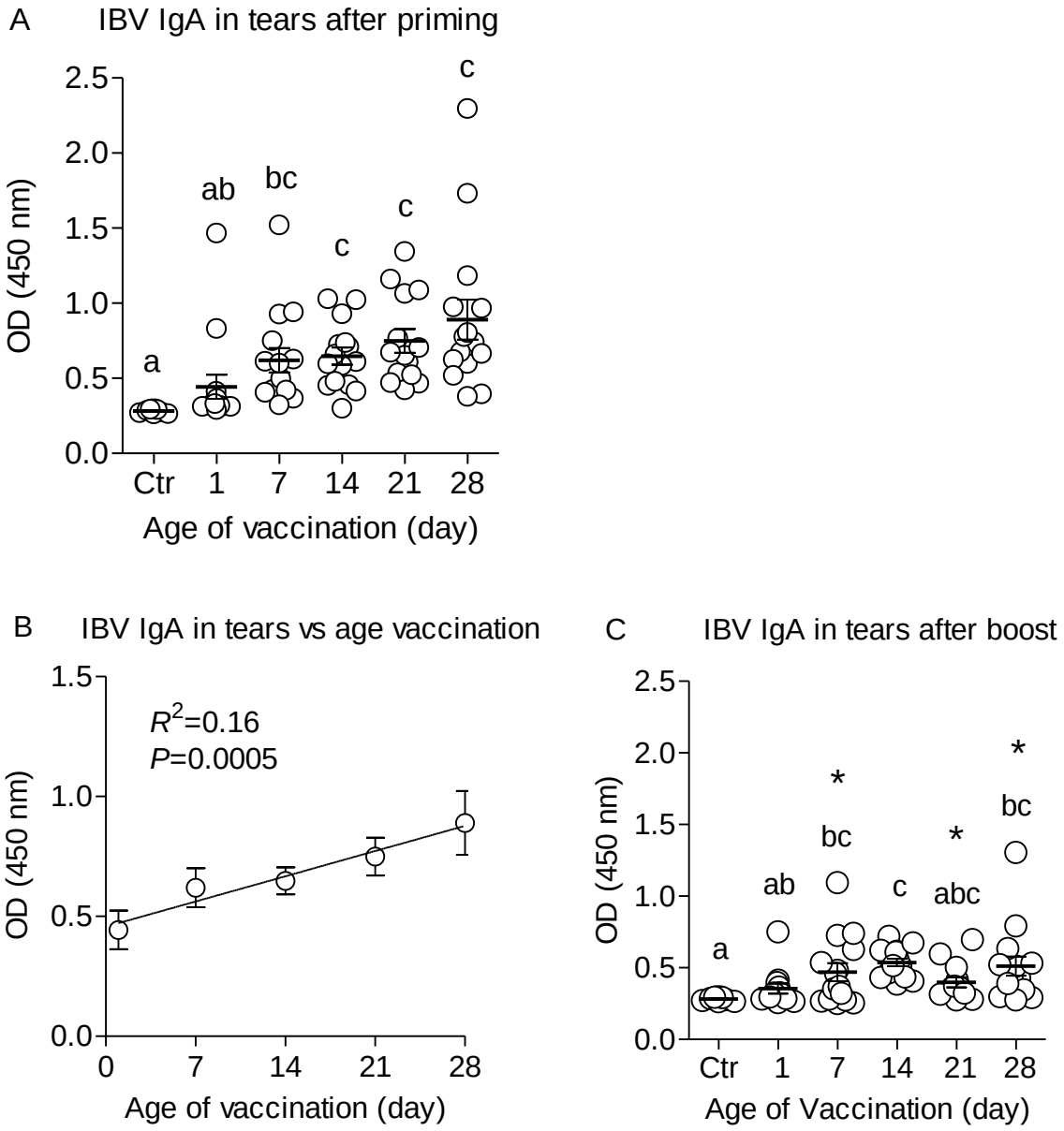

Fig. 5.3. IBV IgA levels (n=15/group) after vaccination determined by ELISA using plates of commercial origin (individual values, mean, and SEM). A) Tear IgA levels two weeks after prime vaccination on days 1, 7, 14, 21, or 28 of age. B) Regression analysis of tear IgA response and increasing age of vaccination. Mean values for each age are shown, but linear regression analysis was carried out using data from individual chickens. C) Tear IgA two weeks after booster vaccination of chickens primed at increasing age. In all graphs error bars indicate SEM.

Ctr=unvaccinated controls. In A and C different letters indicate significant differences at $P<0.05$. In C asterisks indicate significant decreases from IBV-specific IgA antibody levels following prime vaccination ($P<0.05$). Statistical analyses were carried out as described for Figure 5.2.

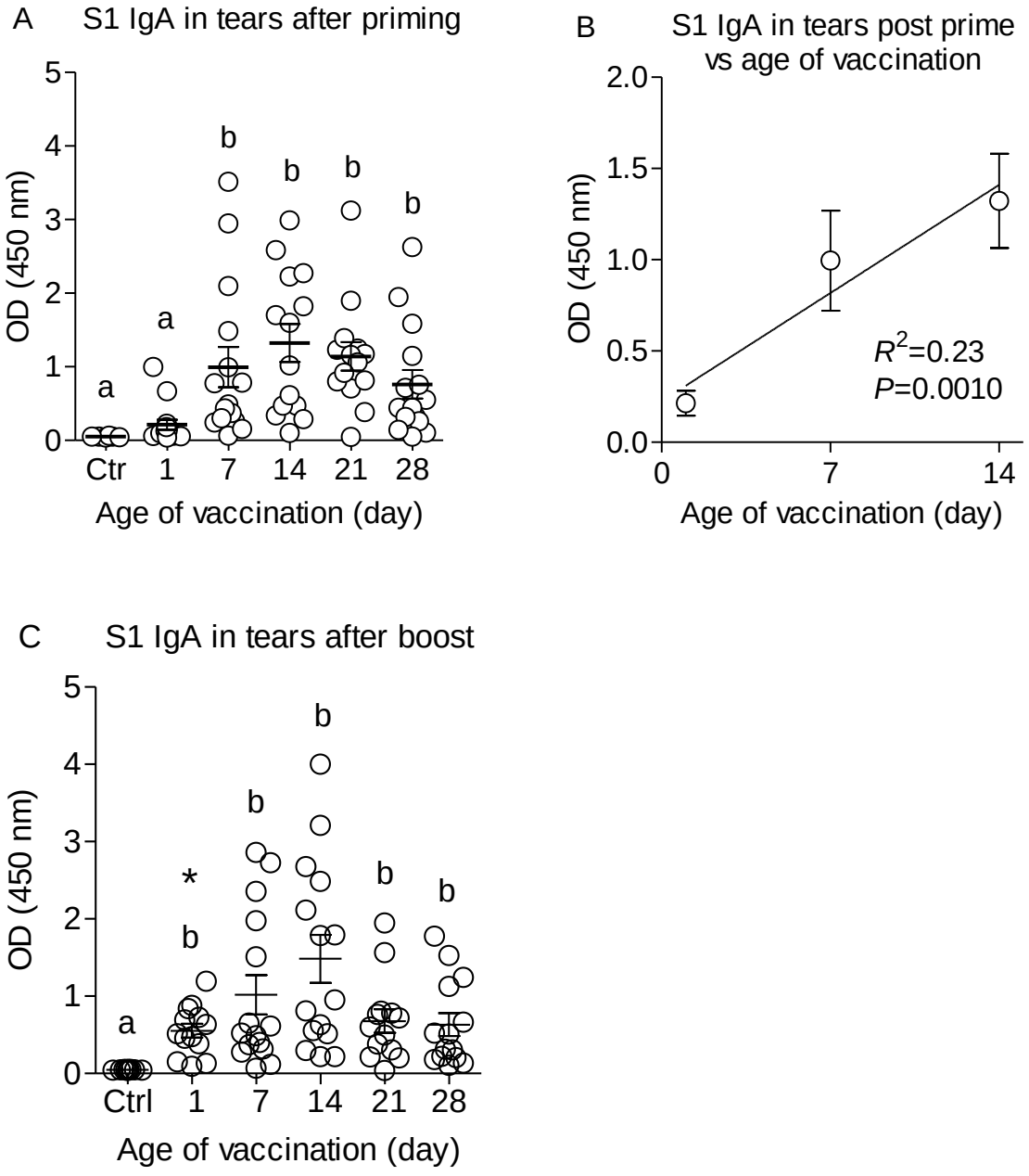

Fig. 5.4. IBV IgA levels (n=15/group) after vaccination determined by ELISA using recombinant Ark-serotype S1 protein bound to wells (individual values, mean, and SEM). A) Tear IgA levels two weeks after prime vaccination on days 1, 7, 14, 21, or 28 of age. B) Regression analysis of tear IgA response and increasing age (days 1, 7, and 14) of vaccination. Mean values for each age

are shown, but linear regression analysis was carried out using data from individual chickens. C) Tear S1 IgA two weeks after booster vaccination of chickens primed at increasing age. In all graphs error bars indicate SEM. Ctr=unvaccinated controls. In A and C different letters indicate significant differences at $P<0.05$. In C asterisks indicate significant increases from IBV-specific IgA antibody levels following prime vaccination ($P<0.05$). Statistical analyses were carried out as described for Figure 5.2.

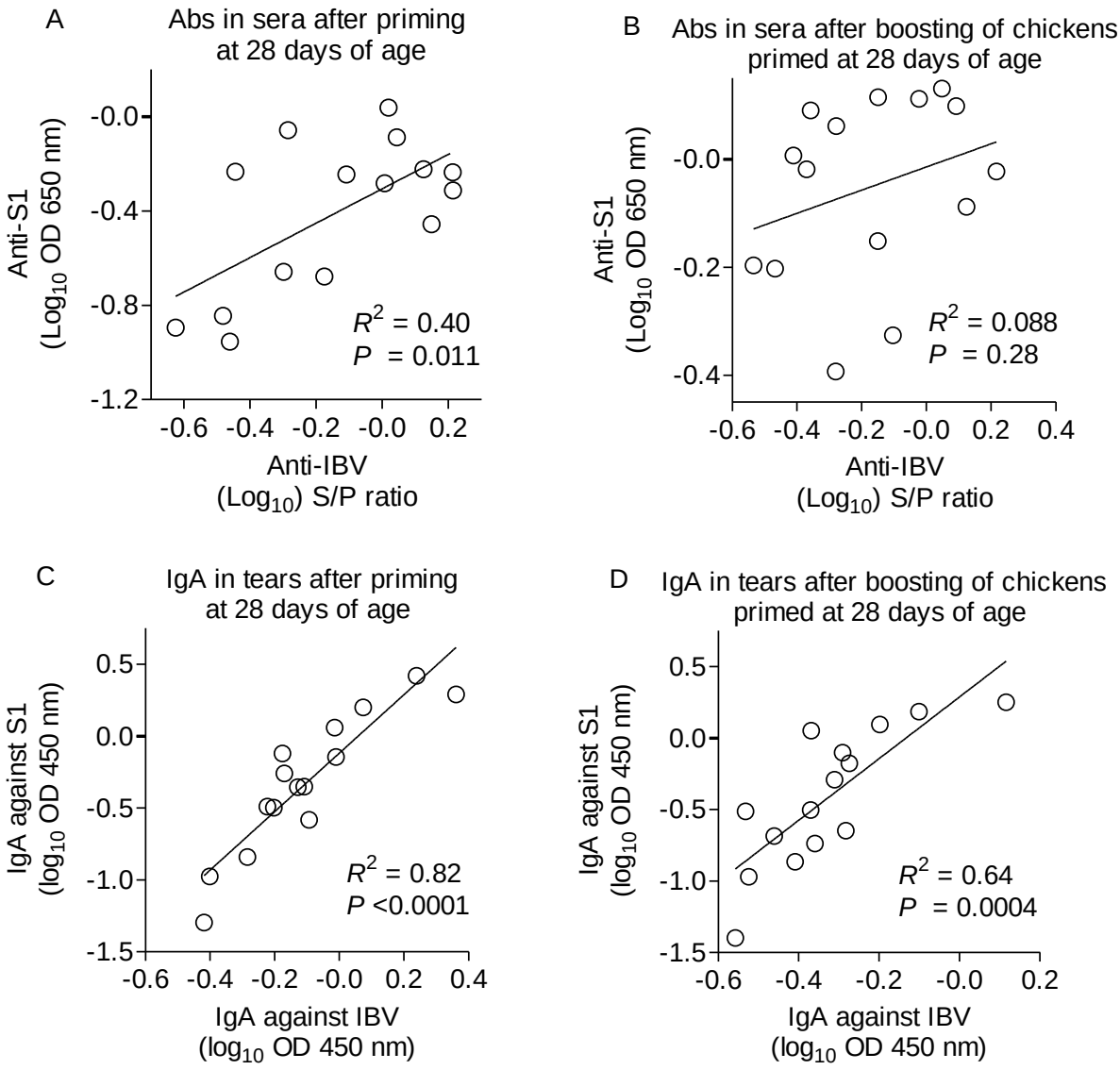

Fig. 5.5. Correlations of IBV-specific and S1-specific antibody levels in sera and tears of individual chickens (n=15) vaccinated at 28 days of age. A) IBV-specific and S1-specfic antibodies in serum after prime vaccination. B) IBV-specific and S1-specfic antibodies in serum after booster vaccination. C) IBV-specific and S1-specific IgA in tears after prime vaccination. D) IBV-specific and S1-specific IgA in tears after booster vaccination. The graphs are shown for chickens vaccinated at 28 days of age because for the correlation shown in A, C, and D chickens vaccinated at 28 days of age showed the highest correlations. Corresponding data in B show lack

of statistically significant positive correlation for IBV-specific and S1-specfic antibodies in serum after booster vaccination. Correlation data for chickens vaccinated at other ages are presented in Table S5.1 (supplemental material).

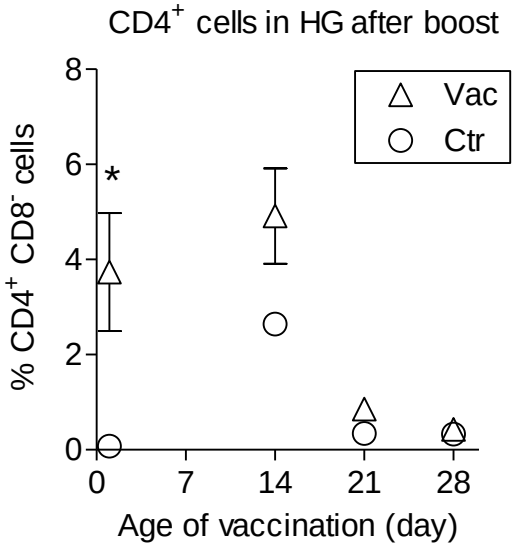

Fig. 5.6. $CD4^+$ lymphocytes in HG of chickens 3 weeks after boosting of chickens primed at different ages. Vac=vaccinated chickens; Ctr=unvaccinated control chickens. Error bars indicate SEM. The asterisk indicates statistically significant difference ($P<0.05$) between three pools of cells from three vaccinated chickens each and a pool of cells from three unvaccinated age-matched control chickens, determined by one-sample *t*-test.

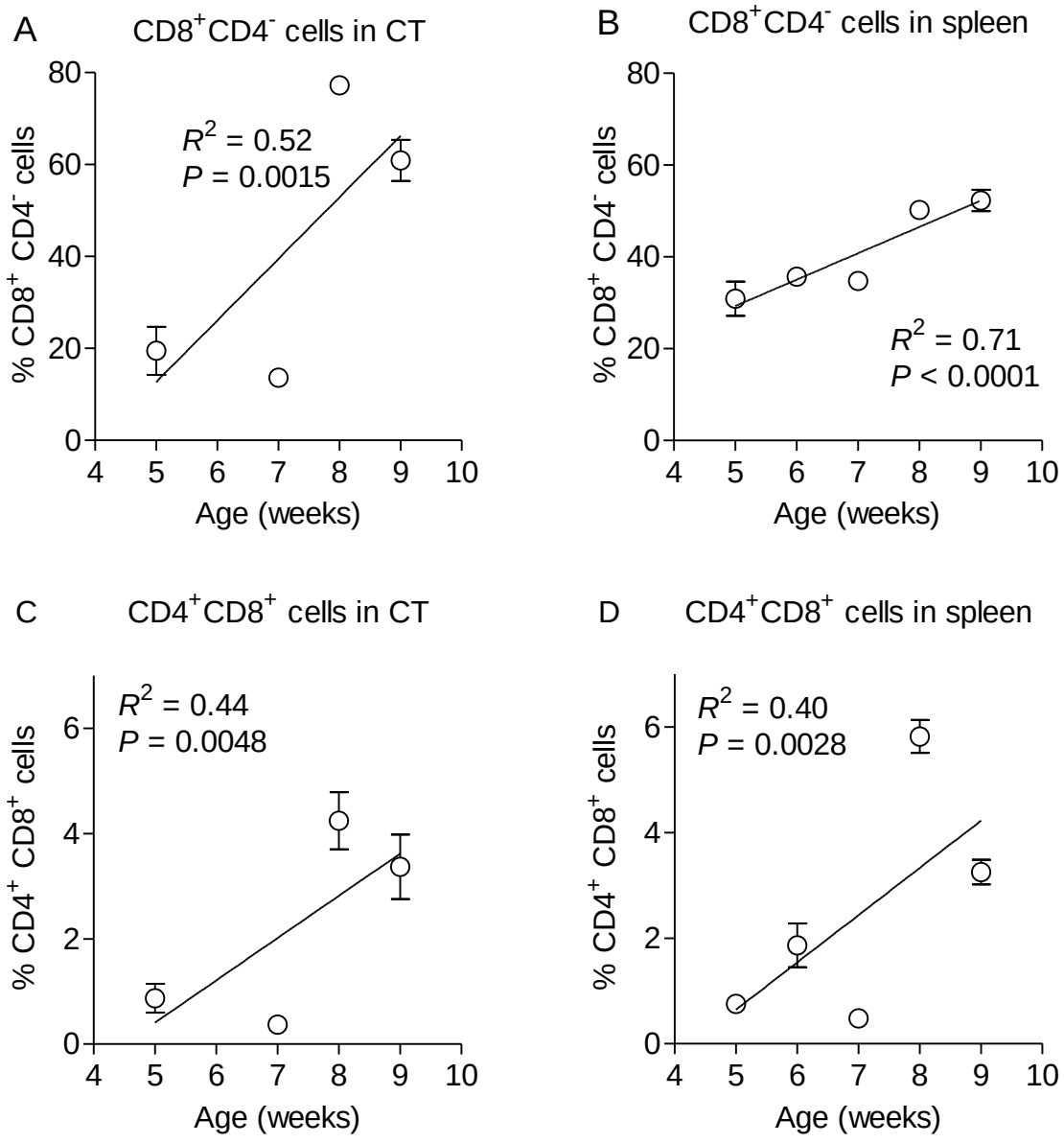
A
CD8+CD4- cells in CT
% CD8+ CD4- cells
R2 = 0.52
P = 0.0015
Age (weeks)
B
CD8+CD4- cells in spleen
% CD8+ CD4- cells
R2 = 0.71
P < 0.0001
Age (weeks)
C
CD4+CD8+ cells in CT
% CD4+ CD8+ cells
R2 = 0.44
P = 0.0048
Age (weeks)
D
CD4+CD8+ cells in spleen
% CD4+ CD8+ cells
R2 = 0.40
P = 0.0028
Age (weeks)

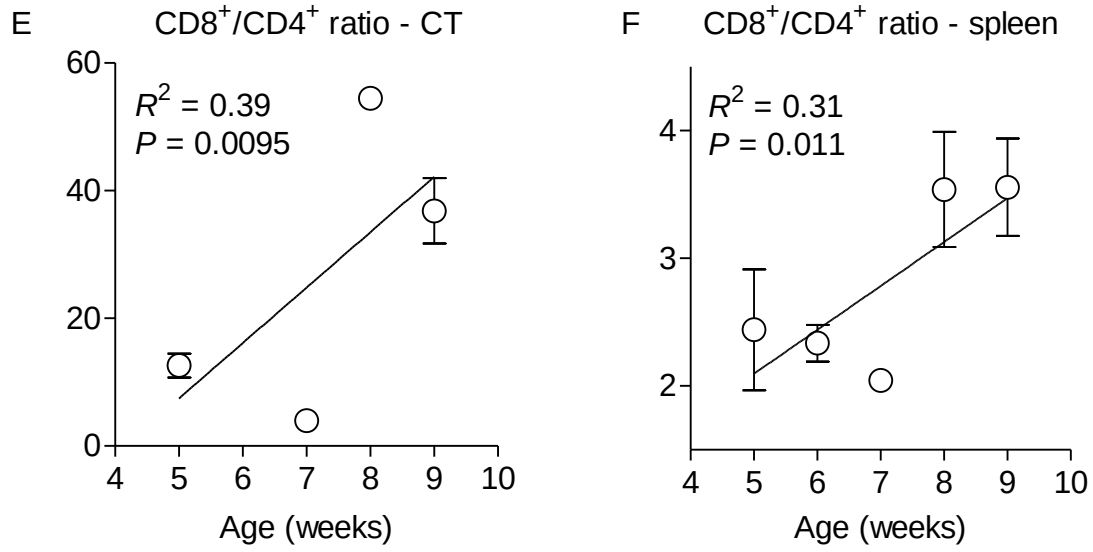

Fig. 5.7. Linear regression analysis of CD8+ and $CD4^+CD8^+$ cells in CT and spleen of chickens at different ages. Because no significant differences were noted between vaccinated and unvaccinated age-matched controls, vaccinated and unvaccinated chickens of the same age were combined in this analysis. Four pools of cells from three chickens each were evaluated at each age. Mean and SEM for each time point and linear regression lines are shown. *P* values for the null hypothesis that the slope of the line is zero are shown. A) $CD8^+CD4^-$ cells in CT correlated with age of chickens. B) $CD8^+CD4^-$ cells in spleen correlated with age of chickens. C) $CD8^+CD4^+$ cells in CT correlated with age of chickens. D) $CD8^+CD4^+$ cells in spleen correlated with age of chickens. E & F) CD8/CD4 cell ratios in CT and spleen correlated with age of chickens.

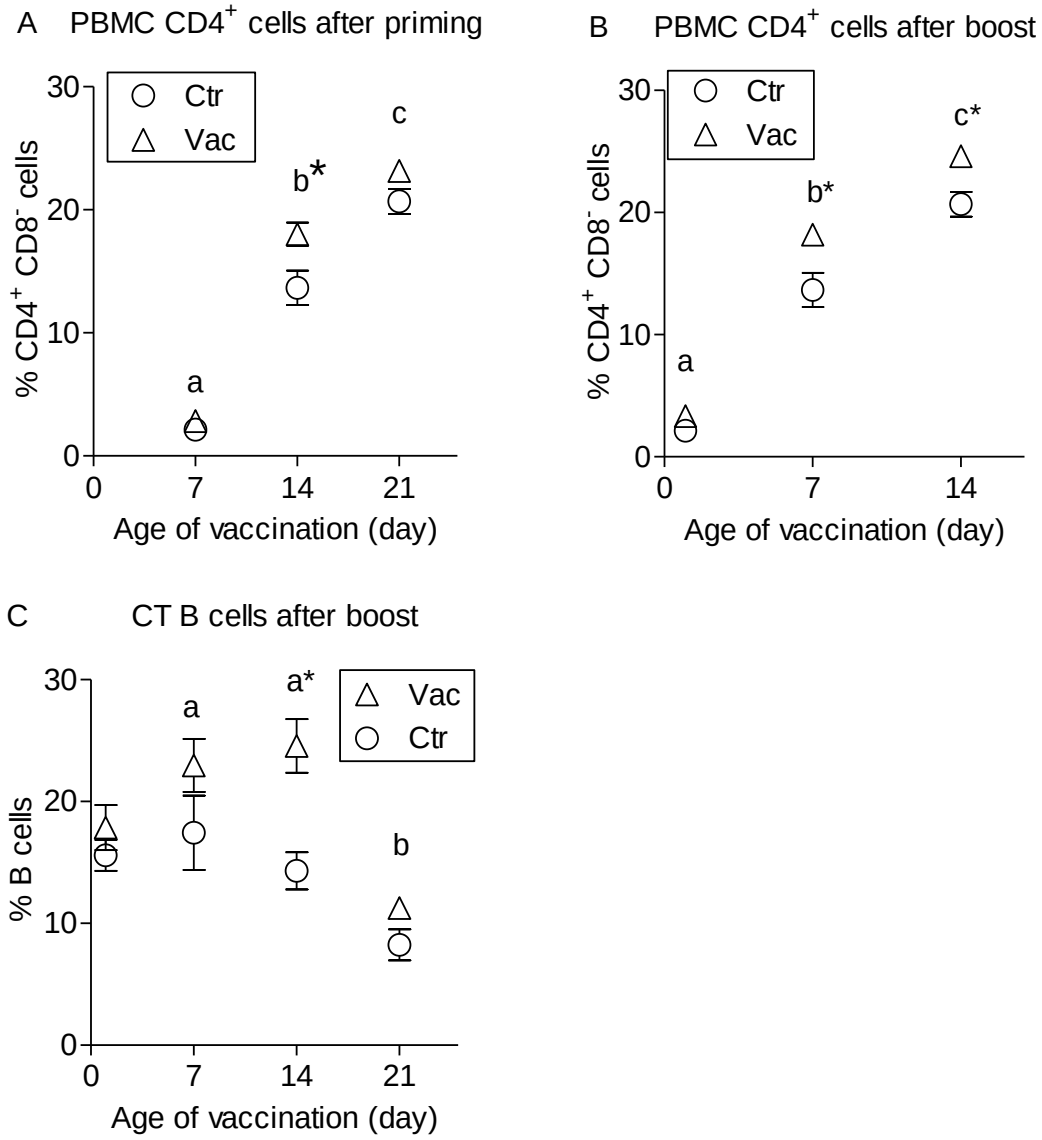

Fig. 5.8. $CD4^+$ lymphocytes in peripheral blood (n=6 chickens/group) determined by flow cytometry 18 days after prime IBV vaccination (A) and 12 days after booster IBV vaccination (B), and B lymphocytes in CT determined by flow cytometry 18 days after booster IBV vaccination (C) in chickens primed on days 1, 7, 14, or 21 days of age. Values of age-matched unvaccinated controls (Ctr) also shown. Vac=vaccinated chickens. Mean and SEM. Different letters indicate significant differences among vaccinated groups at $P<0.05$. Asterisks indicate significant difference between vaccinated and age-matched unvaccinated controls.

Table S5.1. Correlations between antibodies against IBV and S1 and between IgA in tears and antibodies in sera[A]

	Age of primary vaccination (days)	Post prime vaccination		Post booster vaccination	
		Pearson *r*	*p*[B]	Pearson *r*	*p*
IBV and S1 antibodies in serum					
	1	0.29	0.34	0.29	0.32
	7	-0.04	0.89	0.34	0.21
	14	0.63	**0.015**	0.20	0.50
	21	0.55	**0.042**	0.32	0.26
	28	0.63	**0.011**	0.30	0.28
IBV and S1 IgA in tears					
	1	0.17	0.55	0.32	0.10
	7	-0.018	0.95	0.64	**0.01**
	14	0.63	**0.015**	0.49	0.064
	21	0.54	**0.048**	0.58	**0.037**
	28	0.91	**< 0.0001**	0.80	**0.0004**
IBV antibodies in serum and IBV IgA in tears					
	1	0.28	0.35	0.32	0.29
	7	0.32	0.25	0.55	**0.033**
	14	0.09	0.77	0.14	0.64
	21	-0.08	0.79	0.27	0.37
	28	0.42	0.12	0.26	0.35
S1 antibodies in serum and S1 IgA in tears					
	1	0.19	0.51	0.62	**0.02**
	7	0.27	0.33	0.50	0.06
	14	0.13	0.65	0.10	0.73
	21	0.44	0.12	0.07	0.82
	28	0.39	0.15	0.25	0.38

[A]All correlation analyses were preformed using $\log_{10}$ S/P ratios and $\log_{10}$ OD values

[B]*p* values <0.05 are in bold

CHAPTER 6

Role of Changes in S Protein of IBV Field Isolate in Escaping Vaccine-Induced Immune Responses

SUMMARY. In spite of extensive vaccination against Ark-type IBV, Ark-type IBV continues to cause problems in the poultry industry. To understand how IBV field strains are able to escape IBV vaccine-induced immune responses, we previously compared reactivity of antibodies in IBV ArkDPI-vaccinated chickens with the vaccine strain virus and an Ark-type IBV isolated from a vaccinated flock. IBV-specific IgA antibody levels in tears and IgA and IgG antibody levels in plasma measured against the field isolate were lower compared to those against the vaccine strain, suggesting immune escape of the field strain from vaccine-induced immune responses. In order to observe whether differences in antibody levels against the vaccine strain and field isolate in vaccinated chickens included different levels of antibodies recognizing the IBV S proteins, ELISA using trimeric recombinant S-ectodomain proteins with S1 domains representing the vaccine strain and field isolate was conducted. Antibodies in both tears and plasma of vaccinated chickens both post primary vaccination and post boost recognized the S-ectodomain containing the field isolate S1 significantly less ($P<0.05$) than they recognized the vaccine strain S-ectodomain. Our results were consistent with the prediction that IBV field strains escape the host humoral immune responses through aa changes within the S1 protein.

1. INTRODUCTION

The Arkansas (Ark) serotype, followed by Connecticut, Delaware, GA98 and Massachusetts, is the most common serotype of infectious bronchitis virus (IBV) reported in the poultry industry in the United States. Interestingly, based on spike subunit 1 (S1) molecular typing, the most identified Ark serotype IBV in the poultry industry is the same molecular type as the Ark-Delmarva Poultry Industries (DPI) vaccine strain (27, 59, 112). Unlike other IBV vaccine strains, the Ark-DPI vaccine strain persists in vaccinated chickens (27, 59, 112). Whether or not this is due to positive selection of vaccine subpopulations during the process of host invasion (36, 38, 64) is not clear.

The spike (S) protein of IBV mediates viral entry into host cells [reviewed in (67)]. Its highly variable S1 subunit mediates viral attachment to host cells and induces virus-neutralizing antibodies that are important for host protective immune responses (55, 138, 179). Its S2 subunit anchors the protein in the viral envelope and mediates fusion with host cell membranes (49). As is the case for other coronaviruses, the IBV host receptor binding domain (RBD) of the M41 strain has been mapped to S1 (76, 77). The IBV M41 RBD has been further mapped to the S1 N-terminal domain (NTD) of the S1 subunit (amino acids 19-271), which is necessary and sufficient for binding to respiratory epithelium in formalin-fixed chicken tissues (78), but assays with live cells indicate a role in viral attachment for the S1-carboxyl-terminal domain (CTD) as well (52). When the amino acid sequences of the S1 proteins of seven Massachusetts serotype IBV strains were analyzed, two hyper-variable regions were identified in the region including amino acids 19-122, between residues 38-51 and 99-115 (138). It is interesting that important hyper-variable regions are located in the RBD domain that mediates host attachment in the M41 S1 protein. Consistent

with a role for both the S1-NTD and S1-CTD in viral attachment, epitopes recognized by virus-neutralizing antibodies have been mapped within each of these domains (55, 56, 57, 138).

S protein heterogeneity originates from nucleotide insertions, deletions, or point mutations and/or from genetic recombination events occurring during viral replication (134, 135, 136). Amino acid changes of as few as 2-3% in S1 (10-15 residues) can alter serotype, which suggests that a small number of immune-dominant epitopes on S1 are recognized by neutralizing antibodies (85). Emerging strains that accumulate changes in the S1 protein could escape immunity induced by common vaccine types. As for example, an IBV isolated from a Mass serotype H120-vaccinated flock had 5 amino acid substitutions in its S1 aa sequence compared to H120, 4 in the S1-NTD. These changes presumably enabled the virus to successfully evade the Mass vaccine-induced immune response, indicating the important role of a small number of changes in the S protein in host immune escape (139). Interestingly, one of the aa changes was adjacent to an aa position shown to be part of a neutralizing epitope in another Mass-serotype IBV, M41 (138). The continued generation of new IBV variants in the field raises the important question of how mutations in the S gene observed in IBV field isolates contribute to immune evasion by those field strains in vaccinated birds. How the IBV-ArkDPI vaccine-induced humoral immune response cross-reacts with Ark-serotype field isolates obtained from IBV-vaccinated broilers and how small amino acid differences in the S1 protein of field isolates might contribute to immune evasion are not understood. Much less information regarding neutralizing epitopes in Ark-serotype S1 proteins in available compared to neutralizing epitopes in Mass-serotype S1 proteins (55).

To understand how IBV field strains are able to escape IBV vaccine-induced immune responses, we previously compared reactivity of IBV-specific antibodies in IBV ArkDPI-vaccinated chickens with the vaccine strain virus and an Ark-type IBV isolated from a vaccinated

flock. IBV-specific IgA antibody levels in tears and IgA and IgG antibody levels in plasma measured against the field isolate were lower compared to those against the vaccine strain, suggesting immune escape of the field strain from vaccine-induced immune responses. In this study, we compared the reactivity of S-specific antibodies in IBV ArkDPI-vaccinated chickens with the vaccine strain virus and the field isolate to observe whether the lower antibody levels against the field isolate reflected lower the antibody levels against the S protein of the field isolate.

2. MATERIALS AND METHODS

2.1. Chickens

Chickens were hatched from specific pathogen free (SPF) white leghorn chicken eggs purchased from Sunrise Farms (Catskill, NY) and were kept in Horsfall-type isolation units at biosafety level 2. All procedures and animal care were performed in compliance with federal and institutional animal care and use guidelines. Auburn University College of Veterinary Medicine is an Association for Assessment and Accreditation of Laboratory Animal Care-accredited institution.

2.2. Vaccination and sample collection

Twelve chickens were ocularly immunized at 3 weeks of age with 100 µl containing $3x10^5$ 50% embryo infectious doses (EID_{50}) of a commercial live-attenuated IBV Ark serotype (Ark-DPI) vaccine (vaccine D in reference (38) and were ocularly boosted 2 weeks later with the same dose. Tears and plasma were collected 2 weeks after the primary vaccination and after the boost. Tears and plasma were also collected from 8-10 unvaccinated control chickens.

Tear collection was performed as previously described (129). Blood samples were collected from the brachial vein into EDTA-containing Kendall monoject blood collection tubes (Tyco Healthcare Group LP, Mansfield, MA). The blood was incubated on ice for 45 minutes after which it was centrifuged at 500 x g for 30 minutes. Collected plasma and tears were stored at -80 C until used for further analyses.

2.3. Spike Protein-ELISA

S1-specific and S-ectodomain-specific ELISAs were employed to measure specific antibody and IgA antibody levels in plasma and tears, respectively. Soluble trimeric recombinant S1 or S-ectodomain protein was produced in human embryonic kidney (HEK)-293T cells as described (70, 76, 140) and purified from tissue culture supernatants six days post-transfection using *Strep*-Tactin® Sepharose columns according to the manufacturer's instructions (IBA GmbH, Göttingen, Germany). S-ectodomain protein included S1 and S2 lacking the transmembrane and cytoplasmic domains and lacked the furin cleavage site between S1 and S2. ELISA plates (Nunc MaxiSorp Immuno Plates; Thermo Scientific, Rockford, IL) were coated at 4 C overnight with 0.25 µg/ml of recombinant S1 or S ectodomain protein (Ark-DPI major vaccine population, Ark-DPI vaccine subpopulation C2 selected in chickens (64), or field isolate AL/4614/98 (Genbank accession number ABE68839) in PBS. Plates were blocked with 200 µL of ELISA assay buffer (1% BSA and 0.05% Tween 20 in PBS) for 1 hour at room temperature. Individual chicken plasma and tear samples diluted 1:100 in PBS were loaded onto the plates and incubated for 30 min at room temperature. For plasma samples, reagents from a commercial IBV ELISA kit (IDEXX Laboratories, Inc., Westbrook, ME) were used, following instructions in the kit, and absorbance at 650 nm was measured. The enzyme-labeled secondary antibody in this kit is not specific for a

particular chicken antibody isotype. For tear samples, following incubation of the samples on the plate and washing, horseradish peroxidase-conjugated polyclonal goat–anti-chicken IgA antibodies (Southern Biotechnology Associates Inc., Birmingham, AL) and TMB substrate (Invitrogen) were used to detect IgA antibodies.

2.4. Statistical analysis

The data was analyzed using GraphPad Prism 8 for MacOS (GraphPad Software, LLC, San Diego, CA) by repeated measures ANOVA with Tukey's post-test. Post-prime and post-boost samples were compared by ratio paired Student's *t*-test. Differences were considered significant at $P < 0.05$.

3. RESULTS

3.1. Antibody levels to vaccine and field strain S1 proteins

To determine whether differences in antibody levels against the vaccine strain and field isolate in vaccinated chickens included different levels of antibodies recognizing the IBV S1 proteins, we conducted ELISA using trimeric recombinant S1 proteins representing the vaccine strain and field isolate. A very minor subpopulation of the vaccine strain, differing from the major vaccine population in four amino acids in the S1 protein, replicates to much higher levels in chickens than the major vaccine population (38). Because this vaccine subpopulation S1 is identical to that of the field isolate AL/4614/98 at two of those four positions, recombinant S1 protein of the vaccine subpopulation selected in chickens [Ark vaccine (chx)] was also used as ELISA antigen. S1-specific IgA levels in tears of vaccinated chickens recognizing the three S1 antigens tested did not differ significantly and did not increase significantly following boosting

(Fig. 6.1.A). In contrast, S1-specific antibodies in plasma exhibited statistically significant higher levels following boosting (Fig. 6.1.B). Contrary to expectation, plasma antibodies to field isolate S1 protein were statistically significantly higher, rather than lower, than antibodies to the vaccine subpopulation selected in chickens following both primary and boost vaccination (Fig. 6.1.B).

3.2. Antibody levels to vaccine and field strain S-ectodomain proteins

It was demonstrated that trimeric IBV spike-ectodomain (S1 plus S2 lacking the transmembrane and cytoplasmic domains) binds to chicken respiratory epithelium much better than trimeric IBV S1 protein and that chickens vaccinated with trimeric S-ectodomain are better protected against IBV challenge than chickens vaccinated with trimeric S1 protein, suggesting that antibodies generated to S1 protein in the conformation it adopts in association with S2 are important for protection (150150). Therefore, we compared antibodies recognizing trimeric S-ectodomains. To ensure that differences detected in antibody levels to vaccine strain and field isolate S1 in this conformation would be due to differences in S1 and not differences in S2, the vaccine S-ectodomain and the S-ectodomain protein including the field isolate S1 contained identical S2-ectodomains, that of the vaccine strain. In contrast to ELISA results using only the S1 portion of the proteins, antibodies in both tears and plasma of vaccinated chickens both post-primary vaccination and post-boost recognized the S-ectodomain containing the field strain S1 significantly less ($P<0.05$) than they recognized the vaccine strain S-ectodomain (Fig. 6.1.C & 6.1.D). Also in contrast to antibodies recognizing S1 alone, levels of IgA antibodies in tears recognizing the S-ectodomain of the vaccine strain increased after boosting (Fig. 6.1.C). However, the level of antibodies in tears recognizing the field strain S-ectodomain did not increase in response to boosting. With the exception of antibodies post-boost in plasma, recognition of S-

ectodomains representing the major vaccine population and that representing the vaccine subpopulation selected in chickens were indistinguishable, suggesting that the differences between S proteins in the major vaccine population and the minor subpopulation selected in chickens did not result in important antigenic differences.

4. DISCUSSION

It is important to better understand IBV vaccine-induced virus-specific immunity in order to determine how IBV field strains are able to escape IBV vaccine-induced immunity. In this study, we analyzed S-specific mucosal and systemic humoral immune responses induced by a live attenuated Ark-DPI IBV vaccine. We demonstrated significantly lower levels of IgA in tears and antibodies in sera that recognize S-ectodomain protein containing S1 sequences of an Ark-type field strain compared to those recognizing the ArkDPI vaccine strain S-ectodomain protein both post-prime and post-boost in chickens vaccinated with the ArkDPI vaccine strain. All three recombinant proteins used in this study are from the Ark serotype. The field isolate S1 differs from the vaccine strain in 22 amino acid positions. Our results indicate that these amino acid changes might enable the field strain to escape the vaccine-induced host humoral immune response. It is interesting that the levels of IgA in tears recognizing the vaccine S-ectodomain increased following boosting, whereas the levels recognizing the S-ectodomain including the fields strain S1 did not. This may be related to an increase in antibody specificity for the vaccine S protein due to affinity maturation.

ACKNOWLEDGEMENTS

This work was supported by grants from the Alabama Agricultural Experiment Station and from the US Poultry & Egg foundation.

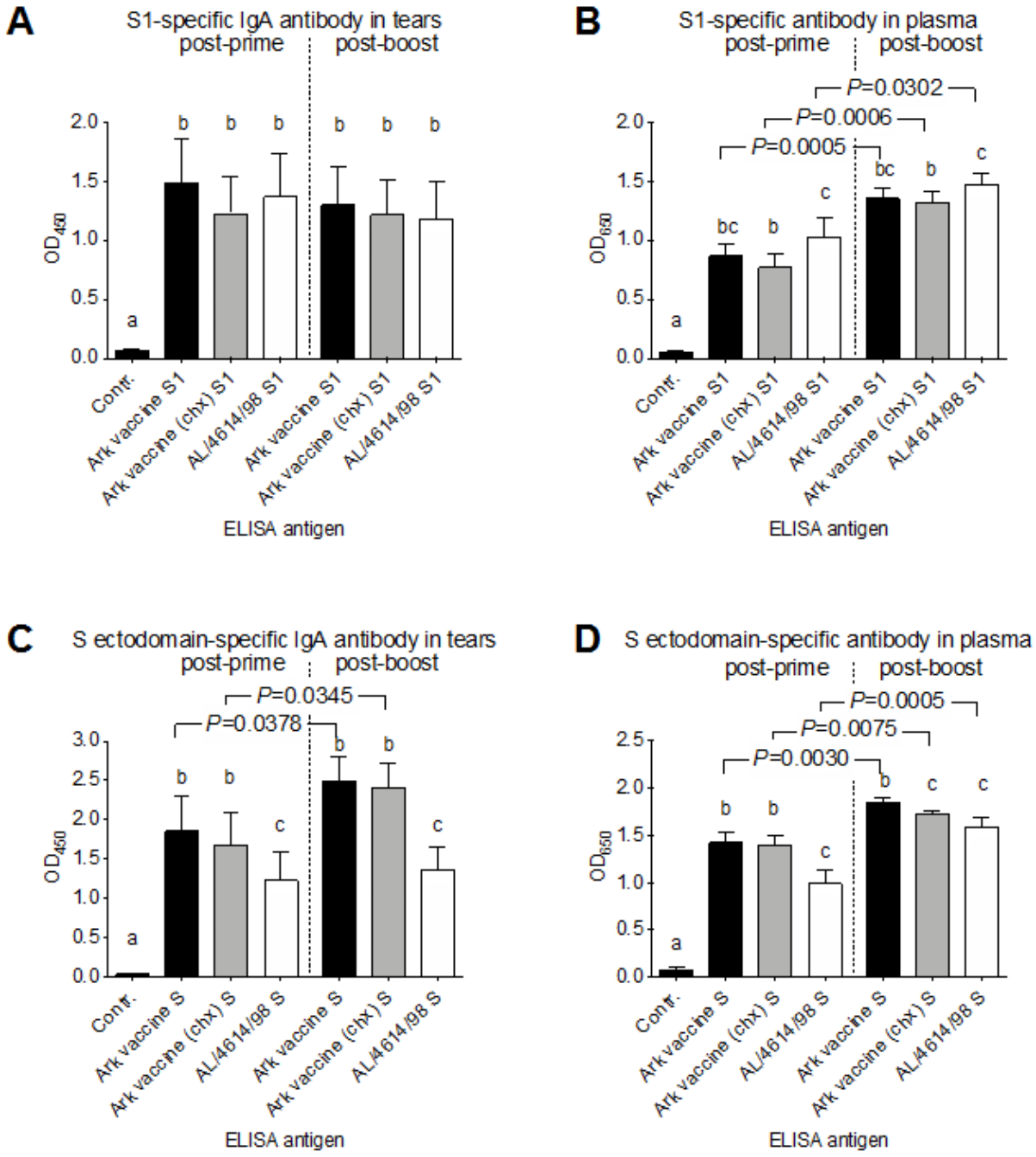

Fig. 6.1. ELISA demonstrating S1- and S-ectodomain-specific IgA antibodies in tears and antibodies in plasma of ArkDPI-vaccinated chickens. (A) S1-specific IgA in tears, (B) S1-specific antibodies in plasma, (C) S-ectodomain-specific IgA in tears, (D) S-ectodomain-specific antibodies in plasma. Antigens used in the ELISA, trimeric recombinant proteins produced in

HEK-293T cells, are indicated below the graphs. Ark vaccine (chx) indicates the vaccine subpopulation selected in chickens after vaccination. Letters indicate significant differences ($P<0.05$) determined by ANOVA (repeated measures ANOVA with Geisser-Greenhouse correction) and Tukey's post-tests, which were carried out separately for post-prime and post-boost samples. Post-prime and post-boost samples were compared by ratio paired *t*- tests; *P* values <0.05 are indicated. Error bars indicate SEM.

CHAPTER 7

CONCLUSIONS

The research presented in this dissertation constitutes a five-part investigation that was conducted to further understand avian infectious bronchitis coronavirus-host interactions at the levels of viral spike protein binding to host cells and host immune responses.

In the first two studies we further characterized a CEK-adapted ArkDPI vaccine strain *in vitro* and *in vivo*. In our first study, we observed the effects of the three amino acids changes in the spike protein of the CEK-adapted virus on attachment to CEK cells by using recombinant S protein in a protein binding assay. We expected that the CEK-adaptation would allow the S protein better binding to CEK cells compared to the ArkDPI vaccine S protein. However, we did not observe the expected improved binding of recombinant S1 or the whole S-ectodomain of CEK-adapted ArkDPI S protein to CEK cells. Instead, we observed no binding to CEK cells at standard protein concentration. Reduced binding of the S protein representing CEK-adapted ArkDPI vaccine virus suggested the possible role in adaptation of changes in other proteins encoded in the genome that also exhibited amino acid changes during CEK-adaptation.

In our second study, we were interested to observe the binding affinity of the S protein of CEK-adapted virus to chicken tissues. Similar to CEK cell binding, the S1 or S-ectodomain protein showed reduced binding to most of the formalin-fixed chicken tissues compared to the S protein of the parental vaccine strain. Exceptions were the epithelium of conjunctiva and choana, where S-ectodomain proteins representing the CEK-adapted and vaccine viruses showed similar binding

affinity. These results suggested that replication of the CEK-adapted vaccine strain in the chicken might be restricted to respiratory-associated tissues in the head, such as conjunctiva and choana. Thus we compared replication of CEK-adapted virus to a commercial ArkDPI-derived vaccine in different tissues after ocular inoculation of 1-day-old SPF leghorn chickens with 10^4 or 10^5 EID_{50} CEK-adapted ArkDPI vaccine, or 10^4 EID_{50} commercial vaccine. Significantly reduced replication as determined by viral RNA levels in tears, choanal swabs, and tracheal swabs was observed in chickens inoculated with CEK-adapted vaccine compared to the commercial vaccine when the same dose (10^4 EID_{50}) was used and in tracheal swabs even when ten times the dose of CEK-adpated virus was used. Reduction of viral loads of CEK-adapted virus in tracheal swabs was not greater than reduction in tears or choanal swabs. Thus, the replication of CEK-adapted vaccine virus was not restricted to respiratory epithelium in the head. However, in spite of substantially lower replication of the CEK-adapted vaccine virus in chickens, reflected in lower vaccine viral loads in tears, it provided effective protection against challenge.

Since amino acid changes in S protein are implicated in determining the host tropism, in our third study we explored the role of differences in the S protein in the altered pathogenesis and extended tropism of an enteric IBV variant CalEnt, expecting that the S protein of CalEnt would bind better to intestinal epithelium compared to a typical respiratory variant Cal99 S protein that has high amino acid identity with CalEnt S. Our results did not support better attachment to intestinal tissues as a reason for CalEnt's extended tropism. In addition, analyses of the S gene sequence using bioinformatic approaches revealed that CalEnt's S2-coding region was likely acquired through a recombination event and encodes a unique amino acid sequence at the putative recognition site for the protease that activates the S protein for fusion. Thus, S2 activation by

tissue-specific proteases might facilitate CalEnt entry into intestinal epithelial cells and compensate for poor binding by its S protein.

In our fourth study, we investigated the effects of early vaccination on immune responses in chickens primed at increasing ages with ArkDPI-type vaccine followed by booster vaccination with the same vaccine. We confirmed that IBV vaccination on the day of hatch induces suboptimal IBV immune responses both in the systemic and mucosal compartments, particularly after prime vaccination. Thus, the routine practice of vaccinating chicks with IBV early after hatch may be contributing to the immunologic escape of the virus and increased persistence of vaccine virus in vaccinated chickens. However, booster vaccination could overcome poor initial responses.

In our final study, we demonstrated significantly lower levels of S-specific IgA in tears and antibodies in sera recognizing an Ark-type field strain S protein compared to ArkDPI vaccine strain S protein both post prime and boost in chickens vaccinated with the ArkDPI vaccine strain. Our results support the concept that IBV field strains escape the host humoral immune responses through aa changes within the S1 protein.

REFERENCES

1. Jackwood MW. Review of infectious bronchitis virus around the world. Avian Dis. 56:634-641; 2012.

2. de Wit JJ, Cook JKA, van der Heijden HMJF. Infectious bronchitis virus variants: A review of the history, current situation and control measures. Avian Pathol. 40:223-225; 2011.

3. Jones RC. Viral respiratory diseases (ilt, ampv infections, ib): Are they ever under control? Br Poult Sci. 51: 1-11; 2010

4. Cavanagh D, Gelb JJ. Infectious bronchitis. In: Y.M. Saif, Fadly AM, Glisson JR, McDougald LR, Nolan LK, Swayne DE, editors. *Diseases of poultry*. 12 ed. Ames, Iowa, USA: Blackwell Publishing Professional. p. 117-135; 2008.

5. Alexander DJ, Gough RE. Isolation of avian infectious bronchitis virus from experimentally infected chickens. Res Vet Sci. 23:344-347; 1977.

6. Animas SB, Otsuki K, Hanayama M, Sanekata T, Tsubokura M. Experimental infection with avian infectious bronchitis virus (kagoshima-34 strain) in chicks at different ages. J Vet Med Sci. 56:443-447; 1994.

7. Toro H, Godoy V, Larenas J, Reyes E, Kaleta EF. Avian infectious bronchitis: Viral persistence in the harderian gland and histological changes after eyedrop vaccination. Avian Dis 40:114-120; 1996.

8. van Ginkel FW, van Santen VL, Gulley SL, Toro H. Infectious bronchitis virus in the chicken harderian gland and lachrymal fluid: Viral load, infectivity, immune cell responses, and effects of viral immunodeficiency. Avian Dis. 52:608-617; 2008.

9. Cavanagh D. Severe acute respiratory syndrome vaccine development: Experiences of vaccination against avian infectious bronchitis coronavirus. Avian Pathol. 32:567-582; 2003.

10. Raj GD, Jones RC. Infectious bronchitis virus: Immunopathogenesis of infection in the chickens. Avian Pathol. 26: 677–706; 1997.

11. Cavanagh D. Coronavirus avian infectious bronchitis virus. Vet Res. 38:281–297; 2007.

12. Crinion RA, Hofstad MS. Pathogenicity of four serotypes of avian infectious bronchitis virus for the oviduct of young chickens of various ages. Avian Dis. 16:351-363; 1972.

13. Hauck R, Gallardo RA, Woolcock PR, Shivaprasad HL. A coronavirus associated with runting stunting syndrome in broiler chickens. Avian Dis. 60:528-534; 2016.

14. Chen BY, Itakura C. Cytopathology of chick renal epithelial cells experimentally infected with avian infectious bronchitis virus. Avian Pathol. 25:675-690; 1996.

15. Franca M, Woolcock PR, Yu M, Jackwood MW, Shivaprasad HL. Nephritis associated with infectious bronchitis virus cal99 variant in game chickens. Avian Dis. 55:422-428; 2011.

16. Gelb JJ, Ladman BS, Pope CR, Ruano JM, Brannick EM, Bautista DA, Coughlin CM, Preskenis LA. Characterization of nephropathogenic infectious bronchitis virus dmv/1639/11 recovered from delmarva broiler chickens in 2011. Avian Dis. 57:65-70; 2013.

17. Karaca K, Naqi SA, Palukaitis P, Lucio B. Serological and molecular characterization of three enteric isolates of infectious bronchitis virus of chickens. Avian Dis. 34:899-904; 1990.

18. Yu L, Jiang Y, Low S, Wang Z, Nam SJ, Liu W, Kwangac J. Characterization of three infectious bronchitis virus isolates from china associated with proventriculus in vaccinated chickens. Avian Dis. 45:416-424; 2001.

19. Ariaans MP, Matthijs MG, van Haarlem D, van de Haar P, van Eck JH, Hensen EJ, Vervelde L. The role of phagocytic cells in enhanced susceptibility of broilers to colibacillosis after infectious bronchitis virus infection. Vet Immunol Immunopathol. 123:240-250; 2008.

20. Bande F, Arshad SS, Omar AR, Bejo MH, Abubakar MS, Abba Y. Pathogenesis and diagnostic approaches of avian infectious bronchitis. Adv Virol. 2016; 2016.

21. Gallardo RA, van Santen VL, Toro H. Effects of chicken anaemia virus and infectious bursal disease virus-induced immunodeficiency on infectious bronchitis virus replication and genotypic drift. Avian Pathol. 41:451-458; 2012.

22. van Ginkel FW, Padgett J, Martinez-Romero G, Miller MS, Joiner KS, Gulley SL. Age-dependent immune responses and immune protection after avian coronavirus vaccination. Vaccine. 33:2655-2661; 2015.

23. Jackwood MW, de Wit S. Infectious bronchitis. In: Swayne DE, Glisson JR, McDougald LR, Nolan LK, Suarez DL, Nair VL, editors. *Diseases of poultry*. Ames, IA.: Wiley-Blackwell Publishing; 2013.

24. Ambali AG, Jones RC. Early pathogenesis in chicks of infection with an enterotropic strain of infectious bronchitis virus. Avian Dis. 34:809-817; 1990.

25. Ignjatovic J, Sapats S. Avian infectious bronchitis virus. Rev sci tech Off int Epiz. 19 493-508; 2000.

26. Sapats SI, Ashton F, Wright PJ, Ignjatovic J. Sequence analysis of the S1 glycoprotein of infectious bronchitis viruses: Identification of a novel genotypic group in australia. J Gen Virol. 77:413-418; 1996.

27. Jackwood MW, Hilt DA, Lee CW, Kwon HM, Callison SA, Moore KM, Moscoso H, Sellers H, Thayer S. Data from 11 years of molecular typing infectious bronchitis virus field isolates. Avian Dis. 49:614-618; 2005.

28. Gelb J, Jr., Cloud SS. Effect of serial embryo passage of an arkansas-type avian infectious bronchitis virus isolate on clinical response, virus recovery, and immunity. Avian Dis. 27:679-687; 1983.

29. Jackwood MW, Hilt DA, Brown TP. Attenuation, safety, and efficacy of an infectious bronchitis virus ga98 serotype vaccine. Avian Dis. 47:627-632; 2003.

30. Eldemery F, Joiner KS, Toro H, van Santen VL. Protection against infectious bronchitis virus by spike ectodomain subunit vaccine. Vaccine. 35:5864-5871; 2017.

31. Johnson MA, Pooley C, Ignjatovic J, Tyack SG. A recombinant fowl adenovirus expressing the S1 gene of infectious bronchitis virus protects against challenge with infectious bronchitis virus. Vaccine. 21:2730-2736; 2003.

32. Abozeid HH, Paldurai A, Varghese BP, Khattar SK, Afifi MA, Zouelfakkar S, El‐Deeb AH, El‐Kady MF, Samal SK. Development of a recombinant newcastle disease virus‐vectored

vaccine for infectious bronchitis virus variant strains circulating in egypt. Veterinary Research. 50:12; 2019.

33. Shirvani E, Paldurai A, Manoharan VK, Varghese BP, Samal SK. A recombinant newcastle disease virus (ndv) expressing s protein of infectious bronchitis virus (IBV) protects chickens against IBV and ndv. Scientific Reports. 8:11951; 2018.

34. Hopkins SR, Yoder HW, Jr. Increased incidence of airsacculitis in broilers infected with mycoplasma synoviae and chicken-passaged infectious bronchitis vaccine virus. Avian Dis. 28:386-396; 1984.

35. Hopkins SR, Yoder HW, Jr. Reversion to virulence of chicken-passaged infectious bronchitis vaccine virus. Avian Dis. 30:221-223; 1986.

36. McKinley ET, Hilt DA, Jackwood MW. Avian coronavirus infectious bronchitis attenuated live vaccines undergo selection of subpopulations and mutations following vaccination. Vaccine. 26:1274-1284; 2008.

37. Toro H, Pennington D, Gallardo RA, van Santen VL, van Ginkel FW, Zhang J, Joiner KS. Infectious bronchitis virus subpopulations in vaccinated chickens after challenge. Avian Dis. 56:501-508; 2012.

38. van Santen VL, Toro H. Rapid selection in chickens of subpopulations within ArkDPI-derived infectious bronchitis virus vaccines. Avian Pathol. 37:293-306; 2008.

39. Lee HJ, Youn HN, Kwon JS, Lee YJ, Kim JH, Lee JB, Park SY, Choi IS, Song CS. Characterization of a novel live attenuated infectious bronchitis virus vaccine candidate derived from a korean nephropathogenic strain. Vaccine. 28:2887-2894; 2010.

40. Quinteros JA, Lee SW, Markham PF, Noormohammadi AH, Hartley CA, Legione AR, Coppo MJC, Vaz PK, Browning GF. Full genome analysis of australian infectious bronchitis viruses suggests frequent recombination events between vaccine strains and multiple phylogenetically distant avian coronaviruses of unknown origin. Vet Microbiol. 197:27-38; 2016.

41. Zhang T, Han Z, Xu Q, Wang Q, Gao M, Wu W, Shao Y, Li H, Kong X, Liu S. Serotype shift of a 793/b genotype infectious bronchitis coronavirus by natural recombination. Infect Genet Evol. 32:377-387; 2015.

42. Schalk AF, Hawn MC. An apparantly new respiratory disease of baby chicks. J Am Vet Med Assoc. 78:413-422; 1931.

43. Lai MMC, Holmes KV. Coronaviridae: The viruses and their replication. In: Knipe DM, Howleyth PM, editors. *Fundamental virology*. 4 ed. Philadelphia: Lippincott Williams and Wilkins. p. 641-663; 2001.

44. Lai MMC. Coronavirus: Organization, replication and expression of genome. Annu Rev Microbiol. 44:303-333; 1990.

45. Lai MMC, Cavanagh D. The molecular biology of coronaviruses. Adv Virus Res. 48:1-100; 1997.

46. Masters PS, Perlman S. Coronaviridae. In: Knipe DM, Howley PM, Cohen JI, Griffin DE, Lamb RA, Martin MA, Racaniello VR, Roizman B, editors. *Fields virology*. 6 ed. Philadelphia, PA.: Lippincott Williams & Wilkins. p. 825–858; 2013.

47. Casais R, Davies M, Cavanagh D, Britton P. Gene 5 of the avian coronavirus infectious bronchitis virus is not essential for replication. J Virol. 79:8065-8078; 2005.

48. Hodgson T, Britton P, Cavanagh D. Neither the rna nor the proteins of open reading frames 3a and 3b of the coronavirus infectious bronchitis virus are essential for replication. J Virol. 80:296-305; 2006.

49. Bosch BJ, van der Zee R, de Haan CA, Rottier PJ. The coronavirus spike protein is a class i virus fusion protein: Structural and functional characterization of the fusion core complex. J Virol 77:8801-8811; 2003.

50. Cavanagh D. Coronavirus IBV: Structural characterization of the spike protein. J Gen Virol. 64:2577-2583; 1983.

51. Cavanagh D, Davis PJ, Pappin DJC, Binns MM, Boursnell ME, Brown TD. Coronavirus IBV: Partial amino terminal sequencing of spike polypeptide S2 identifies the sequence arg-arg-phe-arg-arg at the cleavage site of the spike precursor propolypeptide of IBV strains Beaudette and m41. Virus Res. 4:133-143; 1986.

52. Shang J, Zheng Y, Yang Y, Liu C, Geng Q, Luo C, Zhang W, Li F. Cryo-em structure of infectious bronchitis coronavirus spike protein reveals structural and functional evolution of coronavirus spike proteins. PLoS Pathog. 14:e1007009; 2018.

53. Wickramasinghe INA, van Beurden SJ, Weerts EA, Verheije MH. The avian coronavirus spike protein. Virus Res. 194:37-48; 2014.

54. Cavanagh D, Davis PJ, Cook JK, Li D, Kant A, Koch G. Location of the amino acid differences in the S1 spike glycoprotein subunit of closely related serotypes of infectious bronchitis virus. Avian Pathol. 21:33-43; 1992.

55. Moore KM, Jackwood MW, Hilt DA. Identification of amino acids involved in a serotype and neutralization specific epitope within the S1 subunit of avian infectious bronchitis virus. Arch Virol. 142:2249-2256; 1997.

56. Kant A, Koch G, van Roozelaar DJ, Kusters JG, Poelwijk FA, van der Zeijst BA. Location of antigenic sites defined by neutralizing monoclonal antibodies on the S1 avian infectious bronchitis virus glycopolypeptide. J Gen Virol. 73:591-596; 1992.

57. Koch G, Hartog L, Kant A, van Roozelaar DJ. Antigenic domains on the peplomer protein of avian infectious bronchitis virus: Correlation with biological functions. J Gen Virol. 71:1929-1935; 1990.

58. Niesters HG, Bleumink-Pluym NM, Osterhaus AD, Horzinek MC, van der Zeijst BA. Epitopes on the peplomer protein of infectious bronchitis virus strain m41 as defined by monoclonal antibodies. Virology. 161:511-519; 1987.

59. Toro H, van Santen VL, Li L, Lockaby SB, van Santen E, Hoerr FJ. Epidemiological and experimental evidence for immunodeficiency affecting avian infectious bronchitis. Avian Pathol. 35:455-464; 2006.

60. Fang SG, Shen S, Tay FP, Liu DX. Selection of and recombination between minor variants lead to the adaptation of an avian coronavirus to primate cells. Biochem Biophys Res Commun. 336:417-423; 2005.

61. Toro H, van Santen VL, Jackwood MW. Genetic diversity and selection regulates evolution of infectious bronchitis virus. Avian Dis. 56:449-455; 2012.

62. Nix WA, Troeber DS, Kingham BF, Keeler CL, Jr., Gelb J, Jr. Emergence of subtype strains of the arkansas serotype of infectious bronchitis virus in delmarva broiler chickens. Avian Dis. 44:568-581; 2000.

63. Jackwood MW, Hilt DA, Callison SA. Detection of infectious bronchitis virus by real-time reverse transcriptase-polymerase chain reaction and identification of a quasispecies in the Beaudette strain. Avian Dis. 47:718-724; 2003.

64. Gallardo RA, van Santen VL, Toro H. Host intraspatial selection of infectious bronchitis virus populations. Avian Dis. 54:807-813; 2010.

65. Ghetas AM, van Santen VL, Joiner K, Toro H. Kidney cell-adapted infectious bronchitis virus arkansas delmarva poultry industry vaccine confers effective protection against challenge. Avian Dis. 60:418-423; 2016.

66. Zegpi RA, Breedlove C, van Santen VL, Rasmussen-Ivey CR, Toro H. Kidney cell-adapted infectious bronchitis ArkDPI vaccine is stable and protective. Avian Dis. 61:221-228; 2017.

67. Heald-Sargent T, Gallagher T. Ready, set, fuse! The coronavirus spike protein and acquisition of fusion competence. Viruses. 4:557-580; 2012.

68. Yamada Y, Liu DX. Proteolytic activation of the spike protein at a novel rrrr/s motif is implicated in furin-dependent entry, syncytium formation, and infectivity of coronavirus infectious bronchitis virus in cultured cells. J Virol. 83: 8744-8758; 2009.

69. Walls AC, Tortorici MA, Snijder J, Xiong XL, Bosch BJ, Rey FA, Veesler D. Tectonic conformational changes of a coronavirus spike glycoprotein promote membrane fusion. In: *Proceedings of Proceedings of the National Academy of Sciences of the United States of America*; 2017 Oct. p. 11157-11162.

70. Promkuntod N, Wickramasinghe IN, de Vrieze G, Grone A, Verheije MH. Contributions of the S2 spike ectodomain to attachment and host range of infectious bronchitis virus. Virus Res. 177:127-137; 2013.

71. Li F. Evidence for a common evolutionary origin of coronavirus spike protein receptor-binding subunits. J Virol. 86:2856-2858; 2012.

72. Li D, Cavanagh D. Coronavirus IBV-induced membrane fusion occurs at near-neutral ph. Arch Virol. 122:307-316; 1992.

73. Winter C, Schwegmann-Wessels C, Cavanagh D, Neumann U, Herrler G. Sialic acid is a receptor determinant for infection of cells by avian infectious bronchitis virus. J Gen Virol. 87:1209-1216; 2006.

74. Chu VC, McElroy LJ, Chu V, Bauman BE, Whittaker GR. The avian coronavirus infectious bronchitis virus undergoes direct low-ph-dependent fusion activation during entry into host cells. J Virol. 80:3180-3188; 2006.

75. Winter C, Herrler G, Neumann U. Infection of the tracheal epithelium by infectious bronchitis virus is sialic acid dependent. Microbes Infect. 10:367-373; 2008.

76. Wickramasinghe INA, de Vries RP, Gröne A, De Haan CAM, Verheije MH. Binding of avian coronavirus spike proteins to host factors reflects virus tropism and pathogenicity. J Virol. 85:8903-8912; 2011.

77. Li F. Structure, function, and evolution of coronavirus spike proteins. Annu Rev Virol. 3:237-261; 2016.

78. Promkuntod N, van Eijndhoven RE, de Vrieze G, Grone A, Verheije MH. Mapping of the receptor-binding domain and amino acids critical for attachment in the spike protein of avian coronavirus infectious bronchitis virus. Virology. 448:26-32; 2014.

79. Phillips JJ, Chua MM, Lavi E, Weiss SR. Pathogenesis of chimeric mhv4/mhv-a59 recombinant viruses: The murine coronavirus spike protein is a major determinant of neurovirulence. J Virol. 73:7752-7760; 1999.

80. Jackwood MW, Boynton TO, Hilt DA, McKinley ET, Kissinger JC, Paterson AH, Robertson J, Lemke C, McCall AW, Williams SM et al. Emergence of a group 3 coronavirus through recombination. Virology. 398:98-108; 2010.

81. Ndegwa EN, Joiner KS, Toro H, van Ginkel FW, van Santen VL. The proportion of specific viral subpopulations in attenuated arkansas delmarva poultry industry infectious bronchitis vaccines influences vaccination outcome. Avian Dis. 56:642-653; 2012.

82. Cunningham CH, Spring MP, Nazerian K. Replication of avian infectious bronchitis virus in african green monkey kidney cell line vero. J Gen Virol. 16:423-427; 1972.

83. Otsuki K, Noro K, Yamamoto H, Tsubokura M. Studies on avian infectious bronchitis virus (IBV). Ii. Propagation of IBV in several cultured cells. Arch Virol. 60:115-122; 1979.

84. Binns MM, Boursnell MEG, Tomley FM, Brown TDK. Comparison of the spike precursor sequences of coronavirus IBV strains m41 and 6/82 with that of IBV Beaudette. J gen Virol. 67:2825-2831; 1986.

85. Casais R, Dove B, Cavanagh D, Britton P. Recombinant avian infectious bronchitis virus expressing a heterologous spike gene demonstrates that the spike protein is a determinant of cell tropism. J Virol. 77:9084-9089; 2003.

86. Hulswit RJG, de Haan CAM, Bosch BJ. Coronavirus spike protein and tropism changes. In: Ziebuhr J, editor. *Adv virus res*. p. 29-57; 2016.

87. Ballesteros ML, Sanchez CM, Enjuanes L. Two amino acid changes at the n-terminus of transmissible gastroenteritis coronavirus spike protein result in the loss of enteric tropism. Virology. 227:378-388; 1997.

88. Li W, Zhang C, Sui J, Kuhn JH, Moore MJ, Luo S, Wong SK, Huang IC, Xu K, Vasilieva N et al. Receptor and viral determinants of sars-coronavirus adaptation to human ace2. Embo J. 24:1634-1643; 2005.

89. Ghetas AM, Thaxton GE, Breedlove C, van Santen VL, Toro H. Effects of adaptation of infectious bronchitis virus arkansas attenuated vaccine to embryonic kidney cells. Avian Dis. 59:106-113; 2015.

90. Millet JK, Whittaker GR. Host cell proteases: Critical determinants of coronavirus tropism and pathogenesis. Virus Res. 202:120-134; 2015.

91. Bickerton E, Maier HJ, Stevenson-Leggett P, Armesto M, Britton P. The S2 subunit of infectious bronchitis virus Beaudette is a determinant of cellular tropism. J Virol. 92: e01044-01018; 2018.

92. Sperry SM, Kazi L, Graham RL, Baric RS, Weiss SR, Denison MR. Single-amino-acid substitutions in open reading frame (orf) 1b-nsp14 and orf 2a proteins of the coronavirus mouse hepatitis virus are attenuating in mice. J Virol. 79:3391-3400; 2005.

93. Zust R, Cervantes-Barragan L, Kuri T, Blakqori G, Weber F, Ludewig B, Thiel V. Coronavirus non-structural protein 1 is a major pathogenicity factor: Implications for the rational design of coronavirus vaccines. PLoS Pathog. 3:e109; 2007.

94. Hodgson T, Casais R, Dove B, Britton P, Cavanagh D. Recombinant infectious bronchitis coronavirus Beaudette with the spike protein gene of the pathogenic m41 strain remains attenuated but induces protective immunity. J Virol. 78:13804-13811; 2004.

95. Armesto M, Evans S, Cavanagh D, Abu-Median AB, Keep S, Britton P. A recombinant avian infectious bronchitis virus expressing a heterologous spike gene belonging to the 4/91 serotype. PLoS One. 6:e24352; 2011.

96. Armesto M, Cavanagh D, Britton P. The replicase gene of avian coronavirus infectious bronchitis virus is a determinant of pathogenicity. PLoS One. 4:e7384; 2009.

97. Ammayappan A, Upadhyay C, Gelb J, Jr., Vakharia VN. Identification of sequence changes responsible for the attenuation of avian infectious bronchitis virus strain arkansas dpi. Arch Virol. 154:495-499; 2009.

98. Medvedev KE, Kinch LN, Grishin NV. Functional and evolutionary analysis of viral proteins containing a rossmann-like fold. Protein Sci. 27:1450-1463; 2018

99. Yu K, Ming Z, Li Y, Chen C, Bao Z, Ren Z, Liu B, Tao W, Raoa Z, Lou Z. Purification, crystallization and preliminary x-ray analysis of nonstructural protein 2 (nsp2) from avian infectious bronchitis virus. Acta Cryst. 68:716-719; 2012.

100. Montgomery RD, Boyle CR, Maslin WR, Magee DL. Attempts to reproduce a runting/stunting-type syndrome using infectious agents isolated from affected mississippi broilers. Avian Dis. 41:80-92; 1997.

101. Koo BS, Lee HR, Jeon EO, Han MS, Min KC, Lee SB, Bae YJ, Cho SH, Mo JS, Kwon HM et al. Genetic characterization of three novel chicken parvovirus strains based on analysis of their coding sequences. Avian Pathol. 44:28-34; 2015.

102. Zsak L, Cha RM, Day JM. Chicken parvovirus-induced runting-stunting syndrome in young broilers. Avian Dis. 57:123-127; 2013.

103. Wolf S, Reetz J, Otto P. Genetic characterization of a novel calicivirus from a chicken. Arch Virol. 156:1143-1150; 2011.

104. Otto P, Liebler-Tenorio EM, Elschner M, Reetz J, Lohren U, Diller R. Detection of rotaviruses and intestinal lesions in broiler chicks from flocks with runting and stunting syndrome (rss). Avian Dis. 50:411-418; 2006.

105. Baxendale W, Mebatsion T. The isolation and characterisation of astroviruses from chickens. Avian Pathol. 33:364-370; 2004.

106. Sellers H, Linneman E, Icard AH, Mundt E. A purified recombinant baculovirus expressed capsid protein of a new astrovirus provides partial protection to runting-stunting syndrome in chickens. Vaccine. 28:1253-1263; 2010.

107. Davis JF, Kulkarni A, Fletcher O. Reovirus infections in young broiler chickens. Avian Dis. 57:321-325; 2013.

108. Marguerie J, Leon O, Albaric O, Guy JS, Guerin JL. Birnavirus-associated proventriculitis in french broiler chickens. Vet Rec. 169:394-396; 2011.

109. El-Houadfi M, Jones RC, Cook JK, Ambali AG. The isolation and characterisation of six avian infectious bronchitis viruses isolated in morocco. Avian Pathol. 15:93-105; 1986.

110. Lucio B, Fabricant J. Tissue tropism of three cloacal isolates and massachusetts strain of infectious bronchitis virus. Avian Dis. 34:865-870; 1990.

111. Rimondi A, Craig MI, Vagnozzi A, König G, Delamer M, Pereda A. Molecular characterization of avian infectious bronchitis virus strains from outbreaks in argentina (2001-2008). Avian Pathol. 38:149-153; 2009.

112. Jackwood MW, Hilt DA, McCall AW, Polizzi CN, McKinley ET, Williams SM. Infectious bronchitis virus field vaccination coverage and persistence of arkansas-type viruses in commercial broilers. Avian Dis. 53:175-183; 2009.

113. Roh HJ, Hilt DA, Williams SM, Jackwooda MW. Evaluation of infectious bronchitis virus arkansas-type vaccine failure in commercial broilers. Avian Dis. 57:248-259; 2013.

114. Ndegwa EN, Toro H, van Santen VL. Comparison of vaccine subpopulation selection, viral loads, vaccine virus persistence in trachea and cloaca, and mucosal antibody responses after vaccination with two different arkansas delmarva poultry industry -derived infectious bronchitis virus vaccines. Avian Dis. 58:102-110; 2014.

115. Plachy J, Pink JR, Hala K. Biology of the chicken mhc (b complex). Crit Rev Immunol. 12:47-79; 1992.

116. Briles WE, Briles RW. Genetics and classification of major histocompatibility complex antigens of the chicken. Poult Sci. 66:776-781; 1987.

117. Shiina T, Briles WE, Goto RM, Hosomichi K, Yanagiya K, Shimizu S, Inoko H, Miller MM. Extended gene map reveals tripartite motif, c-type lectin, and ig superfamily type genes within a subregion of the chicken mhc-b affecting infectious disease. J Immunol. 178:7162-7172; 2007.

118. Banat GR, Tkalcic S, Dzielawa JA, Jackwood MW, Saggese MD, Yates L, Kopulos R, Briles WE, Collisson EW. Association of the chicken mhc b haplotypes with resistance to avian coronavirus. Dev Comp Immunol. 39:430-437; 2013.

119. Otsuki K, Huggins MB, Cook JKA. Comparison of the susceptibility to avian infectious bronchitis virus-infection of two inbred lines of white leghorn chickens. Avian Pathology. 19:467-475; 1990.

120. Bacon LD, Hunter DB, Zhang HM, Brand K, Etches R. Retrospective evidence that the mhc (b haplotype) of chickens influences genetic resistance to attenuated infectious bronchitis vaccine strains in chickens. Avian Pathol. 33:605-609; 2004.

121. Cook J, Otsuki K, Huggins M, Bumstead N. Investigations into resistance of chicken lines to infection with infectious bronchitis virus. Adv Exp Med Biol. 276:491-496; 1990.

122. Kameka AM, Haddadi S, Kim DS, Cork SC, Abdul-Careem MF. Induction of innate immune response following infectious bronchitis corona virus infection in the respiratory tract of chickens. Virology. 450-451:114-121; 2014.

123. Guo X, Rosa AJ, Chen DG, Wang X. Molecular mechanisms of primary and secondary mucosal immunity using avian infectious bronchitis virus as a model system. Vet Immunol Immunopathol. 121:332-343; 2008.

124. Kint J, Fernandez-Gutierrez M, Maier HJ, Britton P, Langereis MA, Koumans J, Wiegertjes GF, Forlenza M. Activation of the chicken type i interferon response by infectious bronchitis coronavirus. J Virol. 89:1156-1167; 2015.

125. Collisson EW, Pei J, Dzielawa J, Seo SH. Cytotoxic t lymphocytes are critical in the control of infectious bronchitis virus in poultry. Dev Comp Immunol. 24:187-200; 2000.

126. Ignjatovic J, Galli L. The S1 glycoprotein but not the n or m proteins of avian infectious bronchitis virus induces protection in vaccinated chickens. Arch Virol. 138:117-134; 1994.

127. Seo SH, Collisson EW. Specific cytotoxic t lymphocytes are involved in in vivo clearance of infectious bronchitis virus. J Virol. 71:5173-5177; 1997.

128. Mondal SP, Naqi SA. Maternal antibody to infectious bronchitis virus: Its role in protection against infection and development of active immunity to vaccine. Vet Immunol Immunopathol. 79:31-40; 2001.

129. Toro H, Fernandez I. Avian infectious bronchitis: Specific lachrymal iga level and resistance against challenge. Zentralbl Veterinarmed B 41:467-472; 1994.

130. Brownlie R, Zhu J, Allan B, Mutwiri GK, Babiuk LA, Potter A, Griebel P. Chicken tlr21 acts as a functional homologue to mammalian tlr9 in the recognition of cpg oligodeoxynucleotides. Mol Immunol. 46:3163-3170; 2009.

131. Maslak DM, Reynolds DL. B cells and t-lymphocyte subsets of the head-associated lymphoid tissues of the chicken. Avian Dis. 39:736-742; 1995.

132. Hamal KR, Burgess SC, Pevzner IY, Erf GF. Maternal antibody transfer from dams to their egg yolks, egg whites, and chicks in meat lines of chickens. Poult Sci. 85:1364-1372; 2006.

133. Lowenthal JW, Connick TE, McWaters PG, York JJ. Development of t cell immune responsiveness in the chicken. Immunol Cell Biol. 72:115-122; 1994.

134. Kusters JG, Jager EJ, Niesters HG, van der Zeijst BA. Sequence evidence for rna recombination in field isolates of avian coronavirus infectious bronchitis virus. Vaccine. 8:605-608; 1990.

135. Kusters JG, Niesters HG, Bleumink-Pluym NM, Davelaar FG, Horzinek MC, van der Zeijst BA. Molecular epidemiology of infectious bronchitis virus in the netherlands. J Gen Virol. 68:343-352; 1987.

136. Kusters JG, Niesters HG, Lenstra JA, Horzinek MC, van der Zeijst BA. Phylogeny of antigenic variants of avian coronavirus IBV. Virology. 169:217-221; 1989.

137. Cavanagh D, Naqi S. Infectious bronchitis. In: Saif YM, Barnes HJ, Glisson JR, Fadly AM, McDougald LR, Swayne DE, editors. *Diseases of poultry*. 11 ed. Ames:Iowa State Press.; 2003.

138. Cavanagh D, Davis PJ, Mockett AP. Amino acids within hypervariable region 1 of avian coronavirus IBV (massachusetts serotype) spike glycoprotein are associated with neutralization epitopes. Virus Res. 11:141-150; 1988.

139. Han Z, Sun C, Yan B, Zhang X, Wang Y, Li C, Zhang Q, Ma Y, Shao Y, Liu Q et al. A 15-year analysis of molecular epidemiology of avian infectious bronchitis coronavirus in china. Infect Genet Evol. 11:190-200; 2011.

140. Wickramasinghe IN, Verheije MH. Protein histochemistry using coronaviral spike proteins: Studying binding profiles and sialic acid requirements for attachment to tissues. Methods Mol Biol. 1282:155-163; 2015.

141. van Santen VL, Wickramasinghe INA, Weerts EAWS, Wandee N, de Vrieze G, A. G., Verheije MH. Differential binding of spike proteins of ArkDPI IBV vaccine subpopulations to chicken tissues. In: *Proceedings of Proceedings of the 8th International Symposium on Avian Corona- and Pneumoviruses and Complicating Pathogens Rauischholzhausen, Germany, VVB Laufersweile Verlag* 2014. p. 205-208.

142. Sambrook J, Russell DW. *Molecular cloning: A laboratory manual*. 3rd ed. Cold Spring Harbor (NY): Cold Spring Harbor Laboratory Press; 2001.

143. Roy A, Kucukural A, Zhang Y. I-tasser: A unified platform for automated protein structure and function prediction. Nat Protoc. 5:725-738; 2010.

144. Yang J, Yan R, Roy A, Xu D, Poisson J, Zhang Y. The i-tasser suite: Protein structure and function prediction. Nat Methods. 12:7-8; 2015.

145. Zhang Y. I-tasser server for protein 3d structure prediction. BMC Bioinformatics. 9:40; 2008.

146. Clementz MA, Chen Z, Banach BS, Wang Y, Sun L, Ratia K, Baez-Santos YM, Wang J, Takayama J, Ghosh AK et al. Deubiquitinating and interferon antagonism activities of coronavirus papain-like proteases. J Virol. 84:4619-4629; 2010.

147. Frieman M, Ratia K, Johnston RE, Mesecar AD, Baric RS. Severe acute respiratory syndrome coronavirus papain-like protease ubiquitin-like domain and catalytic domain regulate antagonism of irf3 and nf-kappab signaling. J Virol. 83:6689-6705; 2009.

148. Yang X, Chen X, Bian G, Tu J, Xing Y, Wang Y, Chen Z. Proteolytic processing, deubiquitinase and interferon antagonist activities of middle east respiratory syndrome coronavirus papain-like protease. J Gen Virol. 95:614-626; 2014.

149. Sekellick MJ, Biggers WJ, Marcus PI. Development of the interferon system. I. In chicken cells development *in ovo* continues on time *in vitro*. In Vitro Cell Dev Biol. 26:997-1003; 1990.

150. Eldemery F. *Prevention and pathogenesis of avian infectious bronchitis: The role of infectious bronchitis virus spike proteins in cell attachment and protective immunity* [dissertation]. [Auburn (AL)]: Auburn University; 2017.

151. Toro H, Lavaud P, Vallejos P, Ferreira A. Transfer of igg from serum to lachrymal fluid in chickens. Avian Dis. 37:60-66; 1993.

152. Callison SA, Hilt DA, Boynton TO, Sample BF, Robison R, Swayne DE, Jackwood MW. Development and evaluation of a real-time taqman rt-pcr assay for the detection of infectious bronchitis virus from infected chickens. J Virol Methods 138:60-65; 2006.

153. Cook JKA. The classification of new serotypes of infectious bronchitis virus isolated from poultry flocks in britain between 1981 and 1983. Avian Pathol. 13:733-741; 1984.

154. Cook JKA, Huggins MB. Newly isolated serotypes of infectious bronchitis virus: Their role in disease. Avian Pathol. 15:129-138; 1986.

155. Benyeda Z, Mato T, Suveges T, Szabo E, Kardi V, Abonyi-Toth Z, Rusvai M, Palya V. Comparison of the pathogenicity of qx-like, m41 and 793/b infectious bronchitis strains from different pathological conditions. Avian Pathol. 38:449-456; 2009.

156. Benyeda Z, Szeredi L, Mato T, Suveges T, Balka G, Abonyi-Toth Z, Rusvai M, Palya V. Comparative histopathology and immunohistochemistry of qx-like, massachusetts and 793/b serotypes of infectious bronchitis virus infection in chickens. J Comp Pathol. 143:276-283; 2010.

157. Pantin-Jackwood MJ, Brown TP, Huff GR. Reproduction of proventriculitis in commercial and specific-pathogen-free broiler chickens. Avian Dis. 49:352-360; 2005.

158. Chacón JL, Assayag MS, Jr., Revolledo L, Astolfi-Ferreira CS, Vejarano MP, Jones RC, Piantino Ferreira AJ. Pathogenicity and molecular characteristics of infectious bronchitis virus

(IBV) strains isolated from broilers showing diarrhoea and respiratory disease. Br Poult Sci. 55:271-283; 2014.

159. Wickramasinghe INA, de Vries RP, Weerts EAWS, van Beurden SJ, Peng W, McBride R, Ducatez M, Guy J, Brown P, Eterradossi N. Novel receptor specificity of avian gammacoronaviruses causing enteritis. J Virol. 89:8783-8792; 2015.

160. Waterhouse A, Bertoni M, Bienert S, Studer G, Tauriello G, Gumienny R, Heer FT, de Beer TAP, Rempfer C, Bordoli L et al. Swiss-model: Homology modelling of protein structures and complexes. Nucleic Acids Res. 46:W296-W303; 2018.

161. Martin DP, Murrell B, Golden M, Khoosal A, Muhire B. Rdp4: Detection and analysis of recombination patterns in virus genomes. Virus Evolution. 1:vev003; 2015.

162. Martin DP, Murrell B, Khoosal A, Muhire B. Detecting and analyzing genetic recombination using rdp4. In: Bioinformatics KJe, editor. *Methods mol biol*. Humana Press, New York, NY; 2017.

163. Song J, Tan H, Perry AJ, Akutsu T, Webb GI, Whisstock JC, Pike RN. Prosper: An integrated feature-based tool for predicting protease substrate cleavage sites. PLoS One. 7:e50300; 2012.

164. Gasteiger E, Hoogland C, Gattiker A, Duvaud S, Wilkins MR, Appel RD, Bairoch A. Protein identification and analysis tools on the expasy server. In: Walker JM, editor. *The proteomics protocols handbook*. Totowa, NJ: Humana Press. p. 571-607; 2005.

165. Khanh NP, Tan SW, Yeap SK, Satharasinghe DA, Hair-Bejo M, Bich TN, Omar AR. Molecular characterization of qx-like and variant infectious bronchitis virus strains in malaysia based on partial genomic sequences comprising the s-3a/3b-e-m-intergenic region-5a/5b-n gene order. Avian Dis. 61:442-452; 2017.

166. Williamson MP. The structure and function of proline-rich regions in proteins. Biochem J. 297:249-260; 1994.

167. Yu H, Yan Y, Zhang C, Dalby PA. Two strategies to engineer flexible loops for improved enzyme thermostability. Sci Rep. 7:41212; 2017.

168. Yu H, Zhao Y, Guo C, Gan Y, Huang H. The role of proline substitutions within flexible regions on thermostability of luciferase. Biochim Biophys Acta. 1854:65-72; 2015.

169. Mondal SP, Cardona CJ. Genotypic and phenotypic characterization of the california 99 (cal99) variant of infectious bronchitis virus. Virus Genes. 34:327-341; 2007.

170. Mork AK, Hesse M, El Rahman SA, Rautenschlein S, Herrler G, Winter C. Differences in the tissue tropism to chicken oviduct epithelial cells between avian coronavirus IBV strains qx and b1648 are not related to the sialic acid binding properties of their spike proteins. Vet Res. 45; 2014.

171. Zulperi ZM, Omar AR, Arshad SS. Sequence and phylogenetic analysis of S1, S2, m, and n genes of infectious bronchitis virus isolates from malaysia. Virus Genes. 38:383-391; 2009.

172. Bouwman KM, Delpont M, Broszeit F, Berger R, Weerts EAWS, Lucas MN, Delverdier M, Belkasmi S, Papanikolaou A, Boons GJ et al. Guinea fowl coronavirus diversity has phenotypic consequences for glycan and tissue binding. J Virol. 93:1-11; 2019.

173. Lontok E, Corse E, Machamer CE. Intracellular targeting signals contribute to localization of coronavirus spike proteins near the virus assembly site. J Virol. 78:5913-5922; 2004.

174. Fix AS, Arp LH. Quantification of particle uptake by conjunctiva-associated lymphoid tissue (calt) in chickens. Avian Dis. 35:174-179; 1991.

175. Reemers SS, van Leenen D, Koerkamp MJ, van Haarlem D, van de Haar P, van Eden W, Vervelde L. Early host responses to avian influenza a virus are prolonged and enhanced at transcriptional level depending on maturation of the immune system. Mol Immunol. 47:1675-1685; 2010.

176. Scott TR, Savage ML, Olah I. Plasma cells of the chicken harderian gland. Poult Sci. 72:1273-1279; 1993.

177. Watabe M, Glick B. Graft versus host response as influenced by the origin of the cell, age of chicken, and cellular interactions. Poult Sci. 62:1317-1324; 1983.

178. Wells LL, Lowry VK, DeLoach JR, Kogut MH. Age-dependent phagocytosis and bactericidal activities of the chicken heterophil. Dev Comp Immunol. 22:103-109; 1998.

179. Cavanagh D, Davis PJ, Darbyshire JH, Peters RW. Coronavirus IBV: Virus retaining spike glycopolypeptide S2 but not S1 is unable to induce virus-neutralizing or haemagglutination-inhibiting antibody, or induce chicken tracheal protection. J Gen Virol. 67:1435-1442; 1986.

180. Gelb J, Jr., Nix WA, Gellman SD. Infectious bronchitis virus antibodies in tears and their relationship to immunity. Avian Dis. 42:364-374; 1998.

181. Thompson G, Mohammed H, Bauman B, Naqi S. Systemic and local antibody responses to infectious bronchitis virus in chickens inoculated with infectious bursal disease virus and control chickens. Avian Dis. 41:519-527; 1997.

182. Gurjar RS, Gulley SL, van Ginkel FW. Cell-mediated immune responses in the head-associated lymphoid tissues induced to a live attenuated avian coronavirus vaccine. Dev Comp Immunol. 41:715-722; 2013.

183. Orr-Burks N, Gulley SL, Toro H, van Ginkel FW. Immunoglobulin a as an early humoral responder after mucosal avian coronavirus vaccination. Avian Dis. 58:279-286; 2014.

184. Erf GF, Bottje WG, Bersi TK. Cd4, cd8 and tcr defined t-cell subsets in thymus and spleen of 2- and 7-week old commercial broiler chickens. Vet Immunol Immunopathol. 62:339-348; 1998.

185. Ewald SJ, Lien YY, Li L, Johnson LW. B-haplotype control of cd4/cd8 subsets and tcr v beta usage in chicken t lymphocytes. Vet Immunol Immunopathol. 53:285-301; 1996.

186. Honjo K, Hagiwara T, Itoh K, Takahashi E, Hirota Y. Immunohistochemical analysis of tissue distribution of b and t cells in germfree and conventional chickens. J Vet Med Sci. 55:1031-1034; 1993.

187. Gomez Del Moral M, Fonfria J, Varas A, Jimenez E, Moreno J, Zapata AG. Appearance and development of lymphoid cells in the chicken (gallus gallus) caecal tonsil. Anat Rec. 250:182-189; 1998.